



<https://theses.gla.ac.uk/>

Theses Digitisation:

<https://www.gla.ac.uk/myglasgow/research/enlighten/theses/digitisation/>

This is a digitised version of the original print thesis.

Copyright and moral rights for this work are retained by the author

A copy can be downloaded for personal non-commercial research or study, without prior permission or charge

This work cannot be reproduced or quoted extensively from without first obtaining permission in writing from the author

The content must not be changed in any way or sold commercially in any format or medium without the formal permission of the author

When referring to this work, full bibliographic details including the author, title, awarding institution and date of the thesis must be given

Enlighten: Theses

<https://theses.gla.ac.uk/>
research-enlighten@glasgow.ac.uk

**THE USE OF REAL-TIME PCR FOR THE DIAGNOSIS OF JOHNE'S DISEASE
IN CATTLE AND SHEEP**

BY

RAHUL KUMAR NELLI, B.V.Sc., & A.H.

Dissertation submitted for the Degree in Master of Veterinary Medicine,
University of Glasgow

Institute of Comparative Medicine,
University of Glasgow,

March 2007

© Copyright 2007, all rights reserved by RAHUL KUMAR NELLI

ProQuest Number: 10395731

All rights reserved

INFORMATION TO ALL USERS

The quality of this reproduction is dependent upon the quality of the copy submitted.

In the unlikely event that the author did not send a complete manuscript and there are missing pages, these will be noted. Also, if material had to be removed, a note will indicate the deletion.



ProQuest 10395731

Published by ProQuest LLC (2017). Copyright of the Dissertation is held by the Author.

All rights reserved.

This work is protected against unauthorized copying under Title 17, United States Code
Microform Edition © ProQuest LLC.

ProQuest LLC.
789 East Eisenhower Parkway
P.O. Box 1346
Ann Arbor, MI 48106 – 1346

ABSTRACT

This study was aimed at the rapid and early detection of *Mycobacterium avium paratuberculosis* (*Map*), which is the causative organism for Johne's disease in animals.

The history of Johne's disease and its epidemiology, clinical disease, pathology and diagnosis of Johne's disease was reviewed. The characteristics of *Mycobacterium avium paratuberculosis* and its detection in clinical material were reviewed. The modern diagnostic methods for the identification of pathogens were evaluated and real-time polymerase chain reaction (PCR) was considered worthy of an appropriate tool for the diagnosis of the disease.

The animals used in this study were animals suspected of having Johne's disease which had been admitted to the Farm animal clinic. Six cows and 5 ewes were used in this study. Five of the six cows were antibody positive by Enzyme linked immunosorbent assay (ELISA), faecal smear, intestinal smear and histopathology. Sera of the five sheep were not examined by ELISA but all were positive for acid fast organisms by intestinal smear and post-mortem examination, confirming the presence of the disease. One of the ewes was pregnant and her uterus contained dead twin fetuses.

Real-time PCR for *Map* was developed using a *Map* specific primer/probe set based on IS900 from a published source (SF214/PR265/SR289). A further real-time PCR was developed for the 18S rRNA house keeping gene, using a primer/probe set designed in this study. Optimisation and validation of these primers and probes was performed. The primer/probe set used for detecting *Map* was able to detect 1 log copy of *Map* IS900 DNA with a PCR efficiency of 0.986706 and low standard deviation. The real-time PCR for *Map* detected single log copies of IS900 and calculations confirmed the C_T values (results of real-time PCR) 39.87, 39.07 and 39.65, represented a single cell of *Map*. Gene cloning and sequencing of the PCR product was performed to confirm that the target sequence was present, thereby validating the real-time PCR results. Sequencing of 18S PCR product was not successful and requires further work. The cloned product of *Map* was also used to plot a standard curve for use in quantitation. The real-time PCR assay of the samples examined in this study was carried out in triplicate and the C_T values obtained had a coefficient of variation of less than 10%.

DNA was extracted from faeces/tissue samples, milk and blood from the 6 bovine and 5 ovine cases of suspected Johne's disease using standard protocols (QIAGEN

Ltd, Crawley, UK) *Mycobacterium avium paratuberculosis* DNA was detected in five of the 6 bovine faecal samples by real-time PCR but results for the sixth animal were equivocal.

Mycobacterium avium paratuberculosis was detected in a wide range of bovine tissues. *Map* organisms were demonstrated in blood, lymph nodes, tonsil, mammary tissue, mammary secretions, uterus, liver, spleen, kidney and muscle. Similar results were obtained for the ovine samples where one faecal sample also gave an equivocal result. No organisms were demonstrated in the spleens of adult sheep and retropharyngeal lymph nodes were not examined in this species. The foetal membranes, amniotic and other fluids, spleen and muscle were positive for *Map* but no organisms were detected in the liver.

The approximate number of organisms present in each sample was calculated from the real-time PCR results. Bovine faeces contained a range of 1.73×10^2 organisms to 4.67×10^5 organisms/g. Blood samples contained 1.5×10^1 to 2.61×10^2 organisms/mL in bovine samples and 6.4×10^1 to 1.14×10^2 organisms/mL in ovine samples. Mammary secretions had 1 to 1.56×10^3 organisms/mL in bovine samples and 1.32×10^2 organisms/mL in a single ovine mammary secretion sample analysed. Organisms were detected in most of the lymph nodes, but mesenteric lymph nodes contained 3.25×10^5 organisms/gram in bovine sample and 3.59×10^2 organisms/gram in ovine samples. Bovine liver contained organisms up to 4.20×10^4 organisms/gram higher than that of the other visceral organs like spleen and kidney ($< 1.94 \times 10^3$).

Ovine faeces contained a range from 1 organism to 1.2×10^6 organisms/g. Ileal mucosa with C_T value of 13.58 had the highest number of organisms/gram i.e. 1.5×10^9 . In leg muscle (gastrocnemius) 9.4×10^6 organisms/g were found in one case. The foetal samples (fluids, ileal mucosa, muscle and spleen) contained 3.18×10^2 organisms/mL; 4.35×10^2 organisms/g; 2.12×10^2 organisms/g; 4.7×10^1 organisms/g, respectively.

The real-time PCR for *Map* produced in this study successfully detected *Map* in faeces, blood, mammary secretion and tissues. In some cases it appeared to be superior to other tests. It allowed the enumeration of *Map* organisms in the samples and will provide a guide to the safety of bovine and ovine tissues in veterinary public health and food safety. It will also allow the early detection of *Map* infected animals, the original aim of the study.

DECLARATION

The Studies described in this thesis were carried out in the Institute of Comparative Medicine, Faculty of Veterinary Medicine at the University of Glasgow, between November 2006, and February 2007. The author was responsible for all the results, except where otherwise stated. No part of this thesis has been submitted for any other degree.

RAHUL KUMAR NELLI, March 2007

LIST OF CONTENTS	Page
ABSTRACT	ii
DECLARATION	iv
LIST OF CONTENTS	v
LIST OF TABLES	ix
LIST OF FIGURES	x
ACKNOWLEDGEMENT	xi
CHAPTER I: INTRODUCTION – JOHNE’S DISEASE AND ITS DIAGNOSIS	1
1.1 Definition	2
1.2 History of Johne’s disease	2
1.3 Aetiology	2
1.4 Epidemiology	5
1.4.1 Species Affected	5
1.4.2 Distribution	5
1.4.3 Routes of Infection	6
1.4.4 Incubation Period	6
1.4.5 Survival of the Organism	6
1.5 Clinical Signs	7
1.6 Pathology	7
1.6.1 Pathogenesis	9
1.6.2 Clinical Pathology	9
1.6.3 Gross Pathology	10
1.6.4 Histopathology	10
1.7 Diagnosis	11
1.7.1 Clinical signs	11
1.7.2 Staining of Faecal and Impression Smears	11
1.7.3 Biochemical Tests	13
1.7.4 Culture	13
1.7.4.1 Culture Systems	14
(a) Conventional Culture System	14
(b) Automated Culture System	15
(i) Radiometric System	15

(ii) Non-radiometric System	15
1.7.4.2 Colonial Morphology	15
1.7.5 Cell-Mediated Immunity based Tests	16
(a) Johnin Skin Test	16
(b) Interferon gamma (γ) test	16
(c) Lymphocyte Stimulation Test	17
(d) Leukocyte Migration Agarose Test (LMAT)	17
1.7.6 Serological Tests	17
(a) Agar Gel Immuno Diffusion test (AGID)	17
(b) Complement fixation test (CFT)	18
(c) ELISA (Enzyme linked immuno sorbent assay).	20
1.7.7 DNA probes	22
1.7.8 Polymerase Chain Reaction assay	22
1.7.9 Real-time PCR	23
1.8 Control of Johne's disease	25
1.9 Public health importance	26
1.10 Economic importance	26
1.11 Discussion	27
CHAPTER II: GENERAL MATERIALS AND METHODS	30
2.1 Introduction	31
2.2 Selection of cases	31
2.3 Sample collection	31
2.4 Acid-fast staining	34
2.5 Histopathology	35
2.5 Extraction of genomic DNA templates from samples collected	35
(a) Faeces	35
(b) Tissues	36
(c) Milk, Blood, WBC, etc	37
2.7 Extraction of leukocytes from whole blood samples	37
2.8 Discussion	37
CHAPTER III: RESULTS – CLINICAL AND PATHOLOGICAL	
EXAMINATION OF SUSPECTED CASES	39
3.1 Introduction	40

3.2 Clinical data and examination	40
3.3 Post-mortem examination	40
3.4 Microscopic examination	43
3.4.1 Faecal smears	43
3.4.2 Tissue smears	48
3.4.3 Histopathology	48
3.5 Discussion	48
CHAPTER IV: REAL-TIME PCR ASSAY – INTRODUCTION AND ITS USE	
IN THIS STUDY	51
4.1 Introduction	52
4.1.1 Materials used in real-time PCR assay	52
4.1.2 Dyes used in real-time PCR	52
4.1.3 Principle of real-time PCR assay	52
4.1.3.1 FRET system	53
(a) FRET Hydrolysis probes	53
(i) <i>TaqMan</i> [®] Probes	53
(ii) Molecular Beacons	55
(iii) Scorpion Probes	55
(b) FRET Hybridisation Probe	57
4.1.3.2 DNA-binding agents –SYBR [®] Green dye	57
4.1.4 Analysis of real-time PCR results	58
4.1.5 Selection of primers and probes	58
4.2 Materials and Methods	60
4.2.1 Optimisation of primers and probe concentrations for detection of <i>Map</i> and 18S	60
4.2.2 Detection of <i>Map</i> and 18S template DNA in clinical samples by real-time PCR analysis	64
4.2.3 Validating the real-time PCR results in the detection of <i>Map</i> and 18S	64
(a) Cloning PCR products from <i>Map</i> and 18S reactions	64
(b) DNA extraction from the cloned product	66
(c) Restriction analysis of plasmid DNA obtained from cloned product	67
(d) Sequencing of plasmid DNA from cloned product	67
(e) Agarose gel electrophoresis	68

(f) Polyacrylamide gel electrophoresis	68
4.2.4 Quantification of DNA samples	69
4.2.5 Preparation of <i>Map</i> and 18S templates for standard curve analysis	69
4.3 Results	70
4.3.1 Optimisation of primers and probes concentrations for detection of <i>Map</i> and 18S	70
4.3.2 Validation of real-time PCR products for detection of <i>Map</i> and 18S	70
4.3.3 Results of DNA quantitation	74
4.4 Discussion	77
CHAPTER V: Real-Time PCR results in comparison with other diagnostic results used in this study	80
5.1 Introduction	81
5.2 Materials and methods	81
5.3 Results of the clinical samples to detect <i>Map</i> DNA by real-time PCR	82
(a) Efficiency of DNA extraction	82
(b) Results with <i>Map</i> and 18S primers and probes	82
(c) Results from clinical samples	83
(d) Results with C_T values greater than 40	83
5.4 An approximation of number of organisms present in each tissue	86
5.5 Comparing the results of with other diagnostic results in this study	89
5.6 Discussion	93
CHAPTER VI: GENERAL DISCUSSION	95
6.1 Introduction to Johne's disease	96
6.2 The importance of Johne's disease in animal trade and public health	96
6.3 Current methods of detection and their relationship to control measures	97
6.4 The value of real-time PCR results in diagnosis of Johne's disease	97
6.5 The use of real-time PCR in carcass inspection	98
6.6 Relative costs of major diagnostic methods	98
6.7 The findings of this study in relation to transmission and public health	99
APPENDIX – I	102
APPENDIX – II	105
REFERENCES	108

LIST OF TABLES		Page
Table 1.1	A brief history of Johne's disease	3
Table 1.2	Clinical stages of Johne's disease	8
Table 1.3	Differential Diagnosis of Johne's disease	12
Table 1.4	Evaluation of ELISA	21
Table 1.5	Types of Thermal Cycling	24
Table 2.1	Samples collected from suspected/diseased cattle	32
Table 2.2	Samples collected from suspected/diseased sheep	33
Table 3.1	Clinical findings in cattle	42
Table 3.2	Clinical findings in sheep	42
Table 3.3	Post mortem findings from both bovine and ovine cases used in this study	44
Table 3.4	Results of microscopic examination of clinical samples	47
Table 4.1	Primer/ Probe sets used in detection of <i>Map</i> by Real-time PCR	61
Table 4.2	Different primer/probe dilutions of <i>Map</i>	62
Table 4.3	Different primer/probe dilutions of 18S	62
Table 4.4	<i>Map</i> premix per well in Real-time PCR assay for test samples	65
Table 4.5	18s premix per well in Real-time PCR assay for test samples	65
Table 5.1	Real-time PCR results for <i>Map</i> (C_T values) in various bovine samples	84
Table 5.2	Real-time PCR results for <i>Map</i> (C_T values) in various ovine samples; Right: foetal samples	85
Table 5.3	An approximate number of organisms present in various bovine samples based on their C_T values.	87
Table 5.4	An approximate number of organisms present in various ovine samples based on their C_T values.	88
Table 5.5	Summary of diagnostic results from suspected Johne's disease cattle used in this study	90
Table 5.6	Summary of diagnostic results from suspected Johne's disease sheep used in this study	91

LIST OF FIGURES	Page
Fig. 1.1 Taxonomic tree of <i>Mycobacterium avium</i> subsp. <i>paratuberculosis</i>	4
Fig. 1.2 Agarose gel plate setup for AGID assay	19
Fig. 3.1 General clinical signs of cattle observed in different cases	41
Fig. 3.2 Post-mortem lesions of <i>Map</i> infected GIT	45
Fig. 3.3 Dead ovine foetus recovered from Case 210608	46
Fig. 3.4 Acid-fast stained (ZN-staining) smears of intestinal mucosa <i>Mycobacterium avium</i> subsp. <i>paratuberculosis</i>	49
Fig. 4.1 Fluorescence Resonance Energy Transfer or Förster resonance energy transfer (FRET)	54
Fig. 4.2 Different methods of fluorescence detection in real-time PCR assay	56
Fig. 4.3 Amplification plot of real-time PCR assay	59
Fig. 4.4 Template diagram similar to 96-Well Reaction Plate	63
Fig. 4.5 Line chart representing the C_T values of 18S primer and probe combinations for optimisation	71
Fig. 4.6 Line chart representing the C_T values of <i>Map</i> primer and probe combinations for optimisation	72
Fig. 4.7 Cloned product of <i>Map</i> visualised on a 1.5% agarose gel	73
Fig. 4.8 Gene fragment of cloned product of <i>Map</i>	75
Fig. 4.9 Standard curve generated from C_T values of <i>Map</i> clone	76
Fig 4.10 Standard curve generated from C_T values of 18S	78

ACKNOWLEDGEMENTS

I would like to acknowledge wholeheartedly the efforts of all the individuals in tailoring this project.

Firstly, I would like to thank and express my gratitude to Professor David Taylor for his encouragement; motivation and support to successfully complete this project.

My special thanks, to Dr Libby Graham for her invaluable help, support and advice throughout this project and her suggestions in DNA extractions and real-time PCR assay were valuable.

My sincere thanks, to Dr Steve Dunham for his practical assistance in cloning and sequencing techniques and expert advice on molecular softwares. Also he helped in ordering and designing primers and probes (18S).

I feel happy to thank all the Clinical Scholars of Animal Production and Public Health; Ricardo Bexiga, Ana Mateus and Joachim L Kleen, who gave their support while performing clinical examination, collecting clinical samples and providing clinical reports.

I gratefully acknowledge the help of Richard Irvine and James Baily for assisting with the post-mortem sampling and recording.

I appreciate the help of Kathy, Manuel and Christine in Diagnostic Veterinary Bacteriology, for providing all laboratory needs.

Last but not the least I wish to extend my indebtedness to my parents for their encouragement, confidence in me, without which this work would not have been possible.

CHAPTER I

INTRODUCTION – JOHNE'S DISEASE AND ITS DIAGNOSIS

1.1. Definition

Johne's disease is a severe, chronic, incurable, granulomatous enteritis affecting domestic and wild ruminants caused by *Mycobacterium avium* subsp. *paratuberculosis* (OIE 2004; Cocito *et al.*, 1994; Bauerfeind *et al.*, 1996).

1.2. History of Johne's Disease

The history of Johne's disease has been reviewed by Collins and Manning (2001) in www.johnes.org and started on a German farm in 1894, where a cow failed to gain weight and died. A local veterinarian, Dr Harmes, examined the cow and sent its intestines, stomach, and omentum for pathological examination to the Veterinary Pathology Unit in Dresden. There the tissues were examined by Dr Johne and Dr Frothingham, a visiting scientist from the Pathology Unit in Boston, Massachusetts. Johne and Frothingham concluded that the disease observed in the cow, chronic granulomatous ileitis, was caused by an acid-fast bacterium. The novel disease was pathologically similar to intestinal tuberculosis in cattle which is caused by *Mycobacterium bovis* Johne and Frothingham in 1895. They proposed the name "pseudotuberculous enteritis" for the disease. (Table 1.1)

1.3 Aetiology

Johne's disease is a bacterial disease caused by *Mycobacterium avium* subsp. *paratuberculosis* (*Map*). *Mycobacterium avium paratuberculosis* is an aerobic, non-spore forming, non-motile, acid-fast, weakly gram-positive coccobacillary rod (Clarke, 1997, Bergey's Manual, 2001).

Mycobacterium avium paratuberculosis belongs to a large family of microorganisms, the *Mycobacteriaceae* (Fig. 1.1). The genus *Mycobacterium* includes obligate parasites, saprophytes and intermediate forms and includes type species *Mycobacterium tuberculosis*, *M. leprae*, *M. avium*, and *M. bovis*. Identification of *Map* is based on its mycobactin requirement and its pathogenicity in the host (Thorel *et al.*, 1990). The organism is a slow growing bacterium (Barrow *et al.*, 1993) and has a requirement for the iron-chelating compound mycobactin J, which must be added to any medium used for its cultivation (McCullough and Merkal, 1976). This mycobactin-

Historical Milestones	Historical Events
1 The agent was demonstrated in infected cattle	A cow belonging to a German farmer failed to gain weight; was suspected intestinal tuberculosis, but tuberculin negative. The animal finally died (1894).
2 The agent was isolated and grown in pure culture	An acid-fast bacillus was identified as the cause of disease by Johnne and Frothingham in 1895.
3 Agent was introduced into animals to reproduce disease	Disease was termed Johnne's disease in 1906. Isolation of bacillus in culture by adding <i>Mycobacterium phlei</i> extracts to media was performed by Twort in 1910.
4 Diagnostic developments	Laboratory animals were experimentally infected with isolated bacilli Hagan and Zeissig in 1933. Herd was experimentally infected with cultured bacilli in a 6 year trial. Twort and Ingram used the complement fixation test (CFT) in the diagnosis of Johnne's disease as early as 1913.
	Yokomizo and others developed an ELISA in 1983, which was later modified and used in diagnosis
	In 1989, Green <i>et al.</i> identified a specific gene insertion element, IS900, in <i>Mycobacterium paratuberculosis</i> , this group later developed PCR assay.
	Thorel (1990) carried out numerical taxonomy analysis of <i>Mycobacterium paratuberculosis</i> , which resulted in the current name <i>Mycobacterium avium paratuberculosis</i> .
	Kim <i>et al.</i> , (2002) developed a quantitative PCR method for <i>Mycobacterium avium paratuberculosis</i> .
	Li <i>et al.</i> , (2005), reported the complete genomic sequence of <i>Mycobacterium avium paratuberculosis</i> .

Table 1.1 A brief history of Johnne's disease

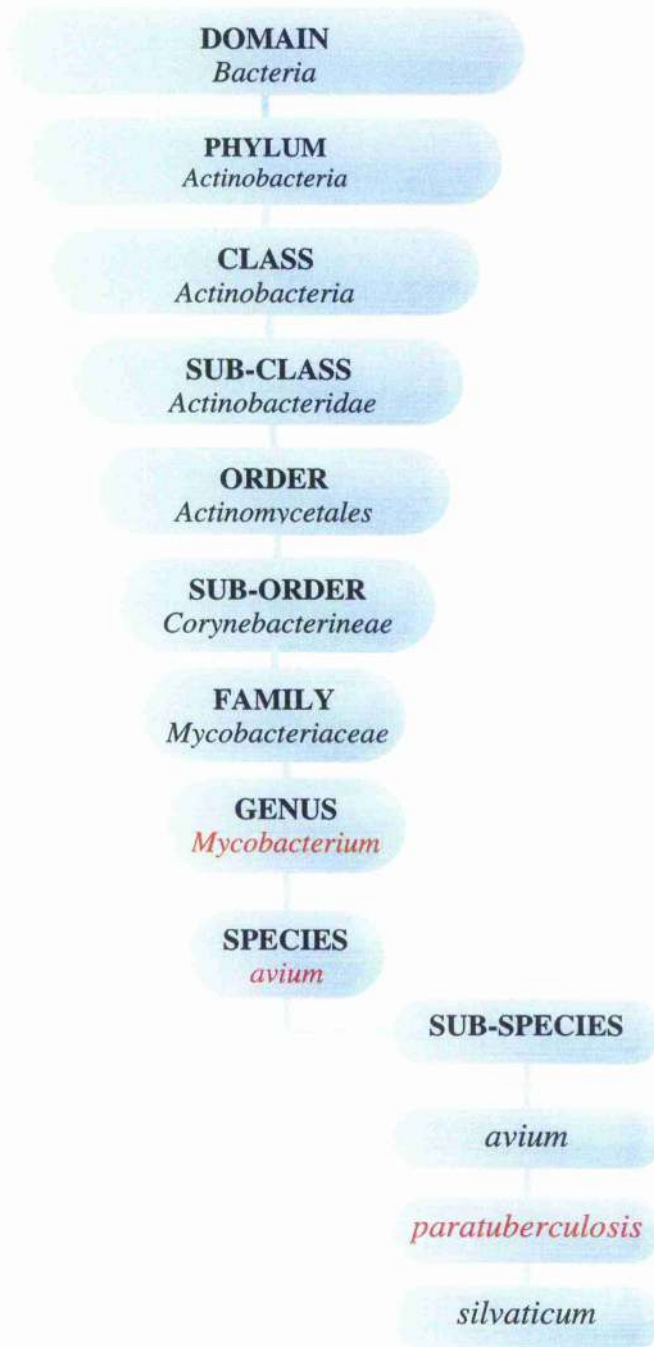


Fig. 1.1 Taxonomic tree (Bergey's Manual, 2001) of *Mycobacterium avium* subsp. *paratuberculosis*

dependency represents a characteristic unique to *Map* (Thorel *et al.*, 1990). Also, *Map* has a complex cell wall like the rest of mycobacteria, which is rich in lipids and relatively impermeable. The lipid-rich complex cell wall confers acid-fast properties, and may enhance its survival in the environment. A prominent lipopolysaccharide (LPS) of the cell wall, lipoarabinomannan (LAM), is thought to have important consequences for hypersensitivity type reactions and the formation of the granulomatous lesions characteristic of the disease. Lipoarabinomannan is also of diagnostic importance, as it is strongly immunogenic (Mutharia *et al.*, 1997). *Map* DNA contains an insertion sequence (IS) element IS900 which is unique to this species and allows *Map* to be differentiated from the other subspecies (Green *et al.*, 1989). Analysis of *Map* DNA showed, >98 percent genetic identity with closely related species *M. avium* subsp. *avium*. The type strain of *Map* is strain ATCC 19698 (Thorel *et al.*, 1990).

Other names proposed for *Map* were *Darntuberculose*; *Mycobacterium enteritidis*; *Bacterium paratuberculosis*; *Bacillus paratuberculosis*; *Mycobacterium johnei* (NCBI taxonomy browser). Finally, *Mycobacterium avium* subsp. *paratuberculosis* was accepted by OIE (Thorel *et al.*, 1990).

1.4 Epidemiology

1.4.1 Species Affected

Mycobacterium avium paratuberculosis is found most often among domestic and wild ruminants. The disease has been reported in cattle; sheep; goats; pigs; deer; mountain goats; elk; alpaca and antelopes. Calves can also become infected (Larsen *et al.*, 1975). Isolated cases have also been reported in horses; rabbits; nonhuman primates; foxes; stoats; weasels and water buffalo. (Chiodini *et al.*, 1984; Greig *et al.*, 1999; Beard *et al.*, 2001; Siva Kumar *et al.*, 2005).

1.4.2 Distribution

The disease has a worldwide distribution and is categorised by the OIE as a list B transmissible disease. The disease is considered to be of socio-economic and/or public health importance within countries and that are significant in the international trade of animals and animal products (OIE, 2005).

1.4.3 Routes of Infection

Mycobacterium avium paratuberculosis most commonly enters the host through the oral route via contaminated water, milk, colostrum and feed material (Chiodini *et al.*, 1984; Streeter *et al.*, 1995; Sweeney, 1996; Grant, 2005). *Mycobacterium avium paratuberculosis* is shed in faecal material which is the major source of infection. Infected cows can also transmit infection to the foetus causing an *in utero* foetal infection, which may be either clinical or subclinical (Sweeney *et al.*, 1992), thus calves may be born infected with *Map* (Sweeney, 1996). Semen can also be infected with *Map* (Larsen *et al.*, 1981). Congenital infection is not common in minimally infected animals but a higher percentage of infection is expected from heavily infected dams (de Lisle, 1980).

1.4.4 Incubation Period

The incubation period may range from 6 months to 15 years. Rarely, incubation periods of less than 6 months and more than 15 years have been observed. In most cases a period of 3-5 years was observed (Chiodini *et al.*, 1984).

1.4.5 Survival of the Organism

Mycobacterium avium paratuberculosis is resistant to drying, acid conditions and many disinfectants, and can survive freezing temperatures of -14°C for a year or longer (Chiodini *et al.*, 1984). Faeces have a bacteriostatic effect on *Map* and urine has a bacteriocidal effect; it survives 163 days in river water and 270 days in pond water (Chiodini *et al.*, 1984). *Mycobacterium avium paratuberculosis* can survive in the environment for long periods, e.g., *Map* was reported to survive for 6 to 18 months in tap or pond water (Larsen *et al.*, 1956) and for about 14-17 months in post inoculated water at different pH; the slowest growing strains were more resistant to chlorine (Manning and Collins, 2001). Other authors have reported survival for 55 weeks in faeces/soil in a dry, fully shaded environment, 48 weeks in a shaded water trough, 36 weeks in an unshaded water trough, 11 months in bovine faeces, 12 weeks in faecal pellets and soil in a terrestrial environment (Chiodini *et al.*, 1984; Whittington *et al.*, 2003a). Destruction of *Map* on surfaces that might be contaminated requires thorough

cleaning with soap and water, followed by application of a disinfectant that is labelled as "tuberculocidal": cresolic disinfectants and sodium orthophenylphenate only kill *Mycobacteria* that are not protected by organic matter (Collins, 2004). *Mycobacterium avium paratuberculosis* is killed within 10 minutes in aqueous solutions of formalin (5%), calcium hypochloride (2%) and phenol (2.5%) (Chiodini *et al.*, 1984) and is killed on exposure to ultra-violet (UV) light for 100 hours or by boiling for 2 minutes.

1.5 Clinical Signs

Johne's disease is a chronic granulomatous enteritis of ruminants, with clinical signs of watery diarrhoea, lowered nutrient absorption and untreatable wasting, eventually resulting in death (Aho *et al.*, 2003). Animals become infected early in life, but often do not develop clinical signs until 2–5 years of age (Larsen *et al.*, 1975). The disease is normally characterised by four stages (Table 1.2) silent infection, subclinical, clinical and advanced clinical infection (Whitlock and Buergelt, 1996). Clinical disease may be precipitated by parturition, lactation or other stress factors (Chiodini *et al.*, 1984). In lactating animals, there will be a fall in milk yield without any pyrexia or toxæmia (Radostits *et al.*, 2000) and also infertility (Bogli-Stuber *et al.*, 2005). Chronic diarrhoea is homogeneous, non-haemorrhagic and non-mucoid (Merkal *et al.*, 1970), but in ovine cases diarrhoea is a less constant feature (Clarke and Little, 1996). Faecal consistency may improve for a few weeks and return with increased severity. Affected animals are usually alert and eat well until the disease enters an advanced stage (Cousins *et al.*, 1999). Severe gradual weight loss occurs due to protein malabsorption and loss caused by the striking cellular infiltrate and oedema that occurs in the intestine (Clarke, 1997). Oedema of submandibular and other areas may be seen in advanced cases and anaemia is detected occasionally (Clarke, 1997). An unthrifty rough coat with alopecia and occasional depigmentation can be seen; sheep exhibit "wool-slip" (Radostits *et al.*, 2000), wool fragility and poor fleece. In sheep, diarrhoea is uncommon, but pasting of soft faeces around the anal region is observed in advanced cases (Clarke and Little 1996). However, clinical signs are not a reliable indicator for diagnosing *Map* in sheep and goats (Whittington and Sergeant, 2001).

1.6 Pathology

Clinical stages	Clinical signs	Diagnostic importance
I. Silent infection stage	No evidence of clinical signs; usually young stock is affected and adult animals	No routine clinical tests or serological tests can detect disease in animals, rarely histopathology can detect. Real-time PCR detection is possible, but as the lowest detection limit cannot precisely be defined (Bogh-Stuber <i>et al.</i> , 2005).
II. Subclinical stage	Doesn't exhibit clinical signs. Intermittent faecal shedding is observed.	Sometimes detectable in serology; cellular immune response; faecal culture tests. All PCR assays can detect
III. Clinical stage	Clinical signs are observed after years of incubation	Detectable in serology; cellular immune response; faecal culture; plasma biochemical tests. All PCR assays can detect
IV. Advanced clinical stage	Weak, lethargic, emaciated, bottle jaw, profuse diarrhoea. Due to severe weight loss animals are culled from the herd.	Detectable in serology; cellular immune response and faecal culture. Also observed in different organs like liver, lymph nodes. All PCR assays can detect

Table 1.2 Clinical stages of Johne's disease

1.6.1 Pathogenesis

Mycobacterium avium paratuberculosis is an intracellular pathogen which replicates in macrophages in the lamina propria of the intestine and is shed into the faeces during disease (Vary *et al.*, 1990). After the organism has been ingested, *Map* undergoes endocytosis by M cells in ileal/Peyer's patches/jejunal regions and then crosses from the lumen of the intestine to the lymphoid system. The intestinal macrophage is the target cell for infection by *Map*. *Mycobacterium avium paratuberculosis* escapes the process of phagocytosis in macrophages. Moreover, LAM in the cell wall induces resistance to macrophage activation and assists in generating cytokines along with peptidoglycan and heat-shock proteins. In addition, *Map* multiplies in the macrophages. The elevated levels of cytokines along with other macrophage products such as tumour necrosis factor- α (TNF- α) and interleukin-1 (IL-1) misdirect the host inflammatory response leading to chronic inflammatory lesions, mainly in the intestinal submucosa (Clarke, 1997). Thus, a diffuse infiltration of lymphocytes, plasma cells and eosinophils occurs in the lamina propria and epithelioid cells in the tips or the bases of the villi. As infection advances, there is an increase in epithelioid cells which gradually compress and destroy the crypts thereby contributing to the gross thickening of the intestine. Changes in the lymphatic tissue are a consistent finding. The earliest lesions develop in the lymphoid tissue of Peyer's patches; lymphatic vessels are surrounded by lymphocytes and plasma cells and clumps of epithelioid cells in the lumen result in epithelioid granulomas that form in the wall and project into the lumen (Cousins *et al.*, 1999). Ultimately necrotic lesions of lymph nodes are observed due to TNF- α activity which encourages tissue catabolism (Beutler and Cerami, 1989). This phenomenon is more common in sheep and goats. According to some authors, *Map* enters the tonsil as the site of primary infection, with subsequent dissemination to other tissues via lymphatics (Payne and Rankin, 1961). The reasons for the long incubation period of the clinical disease are not understood but it may be due to suppressed cell-mediated immunity caused by mycobacterial antigens such as LAM and several other factors.

1.6.2 Clinical Pathology

In infected animals, there are elevated levels of aspartate amino transferase activity, and a decrease in serum concentrations of calcium, total protein and albumin. This is due to loss of albumin bound calcium through the damaged ileal mucosa leading to hypocalcaemia and hypoalbuminaemia. Magnesium and phosphorus levels are very similar to control values and there is no change in serum creatinine or urea concentrations (Jones and Kay, 1996). Histochemical demonstration of succinate dehydrogenase, glucose-6-phosphate dehydrogenase, NADP-dependant isocitrate dehydrogenase, acid phosphatase, alkaline phosphatase and non-specific esterase activity were noted (Merkal *et al.*, 1968a, b). This can only aid as a supportive diagnosis (Jones and Kay, 1996).

1.6.3 Gross Pathology

The focus of pathology is mainly the gut, specifically the jejunum, ileum, ileocaecal junction and immediately adjacent areas like mesenteric lymph nodes which become enlarged, pale and oedematous (Begara-McGorum *et al.*, 1998). In early infections gross lesions may not be evident but some degree of lymphangitis is always present. Lesions are prominent in the distal ileum but usually stop abruptly at the ileocaecal valve. In some cases the ileocaecal valve may be enlarged. It is very rare to find lesions in the duodenum. The classic lesion is thickening of the ileal mucosa which develops into corrugations or transverse folds called "rugae". These folds cannot be smoothed out and they are congested. The ileal serosa is usually oedematous with a granular appearance and the subserosal lymphatics are prominent and dilated (cording). In sheep, lymphatic vessels are knotted and corded, whereas the mucosal surface has a granular appearance and shows pigmentation ranging from light yellow to deep orange. Necrosis of the mucosa occurs very rarely in cattle (Clarke and Little 1996; Clarke, 1997). Necrosis of fat and of the medullary region of lymph nodes is observed; ascites, carcass emaciation and intermandibular oedema are also noted.

1.6.4 Histopathology

Chronic enteritis, chronic intestinal lymphangitis and mesenteric lymph adenopathy are seen. The basic lesion is cellular infiltration of the ileal mucosa. An advanced infection has very distinct histopathological lesions with acid-fast bacilli

when compared to a subclinical infection. Acid-fast bacilli can be demonstrated in the mucosa and submucosa of the intestine. Langhans' giant cells with typical peripheral nuclei are seen, formed by the fusion of large epithelioid cells. Microscopic focal granulomas have been described in liver, tonsil, other lymph nodes and occasionally in kidney and lungs (Hines *et al.*, 1987; Clarke, 1997). In sheep, some advanced cases have granulomatous lesions with very few acid-fast bacilli. Clarke and Little (1996) graded all tissues by the mean number of bacteria per macrophage. Those graded from 0 to 1 were classified as "paucibacillary" and 2 to 3 as "multibacillary". In multibacillary tissues lymphocytic infiltration into the lamina propria is significant and aggregates of large macrophages and Langhans' giant cells with acid-fast rods can be seen. Paucibacillary tissues have far fewer acid-fast rods and there is mild infiltration of lymphocytes when compared to multibacillary tissues. Animals with a pigmented gut (ileum and jejunum) were usually multibacillary and no animal classified as paucibacillary had a pigmented gut. In mild infections, Langhans' giant cells are scattered in the villous lamina propria.

1.7. Diagnosis

1.7.1. Clinical signs

Infected animals are weak and debilitated. They show progressive weight loss and diarrhoea due to chronic enteritis. These signs are accompanied by a decrease in milk production and diffuse oedema (hypoproteinaemia), which ultimately results in the death of the animal. There are different diagnostic possibilities for Johne's disease especially in cattle (Table 1.3).

1.7.2. Staining of Faecal and Impression Smears

Faecal and impression smears of affected regions can be stained by using a hot staining technique such as Ziehl-Neelsen staining (ZN staining), also called acid-fast staining. Other staining methods used to identify *Mav* are cold staining methods, Kinyoun's staining and a fluorescence staining method called auramine-rhodamine staining. Ziehl-Neelsen staining is most widely used and it is the cheapest of all the methods (Somoskovi, 2001). *Mycobacterium avium paratuberculosis* smears stained by

Differential diagnostic disease	Signs
Bovine tuberculosis	Pulmonary lesions.
Intestinal parasites	Eggs and ova in faeces, diarrhoea.
Mucosal disease	Acute diarrhoea, oral lesions.
Left abomasal displacement	Severe colic, increased heart rate, diarrhoea.
Copper deficiency	Anaemia, hair loss, young animals, low Cu and Mo levels in animal.
Septicaemic diseases e.g. Salmonellosis	Increased temperature, acute diarrhoea.
Tumours of gastrointestinal tract	Post-mortem lesions and blood reports, dysentery.
Carbohydrate engorgement	Increased rumen size, respiratory rate, heart rate. Weak pulse.
Toxic conditions	Acute, dark, foetid, sticky diarrhoea.

Table 1.3 Differential Diagnosis of Johne's disease

ZN staining and observed under the light microscope appear as non-capsular, non-motile, non-spore bearing acid-fast rods (pink coloured rods on blue background), which occur in clumps or in groups of 4-10. However some non-acid-fast, lightly acid-fast and cell wall-deficient types are also encountered (Thorel *et al.*, 1990, Clarke 1997). Staining is not a definitive test, as there is every chance of false negative results. Usually in ZN staining cryptosporidial oocysts are observed and appear similar to clumps of 3 more cells of *Map*. A ZN stained section of tissue with cellular changes indicative of Johne's disease should be examined under oil immersion for a minimum of 10 minutes before reporting no evidence of acid-fast organisms.

1.7.3. Biochemical Tests

Characterisation of *Map* based on biochemical properties is difficult due to its low biochemical activity. Biochemical tests like urease, niacin, nitrate reduction, Tween 80 hydrolysis and tellurite reduction were negative and pyrazinamidase and catalase had varied results (Chiodini, 1986). However growth rate and mycobactin dependency are major criteria for positive identification of *Map*. Biochemical evaluations can only be used as supportive evidence (Chiodini, 1986).

1.7.4. Culture

Map was grown in enriched culture media by Twort and Ingram (1912), in which they included extracts from *M. tuberculosis* and *M. phlei*. Later, iron-chelating compounds were added to the culture medium once these compounds were identified as the essential ingredients for growth of *Map*. Detection of *Map* in culture media in conjunction with the presence of characteristic histopathological lesions is regarded as the gold standard test for the diagnosis of Johne's disease. One main disadvantage of the culture technique is that it requires long incubation periods of at least 8-16 weeks. Samples used for cultivation are faeces, milk, intestinal tissues, lymph nodes and foetal tissues (Queen and Russel, 1979; Whittington *et al.*, 1998). To decontaminate these samples various reagents like hexadecylpyridium chloride (HPC), sodium hydroxide, benzalkonium chloride and oxalic acid were used. The solid media used in the cultivation of *Map* are Herrold's egg yolk medium (HEYM), modified Lowenstein-Jensen medium (L-J medium) and liquid media such as Dubos broth and brain heart

infusion broth (BHI broth). The media is supplemented with antibiotics e.g. neomycin; tetracyclines; polymyxin B; nalidixic acid; trimethoprim; azlocillin and vancomycin and with antifungals such as amphotericin B or nystatin. Tween-80 is a surfactant, a supplement to be added to all the media, as it reduces the permeability of the *Map* cell wall, which enhances the growth rate (Masaki *et al.*, 1990). Each medium is supplemented with mycobactin-J (Jørgensen, 1982) Even though there are two types of culture systems; conventional and automated, decontamination of samples is common to both. Tissue samples are digested and centrifuged, then the sediment is treated with HPC, whereas faecal samples are suspended in sterile water and the supernatant is treated with HPC. Samples are then allowed to stand undisturbed for 18 hours at room temperature. The particles that settle to the bottom of the tube are used as the inoculum, and are removed by pipette without disturbing the supernatant fluid. The usual method of decontamination is to use 0.75% HPC; other methods involve oxalic acid and sodium hydroxide. HPC is relatively ineffective in controlling the growth of contaminating fungi. Hence, amphotericin B is added to control fungal overgrowth in inoculated media (Merkal & Richards, 1972). A smear from the sediment can be ZN-stained and observed. The sample after decontamination is used as inoculum by the culture systems.

1.7.4.1. Culture Systems

(a) Conventional Culture System

In this culture system, the inoculum is transferred to each of three slants of HEYM containing mycobactin and to one slant of HEYM without mycobactin. The inoculum is distributed evenly over the surface of the slants. The tubes are allowed to remain in a slanted position at 37°C for approximately 1 week with screw caps loose. The tubes are returned to a vertical position when the free moisture has evaporated from the slants. The lids are tightened and the tubes are placed in an incubator at 37°C. The slants are incubated for 15-20 weeks and observed weekly from the sixth week onwards. The egg in Herrold's medium contributes sufficient phospholipids to neutralise the bactericidal activity of residual HPC in the inoculum. The other media (Modified Dubos and Middlebrook) do not have this property. Due to loss of antifungal activity, storage of HEYM containing amphotericin B should be limited to 1 month at 4°C (OIE, 2004).

(b) Automated Culture System

(i) Radiometric System

This is a more rapid technique for the isolation of *Map*, with the use of a radiometric based detection system, the Bactec 460 system (Becton Dickinson, Oxford, UK). Bactec is highly automated, and is both faster and more sensitive than the conventional culture system. However, it is very expensive and the use of radioisotopes like ^{14}C (carbon) labelled palmitic acid makes it disadvantageous for use in routine diagnosis as disposal of radioactive materials is cumbersome, expensive and potentially hazardous. Growth of mycobacteria is measured by the release of ^{14}C labelled CO_2 from palmitate as a consequence of bacterial metabolism (Collins *et al.*, 1990).

(ii) Non-radiometric System

Recently, various fluorescence-based and other non-radiometric systems have been introduced. These are highly automated; sample cultures are incubated and evaluated simultaneously with results uploaded to a computer. To evaluate these cultures the medium is incorporated with different types of detector systems, which react to the alterations in oxygen, CO_2 or pressure within the sealed tube (Nielsen *et al.*, 2004). Severe problems were encountered during initial experiments on faecal samples, due to overgrowth by other bacteria (spore forms and fungi). However, these methods have been further developed and are now used with some success in many laboratories (OIF, 2004). The various non-radiometric systems available in the market are Bactec MGIT (Mycobacterial Growth Indicator Tube) 960 system and Bactec 9000 MB system (Becton Dickinson, UK), ESP system (Trek Diagnostic Systems Ltd, West Sussex, UK).

1.7.4.2. Colonial Morphology

The primary cultures on mycobactin egg yolk medium are small, smooth, moist, convex and non-pigmented colonies; similar colonial morphology is observed when subcultured on mycobactin-serum agar (Merkal and Curran, 1974). Once *Map* is isolated from infected animals using mycobactin egg yolk media, it can be cultured on a

variety of media (Merkal and Curran, 1974). *Map* when grown on HEYM shows small, smooth to slightly rough, opaque to whitish colonies (OIE, 2004). On L-J medium with sodium pyruvate, *Map* changes from dysgonic to almost eugonic. The colonies are flat and smooth with a slightly raised centre, which grows to form irregular papillae at later stages (Jørgensen, 1982). The use of pyruvate and egg yolk in the medium has the advantage of yielding bigger and more luxuriant colonies, respectively (Merkal and Curran, 1974; Jørgensen, 1982).

1.7.5 Cell-Mediated Immunity based Tests

(a) Johnin Skin Test

This test is an intradermal injection of Johnin, a purified protein derivative (PPD), which is given to the animal under test on the left side of the neck. The thickness of the skin at the injection site is measured 72 ± 2 h after injection with sliding callipers. Thickness of a skin fold 10 cm behind the injection site should also be measured as a control (control site). The increase in thickness is determined by subtracting skin thickness at the control site from skin thickness at the injection site (Kalis *et al.*, 2003). Thickness greater than 2mm is regarded as indicating the presence of delayed type hypersensitivity (DTH), and is regarded as positive in that animal (OIE, 2004). This is no longer widely used due to its poor sensitivity and specificity (de Lisle *et al.*, 1980). It is not as specific as the recent techniques and should not be used as per international animal health regulation for diagnosis or prepurchase testing of animals (Collins, 1996).

(b) Interferon gamma (γ) test

The assay is based on the identification of interferon gamma (IFN- γ) released from sensitised lymphocytes during an 18-36hrs incubation with specific antigen (OIE, 2004). Two methods have been developed to detect bovine IFN- γ ; (i) a bioassay method (Billman-Jacobe *et al.*, 1992), (ii) a sandwich enzyme immunoassay method (EIA) (Rothel *et al.*, 1990). The sandwich EIA is more sensitive and specific than the bioassay for detecting *Map* infected cattle and is available as a commercial kit (BOVIGAM, CSL Ltd., Parkville, Australia).

(c) Lymphocyte Stimulation Test

This test was mainly developed to differentiate cross-reacting pathogenic *Mycobacterium* spp., with non-pathogenic *Mycobacterium* spp., (Muscoplat *et al.*, 1975), but was later used for diagnosing cattle with *Map* (Johnson *et al.*, 1977). In this test lymphocytes were isolated and cultured. Their *in vitro* proliferation in the presence of Johnin PPD or the non-specific mitogen phytohaemagglutinin (PHA) was assessed by the degree of incorporation of tritiated methyl thymidine (³HTdR), measured as counts per minute (CPM) on a scintillation counter. Results were reported based on the Stimulation Index (SI), where SI >2.0 were considered positive (Johnson *et al.*, 1977). It was considered as a poor diagnostic indicator, as it should be repeated over period of several months (Lepper *et al.*, 1989)

$$SI = \frac{\text{CPM of antigen stimulated cultures}}{\text{CPM of control cultures}}$$

(d) Leukocyte Migration Agarose Test (LMAT)

In this test, blood leucocytes were mixed in a HFPES (N-2-hydroxyethyl-piperazine-II'-2-ethanosulfonic acid) buffered liquid medium containing Johnin and 20% inactivated horse serum. This cell suspension was incubated and made completely homogenous, then transferred to wells of an agarose gel plate. Control wells were also prepared and incubated again in a humidified atmosphere. Later cells were fixed at the bottom of the plate with a mixture of methanol, acetic acid and water. Once dry the agarose was removed and the diameter of the migration zone was measured to calculate Migration Index (MI). MI of < 0.80 is considered positive for *Map* (Bendixen, 1977).

$$MI = \frac{\text{radius of migration zone of antigen stimulated cells} - \text{radius of well}}{\text{radius of migration zone of control cells} - \text{radius of well}}$$

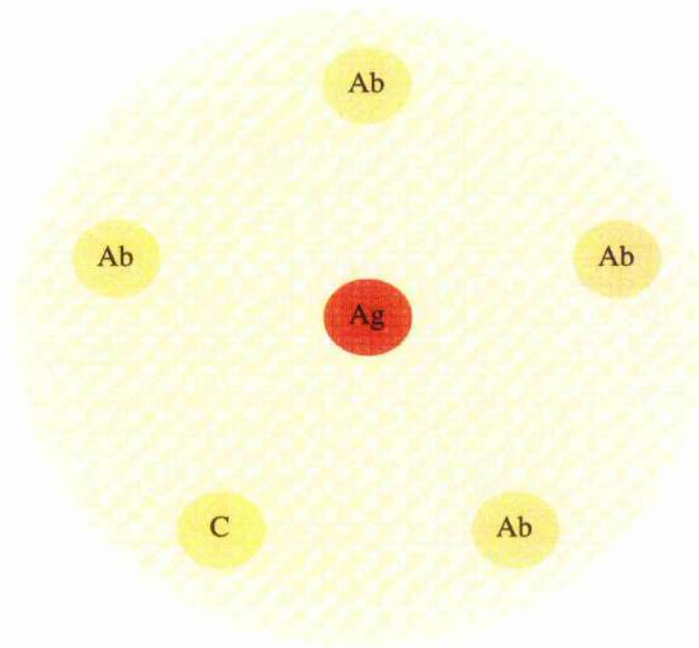
1.7.6. Serological Tests

(a) Agar gel immuno diffusion (AGID) test

The agar gel immuno diffusion test was as described by Merkal *et al.* (1968c) and Goudswaard and Terporten (1972), and was renamed as the ovine gel test by Whittington *et al.*, (2003b). Briefly, 1% agarose gel was prepared in a petri-dish in which six wells are made as shown in Fig. 1.2. The six outer wells are loaded with serum in which five are test sera and one is a positive control serum. Test antigen (mechanically disrupted cells of *Map* strain 316V, ovine test) is placed in the centre well. The plate is incubated at 37.8°C and read over indirect light. The results are recorded as positive when the line of precipitation is detected. The results are confirmed by retesting, in which line of precipitation detected should be confluent with the line produced by the positive control serum in an adjacent outer well. Lines of non-identity were recorded as negative (non-specific) reaction. This test has high specificity and its use varies with animal species, for example it is more widely used in sheep than cattle (Whittington *et al.*, 2003b). The use of an AGID test is highly recommended in animals in late pregnancy and/or those showing clinical signs of Johne's disease. However, AGID also acts as a confirmative test in clinically suspected animals. It has specificity of 100%, but sensitivity is only 26.6% (Sockett *et al.*, 1992)

(b) Complement fixation test (CFT)

Complement fixation testing (CFT) was described by early workers using a carbohydrate antigen (Annau, 1958). Twort and Ingram used CFT in diagnosis of Johne's disease as early as 1913. Although CFT is used extensively, as commented favourably by early workers the test lacks species specificity and is not very sensitive (Colgrove *et al.*, 1989). The sensitivity and specificity of CFT is better than AGID but poorer than the ELISA. The test works well on clinically suspected animals, but does not have sufficient specificity to enable its use in the general population for control purposes. CFT is often required by some cattle importing countries (OIE, 2004). A variety of CF test procedures are used internationally, but the OIE recommended method is the microtitre method in which an aqueous extract of bacteria (strain Map 316F) from which lipid has been removed is used as the antigen. Test sera are inactivated in the water bath at 60°C for 30 minutes and diluted at 1/4, 1/8 and 1/16. Positive and negative controls for the following should be included on each plate; antigen control, complement control and haemolytic system control. The amount of fixation is read by visual comparison with a standard (de Lisle, 1980). The titre of test



Ag represents antigen; Ab represents antibody; C represents control

Fig. 1.2 Agarose gel setup for AGID assay.

sera was given as the reciprocal of the highest dilution of serum giving 50% fixation. A reaction at 1/8 is regarded as positive. It has a specificity of 99%, but sensitivity is only 38.4% (Sockett *et al.*, 1992).

(c) Enzyme linked immuno sorbent assay (ELISA)

The ELISA is, at present, the most sensitive and specific test for serum antibodies to *Map*. Its sensitivity is comparable with that of the CFT in clinical cases, but is greater than that of the CFT in subclinically infected carriers. There are two types of ELISAs; direct ELISA and indirect ELISA; the indirect ELISA is the most widely used in the detection of *Map*. This test utilises an unlabelled primary antibody in conjunction with a labelled secondary antibody. Microwell plates are coated with a sample containing the target antigen, and the binding of labelled secondary antibody with unlabelled primary antibody is quantitated by a colorimetric, chemiluminescent, or fluorescent end point. This has been slightly modified and termed as an indirect absorption ELISA (see below). This was later modified by different researchers and developed into a commercial kit (Milner *et al.*, 1990; Cox *et al.*, 1991), which was later evaluated by Ridge *et al.* (1991) (Table 1.4).

The absorption ELISA combines the sensitivity of ELISA and improves its specificity with an additional absorption step. The serum samples to be tested were diluted with buffer containing soluble *M. phlei* antigen. This procedure eliminates non-specific cross-reacting antibodies, thereby increasing the specificity of the ELISA (Collins *et al.*, 2005). Milk and serum are used as antibody sources whereas LAM is used as an antigen (Jark *et al.*, 1997), hence their names Milk ELISA, Serum ELISA and LAM ELISA respectively.

Four commercial ELISA kits are available for *Map* serum antibody detection. All kits come with all necessary reagents, positive and negative control sera, and interpretation criteria: 'HerdChek[®] *Mycobacterium paratuberculosis* Antibody ELISA kit' (IDEXX Laboratories, West Yorkshire, UK); 'ParaChek[®] Indirect enzyme immuno assay' (Prionics AG, Schlieren, Switzerland); SERELISA ParaTB, Synbiotic Corp., San Diego, CA are licensed by the U.S. Department of Agriculture (USDA); lastly, a kit produced in France, ELISA Paratuberculosis, (Institut Pourquier, Montpellier, France). All antibody assays, except SERELISA, use a serum absorption

Animals	Cases	sensitivity	specificity
Cattle	clinical cases	88.2% ^a	99.8% ^a
	subclinical cases	48.8% ^a	
Sheep	clinical and subclinical cases	35-54% ^b	98.2%-99.5% ^b

^a Ridge et al. 1991; ^b Hope et al., 2000

Table 1.4 Evaluation of ELISA

step to remove antibodies that cross react with *Mycobacterium phlei*, a procedure demonstrated to increase *Map* ELISA specificity.

1.7.7. DNA probes

The discovery of insertion sequence (IS) elements led to the diagnosis of *Map* using DNA probes. The insertion sequence elements are small, mobile genetic elements, containing only genes related to insertion functions; their location within structural genes causes insertional mutations (Green *et al.*, 1989). In 1989, Green and colleagues have exploited the *Map* genome and identified a specific genetic insertion sequence, IS900, which was the first IS element to be found in a mycobacterium and consists of 1415bp. These DNA probes aid in the diagnosis of *Map* by enzymatic amplification of DNA using the polymerase chain reaction (PCR) (Vary *et al.*, 1990). DNA probes have been used to distinguish between *Map* and other mycobacteria, especially those of the *M. avium* group. Commercial diagnostic kits Parath and Parath Realtime Tests (Adiavet) based on the detection of IS900 sequences by PCR have been developed (Adiagène labs, Zoopole, Bruz Cedex, France).

1.7.8. Polymerase Chain Reaction assay (PCR)

The Polymerase Chain Reaction was developed by Mullis in 1983 for which he won the Nobel Prize for chemistry. This invention revolutionised genetic studies drastically. The PCR is covered by patents, one of the reasons to be an expensive assay. The Polymerase Chain Reaction is based on the amplification of a short specific DNA template that lies between two regions of known DNA sequence. It requires a template DNA which is to be amplified; two oligonucleotide primers which are short, single-stranded DNA molecules complementary to the ends of a defined sequence of DNA template; DNA polymerase which copies the region to be amplified; deoxynucleotriphosphates (dNTPs which includes dATP, dGTP, dCTP, dTTP) which acts as building blocks for new DNA strands synthesized by DNA polymerase; Lastly buffer and temperature conditions, which provide a suitable environment for the DNA polymerase to extend the primers to synthesize a new complementary strand. The DNA polymerase at this stage has synthesized a double-stranded DNA molecule. A new strand can again be synthesized by heat denaturation of this double-stranded DNA.

Annealing of primers is by cooling the mixture and primer extension is again by DNA polymerase at a suitable temperature for enzyme reaction. Each repetition of strand synthesis comprises a cycle of amplification. The thermal cycler is a machine designed to run the polymerase chain reaction, which is programmed for an initial denaturation followed by annealing and then extension of primers; these steps are repeated for 25-40 cycles, (Table 1.5) as required for the specific application. Thus a complementary DNA strand is synthesised. PCR products can be detected and analysed depending on the information required; the presence/absence of the target DNA; the length of amplified fragment; quantification of PCR product or sequence analysis. Analysis of the PCR products of DNA is mostly done either by gel electrophoresis or southern blot techniques.

In 1990, Vary and his colleagues used IS900 insertion sequence in the PCR assay. The IS900 PCR assay of faeces is highly specific, as well as sensitive, when faecal shedding is frequent (Thoresen and Saxegaard, 1991; Sockett *et al.*, 1992). Later, other insertion sequences *hspX*, L1/L9 integration sequences and F57 have been evaluated for *Map* (Rajeev *et al.*, 2005). IS900 is present in multiple copies (14-18) in the *Map* genome and is a commonly used target. Reports on the uncertainty of specificity of the IS900 insertion sequence (Cousins *et al.*, 1999) have led to some controversy. More research is it needed to clarify their utility. One drawback of PCR assay is that it detects the DNA of both viable and non-viable organisms.

1.1.7.9 Real-time PCR

The real-time PCR assay is based on the detection and quantitation of a fluorescent dye (Lee *et al.*, 1993; Livak *et al.*, 1995). This signal from the dye increases in direct proportion to the amount of PCR product in a reaction. The amount of fluorescence emitted is recorded at each cycle and is possible to monitor the entire PCR reaction. During the exponential phase of fluorescence detection, the first significant increase in the amount of PCR product correlates to the initial amount of target template. The sooner a significant increase in fluorescence is detected, the higher the starting number of copies of nucleic acid. A significant increase in fluorescence above the baseline value measured during the 3-15 cycles indicates the detection of accumulated PCR product. The procedure was explained in later Chapters. The development of real-time PCR assay helped researchers to completely exploit the nucleic acids, especially the levels of these nucleic acids in various tissues. The results

Step	DNA polymerase activation		PCR			PCR Final Step
	Hold	Denature	Anneal	Extend	Hold	
Two temperature thermal cycling (temp for annealing and extension are same)						
Temperature	95°C	95°C	60-70°C*			72°C
Time	5 min [†]	95°C	60sec/kb			7 min
Three temperature thermal cycling (temp for annealing and extension are different)						
Temperature	95°C	95°C	37-65°C*	72°C		72°C
Time	5 min [†]	95°C	15 sec	60 sec/kb		7 min

*Adjust the temperature according to the primer melting temperature.

† Adjust time according to desired initial enzyme activation.

Table 1.5 Types of Thermal Cycling

can be extrapolated for rapid quantitative estimation of microbial load in various tissues and other sources of infection (O'Mahony and Hill, 2004).

Real-time PCR assay using molecular beacons can detect *Map* in faeces rapidly by giving more sensitive and specific results when compared to conventional PCR and culture techniques (Fang *et al.*, 2002). In 2002, Kim and others developed a real-time PCR assay using *TaqMan* probes for the detection of *Map*. This IS900 *TaqMan* assay was 100-1000 times more sensitive than the conventional PCR with a detection limit of 1CFU (colony forming units) per reaction (Kim *et al.*, 2002). Moreover, real-time PCR assay when coupled with automated culture systems is useful in the detection of viable organisms.

1.8 Control of Johne's disease

The control of Johne's disease in animals is challenging due to various factors. The subclinical form of this disease presents one of the major difficulties, since the affected animal spreads infection without exhibiting any clinical signs. No routinely used diagnostic technique currently available can detect the subclinical infection, especially in large herds where the problem is severe. Although cell-mediated and PCR techniques can detect early infections, they have their own disadvantages. Moreover, early detection of Johne's disease in a herd can be delayed due to lack of awareness by the farmer. An effective vaccine has not yet been developed, though OIE in its 2004 report described a vaccine for Johne's disease which results in a decrease in the rate of faecal excretors when compared with vaccinated and non-vaccinated animals. There is usually good control of clinical disease, but a reduced level of subclinical infection persists (OIE, 2004). Transmission from wildlife has been reported and control in wildlife is a not an easy task, until an effective vaccine is developed. The minimal control measures which can be followed in domestic ruminants include establishing check points at various levels of transmission, annual herd screening, identification of faecal shedders, quarantine of newly acquired animals and bringing in disease free replacement stock. In Australia Johne's disease is endemic, and it launched a programme called the National Johne's Disease Control Program (NJDGP). A policy of zoning on the basis of disease prevalence was adopted using which Johne's disease is controlled effectively in the livestock industry of Australia (Animal Health Australia, 2007). The control programme is performed by demarcating the areas as residual,

control, protected and free depending on the level of disease and the control measures that are followed. In UK, there are currently no such control programmes, but strict surveillance is performed and affected animals are slaughtered (DEFRA, 2007). In Sweden the whole herd is culled if there is any evidence of paratuberculosis. In Spain, some regional authorities ask for certificates to guarantee that cattle, sheep and goats imported into the region are free of paratuberculosis (SAC, 2000).

1.9 Public health importance

In recent years, the increasing reports of isolation of *Map* from Crohn's disease patients, bulk milk samples of dairy cows and recently from muscle tissue of dairy cows (Bosshard *et al.*, 2006; Grant *et al.*, 2002) has raised serious concerns for public health. Because of *Map*'s wide host diversity, the risk of environmental contamination has increased. These environmental contaminations spread through other suspected routes like drinking water, (Whan, 2001) which increases risk through consumption of food. Crohn's disease is a chronic inflammatory disease of humans that primarily affects the intestinal tract. The aetiology of this disease is not known, but various factors have been proposed which include *Map* and a variety of viruses and bacteria, also immune reactions to normal commensal intestinal bacteria. A report by the UK Food Standards Agency (Rubery, 2001) mentioned that Crohn's disease was first reported by Dalzell in 1913 who proposed *Map* as the causative agent. Later Crohn and his colleagues in 1932 described the pathology and reported a series of cases, thus the disease got its name. In early days isolation and culture of *Map* was difficult, but improved culture and DNA technologies increased its detection in Crohn's disease patients. Crohn's disease resembles Johne's disease in some aspects of pathology and clinical signs. However, studies to date have not determined whether *Map* has a causative role, but at the same time it cannot be ruled out.

1.10 Economic importance

The annual economic losses due to animals affected with Johne's disease are estimated to be from \$250 million to 1.5 billion in USA (Ott *et al.*, 1999; Stabel, 1998). In UK, annual economic losses in various animals affected with *Map* are £9.1 million and £3.1 million in dairy and beef cattle respectively; a range of £0.4 -36 million in

sheep; £0.42 ± 0.11 million in goats. Currently Johne's disease has minimal impact on the economy of the UK in live animal trade, especially with EU countries (SAC, 2000). Australia which is a major exporter of animal products like wool was also facing huge economic losses of A\$52.7 millions through sheep alone (Hassall *et al.*, 2003). Increases in Johne's disease cases over the past years will also increase these economic losses.

1.11 Discussion

The growing incidence of Johne's disease worldwide is a major concern in terms of animal and human health, global economics and trade. As *Map* has been identified as the cause of this disease, increased reports of its isolation from a wide host range including domestic ruminants, wildlife and humans make it of great concern. As per reports, entry of *Map* into the food chain and environment through milk, water through farm waste and etc (Sweeney, 1996; Ott *et al.*, 1999; Grant, 2005) is a public health issue. Once an animal is infected with *Map*, the organism can spread into its surrounding environment and to the rest of the herd. The family *Mycobacteriaceae* are rugged microbes; they are very much resistant to extreme environments because of their thick cell wall, as a result it is difficult to completely eliminate these organisms. Thus, animals and their environment should be protected by different means, to minimise contact with *Map*. One such method of prevention/control measure is early detection of *Map*, especially when bringing in new stock from other farms, a major route of herd transmission. So detecting *Map* sufficiently early could prevent this infection from spreading rapidly.

The present study highlights the diagnostic aspect of Johne's disease by detecting *Map* in faeces and various tissue samples using a real-time PCR assay. The early detection of *Map* in Johne's diseased animals has been a major problem since it was first described. Many diagnostic tests have been developed to detect *Map* at an early stage. Out of these the earliest detection method involves observing the cell-mediated immune response, which is the first and strongest immune response (Collins, 1996). However, cell-mediated responses have their own disadvantages like cross-reactivity with environmental mycobacteria (Collins, 1996). Staining of faecal smears was practised ever since the disease was first detected, but faecal shedding of *Map* is below the levels of detection up to the clinical stage of infection (Whitlock and

Buergelt, 1996). The growth of *Map* is slow by conventional techniques requiring 12–16 weeks or longer (Collins, 1996). Serological tests such as CFT, AGID and ELISA, depend on antibody production, which occurs late in the course of infection (Collins, 1996). Hence animals cannot be diagnosed early, during silent infection.

The real-time PCR assay was very sensitive in detection of *Map*, when compared to ELISA which is widely used at present. The real-time PCR assay is relatively simple and robust, and results can be achieved within 24hrs (Khare *et al.*, 2004). Even though there are several diagnostic techniques for detecting *Map*, most of them are specific but none of them are as sensitive as real-time PCR. Furthermore, real-time PCR significantly reduces the time and costs when compared to standard bacteriological culture techniques, making it very practical for the diagnosis of Johne's disease. Detecting *Map* by culture is considered definitive for the diagnosis of Johne's disease, but it is only approximately 50% sensitive even though it is 100% specific (Collins, 1996). The loss in sensitivity may be due to the chemical treatment steps before culture, which will adversely affect the viability of *Map* (Bogli-Stuber *et al.*, 2005), or due to tendency of clumping which makes a non-homogenous distribution of bacteria and inaccurate enumeration (O'Mahony and Hill, 2002; Christopher-Hennings, 2003). The real-time PCR assay is a far more advanced and sensitive technique than the cell-mediated test for the detection of interferon gamma (γ) (Collins, 1996). Presently, ELISA is a more widely used rapid diagnostic test than AGID and CFT because ELISA is analytically more sensitive. Its sensitivity is as low as 15% in low-level faecal shedders and as high as 87% in animals showing clinical signs (Collins, 1996); specificity ranges from 98.2–99.8% (Ridge *et al.* 1991; Hoop *et al.*, 2000). Faecal shedding of *Map* is high in the animals showing clinical signs and can exceed 10^{10} /gram faeces (Bogli-Stuber *et al.*, 2005), so at this stage most of the diagnostic tests like ELISA are effective. To get more specific and sensitive results, molecular techniques like PCR are one step ahead. Both conventional PCR and real-time PCR have 100% specificity, their sensitivity range varies from 93-100% and 85-100% respectively (Christopher-Hennings, 2003). Out of these, real-time PCR is much superior to conventional PCR, as results are obtained rapidly with higher throughput because reactions can be set up in a 96-well plate and post-PCR analysis is obtained from a computer. Also, DNA contamination is minimised in real-time PCR as tubes are never opened for post-PCR analysis unlike southern-blotting procedures. Results stored on a computer can be analysed for further quantification to determine bacterial load in

samples. Real-time PCR has potential to detect 4 fg (femtogram) of *Map* specific DNA. Theoretically a *Map* cell contains 6.8 fg of DNA, after extraction losses it is adjusted to 5.1 fg (Ravva and Stanker, 2005). Thus, it can detect even 1CFU/reaction (Kim *et al.*, 2002), and can assist in early detection of *Map* infected animals.

The objective of this study was to improve rapid and early diagnosis for Johne's disease by improving the specificity and sensitivity *Map* in various field samples of real-time PCR.

CHAPTER II

GENERAL MATERIALS AND METHODS

2.1 Introduction

The materials and methods described in this Chapter are those used in the examination of the cases suspected of Johne's disease in this study. Detailed methods used for the individual studies are described in the Chapters concerned. The evaluation and standardisation of the real-time PCR was a major part of the project and is described in Chapter 4.

2.2 Selection of cases

Cattle and sheep which were suspected on clinical grounds or confirmed positive for Johne's disease by ELISA were purchased by the Division of Animal Production and Public Health, Faculty of Veterinary Medicine, University of Glasgow. The cases were purchased for teaching purposes and confirmed as having Johne's disease either by ZN stained faecal smears or ELISA. Most cases were ZN positive and were later confirmed as Johne's disease by post-mortem (PM) examination. Cases diagnosed as or suspected of being Johne's disease were examined clinically before post-mortem and samples were taken at post-mortem examination for this study.

2.3 Sample collection

Samples were collected by the author in the post mortem room of the Faculty of Veterinary Medicine, University of Glasgow, UK, except for the faecal samples which were collected before slaughtering the animal. Collection of faeces from cattle was performed by rectal pinch, where the hand is passed deep into the rectum and faeces is collected by pinching along with some mucosal tissue. Occasionally, smears were made on the spot, taking pinched mucosa and smearing it over the slide for immediate examination. All other samples were collected in an aseptic environment, using sterile instruments. The list of samples collected from cattle and sheep is given in Table 2.1 and Table 2.2. Blood samples were collected in 15% tripotassium ethylenediamine tetra-acetic acid (K3E) vacutainer tubes (Becton Dickinson and company, Oxford, UK) with the assistance of clinical scholars. Tissue samples were collected in 7mL polystyrene bijoux tubes (Bibby Sterilin, UK). Mammary secretions

Samples	210444	210716	210717	211253	212260	212261
Faeces	C	C	C	C	C	C
Ileal mucosa	U	C	C	C	C	C
Blood	C	C	C	C	C	C
Lymph Nodes						
Mesenteric	U	C	C	C	C	C
Ileocaecocolic	U	C	C	C	C	C
Iliac	U	C	U	C	C	C
Precapular	U	U	U	U	C	C
Retropharyngeal	U	C	U	C	C	C
Popliteal	U	C	U	U	C	C
Supra mammary	U	C	U	C	C	C
Tonsil	U	C	U	C	C	C
Mammary Secretions	U	C	C	U	C	U
Mammary tissue	U	C	U	C	C	C
Uterus	U	C	C	C	C	U
Liver	U	U	U	C	C	U
Spleen	U	U	U	C	C	U
Kidney	U	U	U	C	C	U
Muscle	U	U	U	C	C	C
Ileocaecal valve	U	U	C	U	C	U

C collected samples, U unable to collect

Table 2.1 Samples collected from suspected/diseased cattle

Samples	209942	210552	210608	211056	212384
Faeces	C	C	C	C	C
Ileal mucosa	C	C	C	C	C
Blood	C	U	C	U	U
Lymph Nodes					
Mesenteric	U	U	C	C	C
Ileocaecocolic	U	U	U	U	C
Iliac	U	U	C	U	C
Prescapular	U	U	C	U	C
Popliteal	U	U	U	U	C
Supra mammary	U	U	U	U	C
Mammary Secretions/ Milk	U	U	U	U	C
Mammary tissue	U	U	C	U	C
Uterus	U	U	C	U	C
Liver	U	U	C	U	U
Spleen	U	U	C	U	U
Kidney	U	U	C	U	U
Muscle	U	U	C	U	C
Any other samples	U	U	#	U	U

Foetal Samples: F. membranes, F. fluids, F. intestines, F. muscle, F. spleen, F. Amniotic fluid
 C collected samples; U unable to collect

Table 2.2 Samples collected from suspected/diseased sheep

were collected from the cistern of the mammary gland using sterile syringes (Becton Dickinson and company, UK). The necrosed medullary region in lymph nodes and the mucosa from the rugae of the pathognomonic lesion in intestine (distal ileum/jejunum) were collected. Faecal smears and intestinal impression smears were also made using clean dry glass slides. All samples were labelled appropriately. Samples collected from the post-mortem room were brought to the lab. Tissues samples were further processed into pieces of 10-30mg and transferred into 1mL cryotubes (NUNC A/S, Denmark) under aseptic conditions. Faeces and milk samples were also transferred into cryotubes and all samples were kept at -80°C for later use. Blood samples were further processed to extract leucocytes and stored at -20°C , see section 2.4.3.1. Samples were submitted routinely to Veterinary Diagnostic Services of University of Glasgow for haematology, biochemistry, microbiology, parasitology and pathology by the veterinary surgeon in charge for clinical purposes. Blood samples were routinely sent to SAC Veterinary Services, Inverness for the diagnosis of Johne's disease. Serum antibodies to *Map* were detected by ELISA. The results of this test were used to determine whether animals were Johne's disease positive or negative.

2.4 Acid-fast staining

Faecal smears were prepared based on the consistency of the faeces. If the faeces were watery, a loopful of faeces was placed on the slide and a thin smear was prepared. If the faeces were pelleted, a loopful of sterile water was placed on the slide and using sterile loop the outer edge of the pellets were scrapped and mixed with water placed on the slide to make a thin smear. Smears of ileal mucosa collected from the animals were prepared by gently rubbing the ileal mucosa over the slide. All smears were stained by Ziehl-Neelsen's method as described by Quinn & Carter, (1994). The smears were initially heat fixed over the flame for a few seconds and then stained by placing the 1% carbol fuchsin over the slide and steaming it for 10 minutes, then washed under running tap water. Differentiation was carried out using 3% acid alcohol for 15 minutes, and the slide was then washed under running tap water. The smear was then counterstained using 1% Loeffler's Methylene Blue for 20secs and again washed under running tap water. The smear was allowed to dry and observed under oil immersion at 1000X magnification.

2.5 Histopathology

At necropsy, samples from intestines and lymph nodes were collected as the primary sites for confirmation of the diagnosis by histopathology. Samples of full thickness of approximately 5mm width were taken from the intestinal wall (distal ileum/jejunum). The local mesenteric lymph nodes were excised and a 5mm thick cross section was taken. Samples were fixed in 10% neutral buffered formalin for 24 hours before undergoing routine histological processing using a Shandon Excelsior automated processor in the histopathology laboratory of the Division of Pathological Sciences. These dehydrated samples were then embedded in paraffin wax using a Sakura Tissue-Tek TEC histoembedder and cut at 5 micrometer thickness with a Shandon Finesse microtome before being stained with haematoxylin & eosin and by the Ziehl-Neelsen method for acid fast bacteria. All sections were evaluated using an Olympus BH-2 light microscope.

2.6 Extraction of genomic DNA from samples collected

(a) Faeces

DNA extraction from faeces was performed using the QIA amp[®] DNA stool mini kit, (QIAGEN Ltd, Crawley, UK). 200mg of solid faeces was aliquoted into a 2mL safe-lock microcentrifuge tube (Eppendorf AG, Germany). To this tube 1.4mL of buffer ASL was added and then vortexed (Vortex Genie2, Scientific Industries Inc, USA) for 1 minute until homogenised. The suspension was heated on a heat block for 20 minutes at 95°C and sonicated for 8 minutes followed by centrifugation (Eppendorf 5415 D, Eppendorf AG, Germany) at 15304 ×g for 1 minute to pellet faecal particles. The sonication step was done to disintegrate and homogenise the faecal matter, this step is added to increase the amount of DNA. A volume of 1.2mL supernatant was pipetted into a 2mL safe-lock microcentrifuge tube (Eppendorf AG, Germany), and the pellet was discarded. One inhibitex tablet (provided with the kit) was added to the supernatant which was then vortexed immediately and continuously for 1 minute at room temperature. The mixture was then incubated for 1-2 minutes before centrifugation at 15304 ×g for 5 minutes. The supernatant was then placed into a fresh 1.5µL safe-lock microcentrifuge tube and centrifuged as before. Two hundred microlitre of this

supernatant was then added to 15 μ L of proteinase-K previously placed into a fresh 1.5 μ L safe-lock microcentrifuge tube. A 200 μ L volume of buffer AL was then added, and the mixture vortexed for 15sec, prior to incubation for 10 minutes at 70°C followed by centrifugation at 15304 \times g for 30sec to remove all drops from inside the tube lid.

A volume of 200 μ L 96-100% ethanol was then added and the mixture vortexed for 15sec, followed by centrifugation for 30sec, to remove all drops from inside the tube lid. The centrifuged mixture was then carefully applied to the QIA amp spin column in a 2mL collection tube, the cap was closed and the tube was centrifuged at 15304 \times g for 1 minute. The 2mL tube containing the filtrate was discarded, and the QIA amp spin column was placed in a new 2mL collection tube. The QIA amp spin column was carefully opened and 500 μ L of buffer AW1 was added before centrifugation for 15304 \times g for 1 minute. The filtrate in the 2mL tube was poured off and the mouth of the tube was blotted, and the QIA amp spin column was placed in the same 2mL collection tube. Five hundred microlitre of buffer AW2 was then added to the spin column and it was centrifuged for 1minute, after which the 2mL tube containing the filtrate was discarded. The QIA amp spin column was now placed in a fresh 2mL collection tube, and centrifuged for 10 minutes, the additional spin was done to remove any left over buffers, which actually interact with the elute DNA. Finally, the QIA amp spin column was transferred into a new 1.5mL safe-lock microcentrifuge tube, 50 μ L of buffer AE was added and then incubated for 1minute followed by centrifugation for 1minute to elute DNA. Volume of AE buffer was changed to concentrate the final DNA concentration. Eluted DNA was stored at -70°C for later use.

(b) Tissues

DNA extraction from tissues was performed using the QIA amp @ DNA mini kit, (QIAGEN Ltd, UK). 25mg cut tissue was placed in a 1.5mL safe-lock microcentrifuge tube. To this tube 180 μ L of buffer ATL was added, followed by 20 μ L of proteinase K; the mixture was then vortexed for 1 minute until homogenised. Subsequently, the suspension was incubated at 56°C for 1.5hr until the tissue lysed completely. The suspension was vortexed again for 15sec followed by centrifugation at 15304 \times g for 30sec to remove all drops from inside the tube lid. Next, 200 μ L of buffer AL was added to this suspension then vortexed for 15sec. This mixture was incubated at 70°C for 10 minutes followed by centrifugation at 15304 \times g for 30sec to remove all

drops from inside the tube lid. The procedure from here was as described above in Section 2.5.1, except that 50 μ L AE buffer was added to elute DNA.

(c) Milk, Blood, WBC, etc

A volume of 20 μ L proteinase K was placed in a new 1.5 μ L safe-lock microcentrifuge tube to which a 200 μ L sample of milk, whole blood, plasma, serum, body fluids, or up to 5 \times 10⁶ lymphocytes in 200 μ L PBS was added, followed by 200 μ L buffer AL. The mixture was then vortexed for 15sec and incubated at 56°C for 10 minutes followed by centrifugation at 15304 \times g for 30sec. The procedure from this point was as described above in Section 2.5.1, except that 50 μ L AE buffer was added to elute DNA.

2.7 Extraction of leucocytes from whole blood samples

Ten millilitre of blood samples were collected, and were aliquoted into 5 universal containers (30mL) (Bibby Sterlin, UK). 10mL of ammonium chloride lysis buffer was added to all the tubes and mixed gently and incubated for 5-10 minutes at room temperature until RBC lysis was complete. All the tubes were centrifuged at 228 \times g for 10 minutes. The supernatant was discarded and the WBC washed three times using phosphate buffer saline (PBS), by centrifugation at 514 \times g for 5 minutes. WBC count was made using a haemocytometer and recorded. Aliquots of 5 \times 10⁶ lymphocytes were pelleted and stored at -20°C for later use.

2.8 Discussion

In this study, the collection and processing of samples was done carefully and strict aseptic conditions were maintained all through. Asepsis is particularly important to sampling for real-time PCR because of the sensitivity of PCR techniques used. The effectiveness of aseptic techniques used is described in Chapter 5 where the results of the real-time PCR are presented. Although the methods described here were carried out for most cases, consistent sample collection was not performed on every case for various practical reasons. Where sampling could not be carried out is indicated in the results.

In this study, DNA extraction was performed using a commercially available stool kit, the use of a commercial kit format results in better removal of PCR inhibitors and a greater amount of DNA with less possibility of carry-over contamination, leading to more accurate results (Christopher-Hennings, 2003). In initial extractions the results suggested that low amounts of DNA were being extracted. Later, some additional steps were added to this method in order to extract more DNA as mentioned in the manual of Artus[®] M. paratuberculosis PCR kit by QIAGEN, Hamburg (March, 2006).

These materials and methods described here and used for all the cases were adopted following initial familiarisation with the method and the adoption of minor modifications to those previously published. Modifications have been indicated in the text.

CHAPTER III

RESULTS – CLINICAL AND PATHOLOGICAL EXAMINATION OF SUSPECTED CASES

3.1 Introduction

This Chapter describes the results obtained from the cattle and sheep cases of suspected Johne's disease used in the study. The results of the real-time PCR examinations are described in Chapter 5 and are informed by the results presented here. The materials and methods used in the Chapter were described in Chapter 2.

3.2 Clinical data and examination

A total of 11 cases of animals with suspected Johne's disease were examined, of which 5 were sheep cases and 6 were cow cases. The case history of animals used in this study revealed that more than 80% were from farms with a history of Johne's disease.

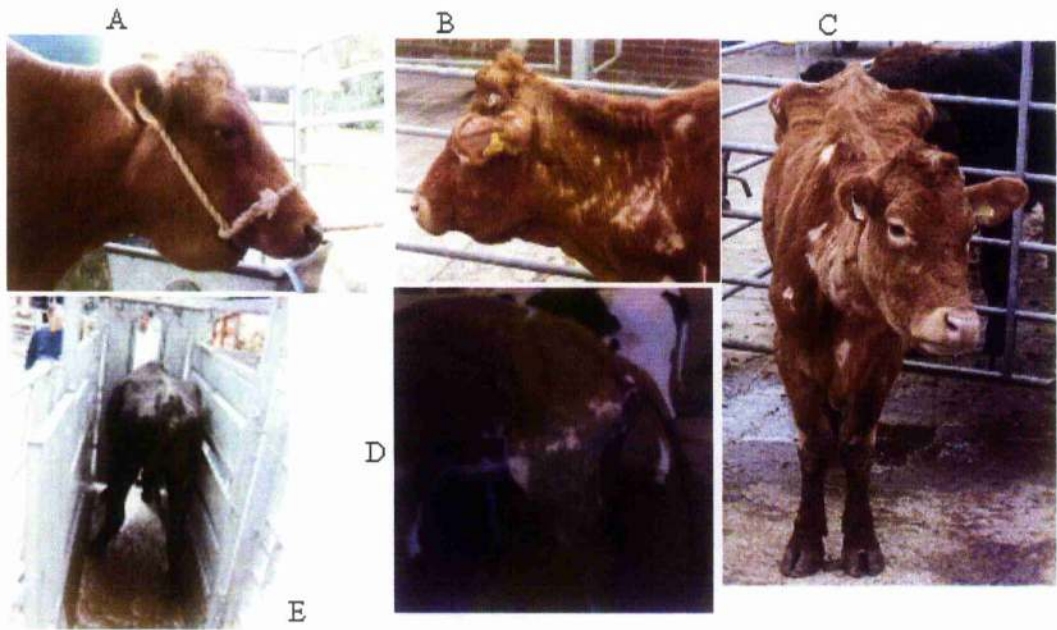
The cows used in this study were aged 4–8 yrs and had common symptoms of chronic diarrhoea, alopecia, chronic wasting and anaemia (Fig. 3.1; Table 3.1). 4/6 of the cases showed submandibular oedema but it was an inconsistent finding and none showed any signs of pyrexia. Strongyle eggs were demonstrated in 4/6 of cases. The reports of Case 212260 had confirmed that the animal was positive for salmonellosis.

The sheep used in this study were aged of 3-4 yrs and showed signs of alopecia, severe anaemia and chronic wasting (Table 3.2). Often they suffered from intermittent diarrhoea which was pasty in consistency, 3/5 showed signs of diarrhoea. The cases presented with a "stary" hair coat and a very poor body condition where most of the vertebral bones and ribs could be palpated. A parasitic burden was demonstrated in 4/5 cases, of which 2 Cases (209942, 210608) had *Moniezia* eggs and 2 Cases (211056, 212384) had strongyle eggs. Case 212384 appeared to have *Pasteurella pneumonia*, which was later confirmed. No blood samples were sent for ELISA testing due to economical constraints.

One common finding observed from the clinical pathology reports from both cattle and sheep was that all Johne's disease positive cases had decreased blood calcium levels (hypocalcaemia).

3.3 Post-mortem examination

Post-Mortem examination revealed that most bovine cases had common gross lesions such as thickened distal ileum/jejunum, enlarged lymph nodes a



A shows submandibular oedema; B shows alopecia; C shows emaciation with rough, 'stary' hair coat; D severe straining with diarrhoea; E chronic diarrhoea

Fig. 3.1 General clinical signs of cattle observed in different cases

Case.Nos	Age	Breed	Body Condition Score	Wasting	Diarrhoea	Oedema	Alopecia/ Rough hair coat
210444	8yrs	Sim X	1	++	++	+	++
210716	5yrs	Lim	1	++	+	+	++
210717	4yrs	Lim	1	++	+	n	++
211253	6yrs	Lim X	1.5	+	++	++	++
212260	5yrs	HF	1.5	+	+	+	+
212261	6yrs	HF	1.5	+	++	n	+

+ mild; ++ severe; n not observed; Sim X Simmental cross; Lim Limousin; Lim X Limousin cross; HF Holstein Friesian.

Table 3.1 Clinical findings in cattle

Case.Nos	Age	Breed	Body Condition Score	Wasting	Diarrhoea	Oedema	Alopecia/ Rough hair coat
209942	3	Mule ewe	1	++	-	n	÷
210552	4	SBF	1	++	p	-	++
210608	4	SBF	1	+	p	-	+
211056	3.4	SBF	1	n	n	n	n
212384	3	CB	1	++	p	-	++

- negative; + mild; ++ severe; n not observed; p pasty faeces; SBF Scottish Black Face; CB Cross Breed.

Table 3.2 Clinical findings in sheep

lymphatic cording, depending on the degree of infection. The exception was Case 210444, which had poor body condition with bottle jaw, emphysema and multiple nodulation of the abomasum, and the intestines were slightly thickened with a granular appearance. On gross pathology this case was negative for Johne's disease. Other gross lesions were observed in individual cases, e.g. Case 210716 had bottle jaw, anasarca, oedematous intestines with mild pleurisy and liver damage; Case 210717 had severe oedema of the abomasal folds along with a thickened and an ulcerated abomasum, oedema of the mesenterics, fibrous pleural adhesions of the cranial lobes of the lung; Case 212260 had a thickened caecum with some haemorrhagic areas. (Table 3.3)

Based on the degree of infection ovine cases had gross lesions such as thickened distal ileum/jejunum, enlarged and necrosed lymph nodes and lymphatic cording, upon post-mortem examination. Gross lesions observed in individual cases were; Case 209942 had patchy orange pigmentation of the intestines (Fig. 3.2; Table 3.3), lymphatic cording and mild consolidation of the lungs; Case 210552 had pigmented intestines; Case 210608 had dead foetuses (Fig. 3.3), ascitic fluid with fibrous strands, consolidated lungs with an occasional focal abscess. At post-mortem examination the uterus was handled carefully and was examined separately in aseptic conditions, which further revealed twins inside the uterus. Different samples were collected from these foetuses aseptically. Case 211056 had pigmented intestines, gelatinous oedema of the mesentery and lymph nodes and catabolism of fat; Case 212384 had slightly pigmented intestines and lungs severely affected with pneumonia.

During post-mortem examination, no gross pathological lesions were observed in visceral organs like liver, spleen, kidneys, also in uterus, mammary gland, and muscle tissue.

3.4 Microscopic examination

3.4.1. Faecal smears

Two sets of faecal smears were prepared, one before PM and the other at the time of PM. The positive smears had *Map* clumps stained in pinkish red with blue background. The results of faecal smears from both cattle and sheep after ZN staining are given in Table 3.4. Careful observations were made to avoid false positive results obtained with cryptosporidial oocysts which look similar to the clumps of *Map*.

Case.Nos	Ileum		Lymph nodes		Lymphatic cording
	Thickened	Pigmented	Enlarged	Necrosed	
Cattle					
210444	+	-	-	-	-
210716	++	-	0	0	0
210717	++	-	0	0	0
211253	++	-	0	0	0
212260	++	-	++	++	0
212261	++	-	0	0	0
Sheep					
209942	++	0	0	0	0
210552	n	n	n	n	n
210608	++	-	0	0	0
211056	++	0	0	0	0
212384	+	0	0	0	0

- negative; + mild; ++ granulomatous/oedematous appearance; 0 observed; n no data

Table 3.3 Post mortem findings from both bovine and ovine cases used in this study



A. The granular appearance over folds is observed in bovine sample 211253; B. the pigmented gut was observed in ovine sample 209941; C. the non-pigmented gut was observed in ovine sample 210608.

Fig. 3.2 Post-mortem lesions of *Map* infected GIT



The foetus from ovine case no. 210608 samples were collected aseptically from the foetus and were known to be positive on real-time PCR assay.

Fig. 3.3 Dead ovine foetus recovered from case 210608.

Case no.	ZN Staining Faecal	ZN Staining Tissue	Histo pathology
Cattle			
210444	-	n	-
210716	+	+	+
210717	+	+	+
211253	+	+	+
212260	+	+	+
212261	+	+	+
Sheep			
209942	+	+	+
210552	÷	+	+
210608	+	÷	S
211056	+	+	+
212384	+	÷	+

+ positive; - negative; n not collected; S suspected

Table 3.4 Results of microscopic examination of clinical samples

3.4.2. Tissue smears

Different tissue impression smears were prepared with ileal mucosa and lymph nodes. The results of tissue impression smears (Fig. 3.4) from both cattle and sheep after ZN staining are given in Table 3.3. Clear *Map* clumps can be appreciated in the tissue impression smear which was a classical example of a positive case of Johne's disease.

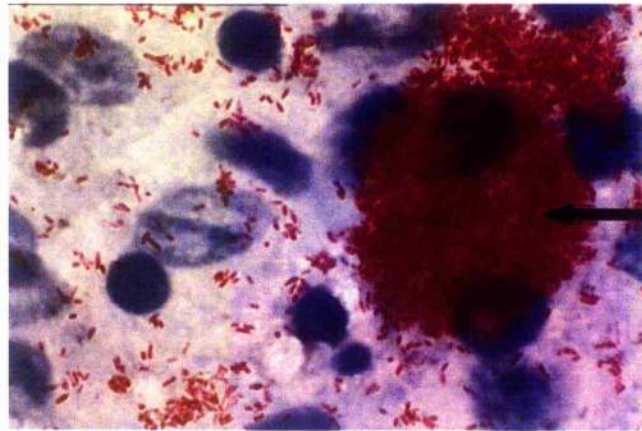
3.4.3. Histopathology

The results of histopathology in the bovine cases are as given in Table 3.4. Case 210444 was reported as of not having any evidence that the enteropathy was due to Johne's disease, on all tissue sections examined; Cases 211253, 212260, 212261 were reported to be granulomatous enteritis with Johne's disease.

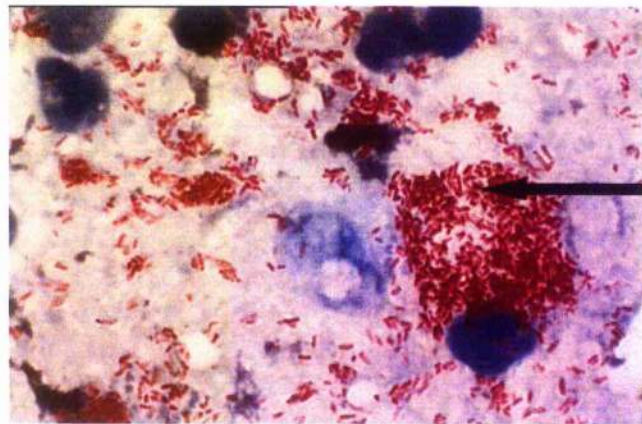
In ovine cases the report for Case 210608 was consistent with ovine pneumonic manheimiosis but was a suspect Johne's disease based on faecal and tissue smears, this was not confirmed on histopathological examination. All other results were provided in Table 3.4

3.5 Discussion

The clinical signs found in both the cattle and the sheep cases were consistent with a diagnosis of Johne's disease. In no case was it possible to identify them unequivocally as Johne's disease without further laboratory testing. The results of clinical and laboratory testing confirmed the presence of other agents in 4/6 bovine cases and 4/5 ovine cases were suffering from other infections like parasitic burdens and secondary bacterial infections. It was not clear from the information available whether these infections followed the initial development of Johne's disease or preceded them. The pregnant ewe (Case 210608) was a good example as the foetuses were dead and were putrefied even before post-mortem and there was ascitis. Their death might have been due to chronic wasting/anaemia. Upon foetal post-mortem examination, no pathological lesions were observed in any tissue. In microscopic examination both faecal and tissue smears were positive. The absence of histopathological confirmation of the infection is an example of the difficulties of making consistent observations even



Map clumps



Map clumps

Pink/ red colored clumps are *Map* over blue background of intestinal mucosa

**Fig. 3.4 Acid-fast stained (ZN-staining) smears of intestinal mucosa
Mycobacterium avium subsp. *paratuberculosis***

when following a standard protocol. Pathological findings were largely consistent with a diagnosis of Johne's disease. They were least obvious in bovine Case 210444, where the histopathology provided no evidence for the presence of organisms and neither did they in ovine Case 210608. Case 210608 showed histological changes similar to Johne's disease. Other examinations (tissue smear and faecal smear) supported pathology in all the cases with exception of bovine Case 210444, which could not be confirmed as a case of Johne's disease by the methods described in this study. The limitations of the diagnostic methods commonly used to confirm Johne's disease in cattle and sheep were thus demonstrated in this small sample of animals.

CHAPTER IV

REAL-TIME PCR ASSAY – INTRODUCTION AND ITS USE IN THIS STUDY

4.1 Introduction

Real-time PCR is a quantitative assay in which the amount of a nucleic acid target is measured during each amplification cycle of the PCR. The target may be DNA, cDNA, or RNA. There are three types of quantitation assay; DNA/cDNA quantitation; RNA quantitation using one-step reverse transcription polymerase chain reaction (RT-PCR); RNA quantitation using two-step RT-PCR. The technology used is reviewed here. This chapter also describes the optimisation and validation of a real-time PCR assay for *Map* based on the detection of IS900 gene. In addition an 18S rRNA assay was used to accurately quantify of the amount of DNA input in to each real-time PCR reaction.

4.1.1 Materials used in the real-time PCR assay

Ready master mix; primers; probes; sample template DNA; PCR grade water; 96 well reaction plate; adhesive film cover; real-time PCR system and its software; pipettes; microcentrifuge tubes; microcentrifuges.

4.1.2 Dyes used to label probes

In general there are three different dyes called reporter dyes, quencher dyes and internal reference dyes. The reporter and quencher dyes are labelled to probes. The classical reporter dye is 6-FAM (6-carboxyfluorescein); other reporter dyes include Joe and Vic. The classical quencher dye is TAMRA (6-carboxytetramethylrhodamine), other quencher dyes are DABCYL (1-(4, 4'-Dimethoxytrityloxy)-3-[O-(N-4'-carboxy-4-(dimethylamino)-azobenzene)-3-amino propyl]-propyl-2-O- succinoyl-1caa), and BHQ (Black Hole Quenchers). Internal reference dyes like ROX are used in some probe reactions quenched by dark dyes like BHQ and DABCYL (Dorak MT, 2004). SYBR green dye is a dye which binds to double-stranded DNA.

4.1.3 The principles of real-time PCR assay

Two different methods are used for quantitative detection: FRET (fluorescence resonance energy) system and DNA binding agents. In general probes

using the FRET system are sequence specific, whereas DNA binding agents are non-specific.

4.1.3.1 FRET system

When the reporter dye is excited by light from the real-time cycler instrument, energy is transferred from the reporter (fluor) to the quencher dye, which is fluorescence resonance energy transfer or Förster resonance energy transfer (FRET) (Hiyoshi and Hosoi, 1994; Chen and Lentz, 1997) (Fig 4.1). However, the quencher does not completely quench the fluorescence of the reporter dye. The energy transfer causes the quencher dye to excite and emit light at a longer wavelength, so longer wavelength fluorescence is observed. The release of the reporter dye away from the close vicinity of the quencher (e.g. due to probe hydrolysis) (Holland *et al.*, 1991) ends the activity of the quencher (no FRET) and the reporter dye starts to emit fluorescence. The fluorescence intensity of the reporter dye increases, when compared to the longer wavelength fluorescence which was observed before. Hence the increase in measured fluorescent signal is directly proportional to the amount of accumulating target DNA. This process repeats in every cycle and does not interfere with the accumulation of PCR product. Accumulation of PCR products is detected by monitoring the increase in fluorescence of the reporter dye. In the FRET system, hydrolysis probes require one hybridization event for signal generation, whereas hybridization probes require two independent hybridizations.

(a) FRET Hydrolysis chemistry

For all hydrolysis chemistry, both the reporter dye and quencher dye are labelled to the same probe. These can be used for multiplex assays by designing each probe with a spectrally unique fluor/quench pair. However they are relatively expensive to synthesize.

(i) *TaqMan*[®] chemistry

TaqMan[®] chemistry depends on the 5'-nuclease activity of the DNA polymerase used for PCR to hydrolyse an oligonucleotide that is hybridised to the target

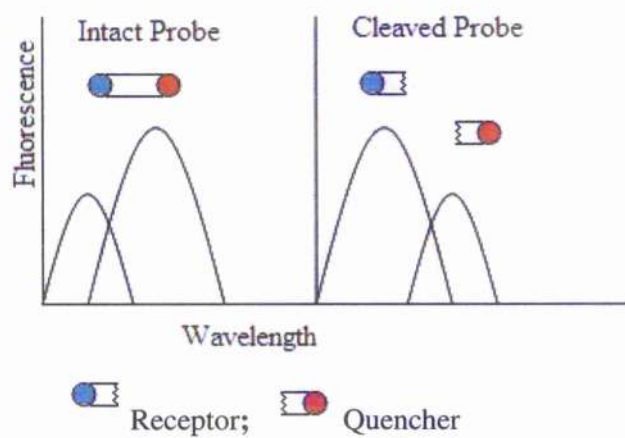


Fig. 4.1 Fluorescence Resonance Energy Transfer or Förster resonance energy transfer (FRET)

amplicon (Fig 4.2). *TaqMan*[®] probes are oligonucleotides labelled with a fluorescent reporter dye on the 5' end, and a quenching dye on 3' end. They are usually 20-30 bases long with a T_m value 10°C higher than primers. During PCR, the probe anneals specifically between the forward and reverse primer to an internal region of the PCR product. The polymerase then carries out the extension of the primer and replicates the template to which the *TaqMan*[®] probe is bound. The 5' exonuclease activity of the polymerase cleaves the probe, releasing the reporter molecule away from the close vicinity of the quencher (Holland *et al.*, 1991), thereby ending the activity of the quencher (no FRET). *TaqMan* assay uses universal thermal cycling parameters and PCR reaction conditions. Because the cleavage occurs only if the probe hybridises to the target, the origin of the detected fluorescence is specific amplification. The process of hybridisation and cleavage does not interfere with the exponential accumulation of the product. One specific requirement for fluorogenic probes is that 'G' should not be at the 5' end. A 'G' adjacent to the reporter dye quenches reporter fluorescence even after cleavage.

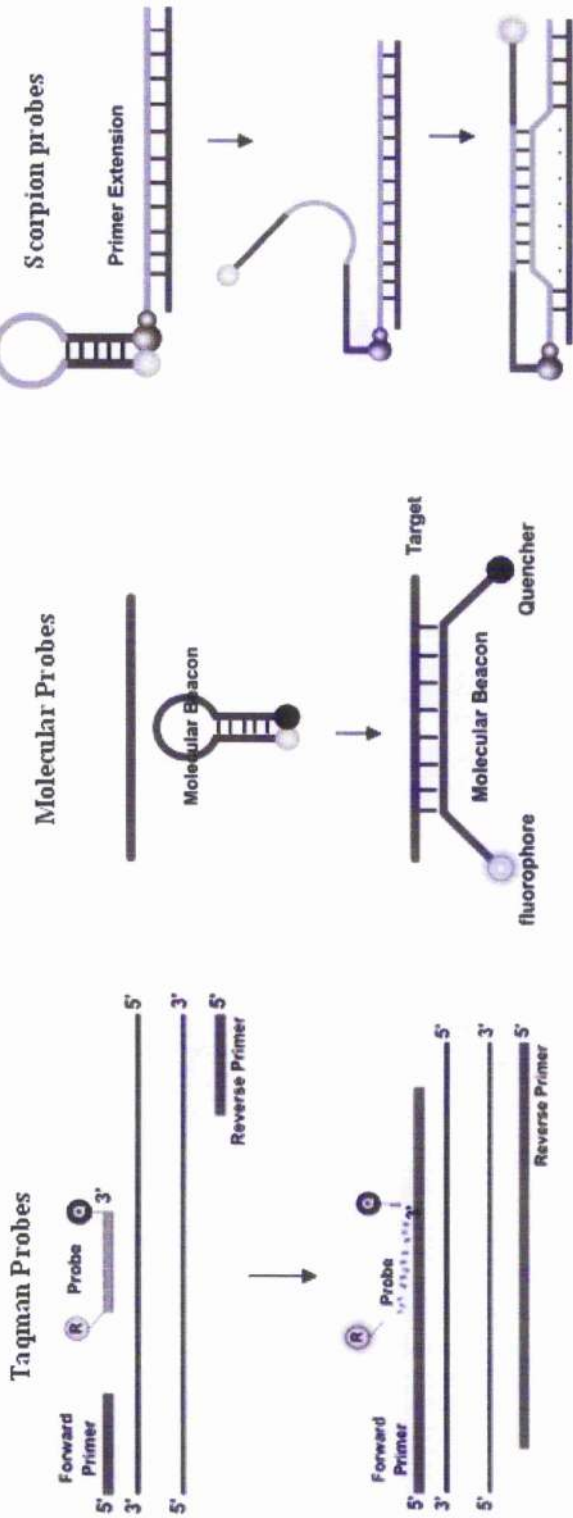
(ii) Molecular Beacons chemistry

Molecular beacons also contain a fluorescent dye, usually on the 5' base, and a quenching dye on the 3' base (Fig 4.2). However, they differ from *TaqMan*[®] chemistry, as they are designed to adopt a hairpin structure while free in solution to bring the fluorescent dye and the quencher in close proximity for FRET to occur (Täpp *et al.*, 2000). The close proximity of the reporter and the quencher in this hairpin configuration suppresses reporter fluorescence. Thus at the annealing step, the reporter dye is separated from the quencher (no FRET) and the reporter fluoresces. Molecular beacons regain their hairpin loop during denaturation and must rebind to their target sequence every cycle for fluorescence emission.

(iii) Scorpion Probe chemistry

Scorpion probes achieve sequence specific priming and PCR product detection using a single oligonucleotide (Fig 4.2). The Scorpion probe maintains a stem loop configuration in the unhybridised state. The 3' portion of the stem also contains a sequence that is complementary to the extension product of the primer. This sequence is

Hydrolysis Probes



Hybridisation Probes



Courtesy: website of premier biosoft (http://www.premierbiosoft.com/tech_notes/index.html), except hybridisation probes and SYBR green which was redrawn based on the chemistry.

Fig. 4.2 Different methods of fluorescence detection in real-time PCR assay

linked to the 5' end of a specific primer via a non-amplifiable monomer. After extension of the Scorpion primer, the specific probe sequence is able to bind to its complement within the extended amplicon thus opening up the hairpin loop. This prevents the fluorescence from being quenched (no FRET) and a signal is observed (Thelwell *et al.*, 2000). Unlike Molecular Beacons and *TaqMan*[®] probes, Scorpion probes don't require separate probe and primers (Thelwell *et al.*, 2000).

(b) FRET Hybridisation

In hybridisation chemistry, the reporter dye and quencher dye are labelled to two separate probes (Fig 4.2). Probe 1 is labelled at its 3' end with a reporter dye and probe 2 is labelled at its 5' end with a quencher dye. The free 3' hydroxyl group of probe 2 must be blocked with a phosphate group to prevent *Taq* DNA polymerase extension. To avoid any steric problems between the quencher and the reporter dye on both probes, there should be a spacer of 1 to 5 nucleotides to separate the two probes from each other. Initially the reporter dye's fluorescence is detected as background fluorescence by the real-time cycler instrument's optical unit. At the time of the annealing step of real-time PCR, the PCR primers and the probes hybridize to their specific target regions causing the reporter dye to come into close proximity to the quencher dye. So no fluorescence of reporter dye develops instead there is transfer of energy to the quencher dye (FRET). The quencher dye now emits this energy at a longer wave length, which is detected by the cycler instrument.

4.1.3.2 DNA-binding agents –SYBR[®] Green dye

SYBR[®] Green is a fluorescent dye that offers a simple and most economical method for detecting and quantifying real-time PCR products (Fig 4.2). SYBR[®] Green binds to double-stranded DNA, and upon excitation emits fluorescence (Wittwer *et al.*, 1997). Thus, as the PCR product accumulates, fluorescence increases. For single PCR product reactions with well designed primers, SYBR[®] Green can work extremely well, with spurious non-specific background only showing up in very late cycles. Since the dye binds to double-stranded DNA, there is no need to design a probe for any particular target being analyzed. However, detection by SYBR[®] Green requires extensive optimization as the dye cannot distinguish between specific and non-specific product

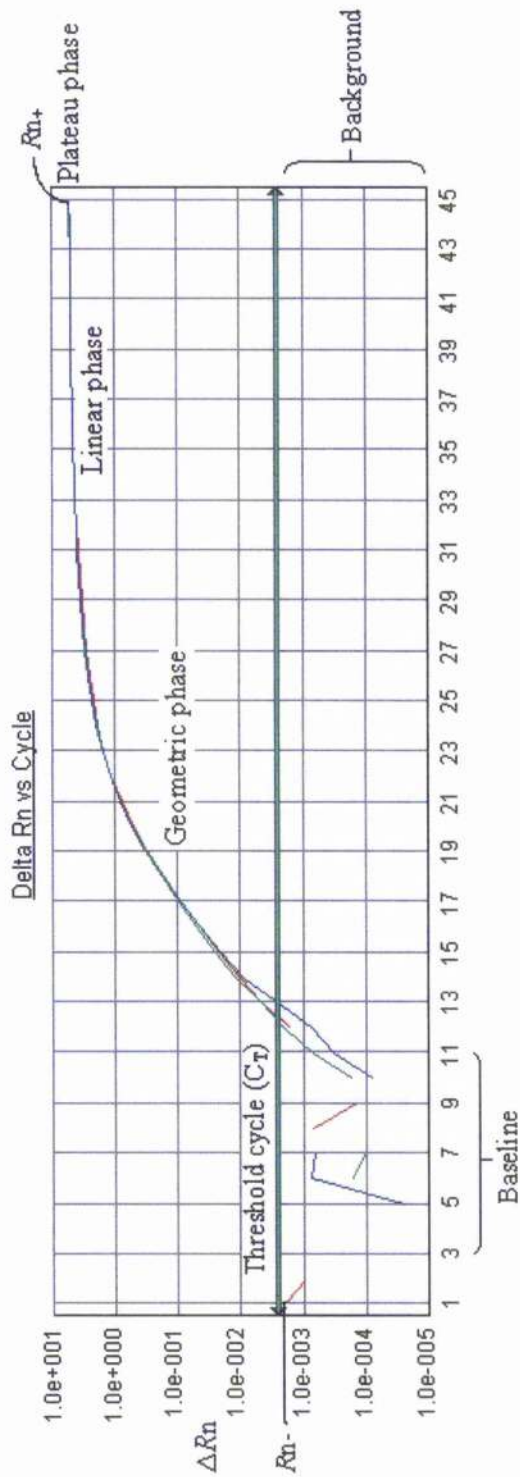
accumulated during PCR. The advantages of SYBR[®] Green are that it is cheap, easy to use, and sensitive. The disadvantage is that SYBR[®] Green will bind to any double-stranded DNA in the reaction, including primer-dimers and other non-specific reaction products, which can result in an overestimation of the target concentration.

4.1.4 Analysis of real-time PCR results

The data of fluorescence is stored in an .SDS file for analysis. The data is visualised (Fig 4.3) using an amplification plot, which reflects the fluorescence of the reporter dye during amplification and is directly related to the formation of PCR products. R_n is the fluorescence emission intensity of the reporter dye divided by the fluorescence emission intensity of the passive reference dye (ROX), which provides an internal reference to the reporter dye signal and is normalised during data analysis. The threshold should be set in the region associated with an exponential growth of PCR product. It is either chosen or calculated automatically as the average standard deviation of the background fluorescence (R_n for earlier cycles) multiplied by an adjustable factor. The first cycle which is above threshold is defined as the threshold cycle (C_T), thus representing the earliest point in the amplification curve which can be used for quantification of amplified product. An early detection of increased fluorescence results from a higher concentration of target DNA. No template control (NTC) is a sample that does not contain template DNA (e.g. PCR grade water), in which no signal should be observed above the threshold. Using the standard curve generated with a target DNA sequence of known copy number, the starting amount of target DNA in unknown samples can be determined.

4.1.5 Selection of primers and probes

The primers and probes are selected based on the target gene to be amplified. In this study *Map* specific target primers and probes were selected from published sources (Ravva and Stanker, 2005). These primers and probes were designed to target the IS900 sequence, which is present as 14-18 copies in each *Map* genome (Vary *et al.*, 1990). In the complete genome sequence of a *Map* organism, 17 copies of IS900 were detected (Li *et al.*, 2005). The 18S rRNA gene is a house keeping gene and acts as an internal



Baseline is the initial cycles of PCR where there is little change in fluorescence signal (3-11 cycles), usually set based on NTC; Threshold cycle (C_T) is the fractional cycle number at which the fluorescence passes the fixed threshold; $\Delta Rn = (Rn_+) - (Rn_-)$, where Rn_+ is the value of a reaction containing all components, including the template, Rn_- is the value of a reaction that does not contain any template or an un-reacted sample whose value is obtained from the early cycles of reaction.

Fig. 4.3 Amplification plot of real-time PCR assay

control in all the real-time PCR assays. The 18S rRNA gene is present in almost all eukaryotic cells and can be used for quantitation of total number of cells.

4.2 Materials and Methods

4.2.1 Optimisation of primers and probe concentrations for detection of *Map* and 18S

Working stock solutions were prepared from primers (Operon Biotechnologies GmbH, Germany) and probes (Eurogentec S.A, Belgium) of both *Map* and 18S (Table 4.1). These stock solutions had a primer concentration of 400nM and probe concentration of 200nM. Two sets of premix solutions were prepared for *Map* and 18S with different concentrations of primers and probes (Table 4.2. and Table 4.3.). A set of primers and probes targeting conserved regions of the 18S ribosomal gene (18S rRNA), a house keeping gene, were designed. In the real-time PCR assay this gene was used to evaluate false negative results and also to check the DNA extraction procedure. To design *TaqMan*[®] probes and primers for 18S sequence 'Primer Express' software (Applied Biosystems, Cheshire, UK) was used with default settings. The premix solutions were prepared in 2mL microcentrifuge/eppendorf tubes (Eppendorf AG, Germany) using *TaqMan*[®] master mix (Applied Biosystems, Cheshire, UK), PCR grade nuclease free water (Ambion Inc, UK) and primers and probes. The premix solutions were vortexed for 5sec and then briefly centrifuged (Eppendorf 5804 R, Eppendorf AG, Germany) to remove any drops splashed inside the tube lid. A volume of 20µL premix was loaded into each well of MicroAmp[™] Optical 96-Well Reaction Plate (Applied Biosystems, Cheshire, UK) according to the template Fig. 4.4. The template was prepared before the start of each experiment with different combinations of primers and probes. When setting up the 96-Well Reaction Plate a total of 4 controls were used; *Map* positive control; *Map* negative control; 18S positive control; and 18S negative control. For the positive control (C_{TP}), DNA of a known positive sample and for the negative control nuclease free pure water (designated 'no template control' (NTC)) were used. Volumes of 5µL of known positive sample DNA, nuclease free water and test samples were added into the wells as per the labelled template. All samples were evaluated in triplicate and reaction volumes of 25µL were used throughout the optimisation process. Once the wells were filled the plate was sealed with MicroAmp[™] Optical Adhesive Film (Applied Biosystems, Cheshire, UK) to prevent evaporation. The

Sequence name	Sequence (5'-3')	Amplicon size (bp)	Source	Region of Gene
18s				18s rRNA gene
Forward primer	GCCGCTAGAGGTGAAATTCCTTG			949 – 970 bp
Reverse primer	CATTCCTGGCAAATGCTTTCG	66	See below ^a	994 – 1014 bp
Probe	TCGGCCAAAGACGGACCAGA			973 – 992 bp
<i>Map</i>				IS900 insertion sequence
Forward primer (SF214)	ATGACGGTTACGGAGGTGGTT			705 – 726 bp
Reverse primer (SR289)	TGCAGTAATGGTCGGCCTTAC	76	Ravva and Stanker ^b	760 – 780bp
Probe (PR265)	CGACCCACGCCCGCCACAGA*			739 – 756 bp

Primers (Operon Biotechnologies GmbH, Germany) and probes provided by manufacturer Eurogenetic S.A., Belgium. Both the probes were tagged with 6-FAM reporter dye on 5' end and with BHQ-1 quencher dye on 3' end. *Probe designed for reverse strand. 18s primers and probes were designed for this project. All primers and probes were based on ^a Gene bank accession DQ222453, GI: 83321215; ^b Gene bank accession AJ250017, GI: 8919133.

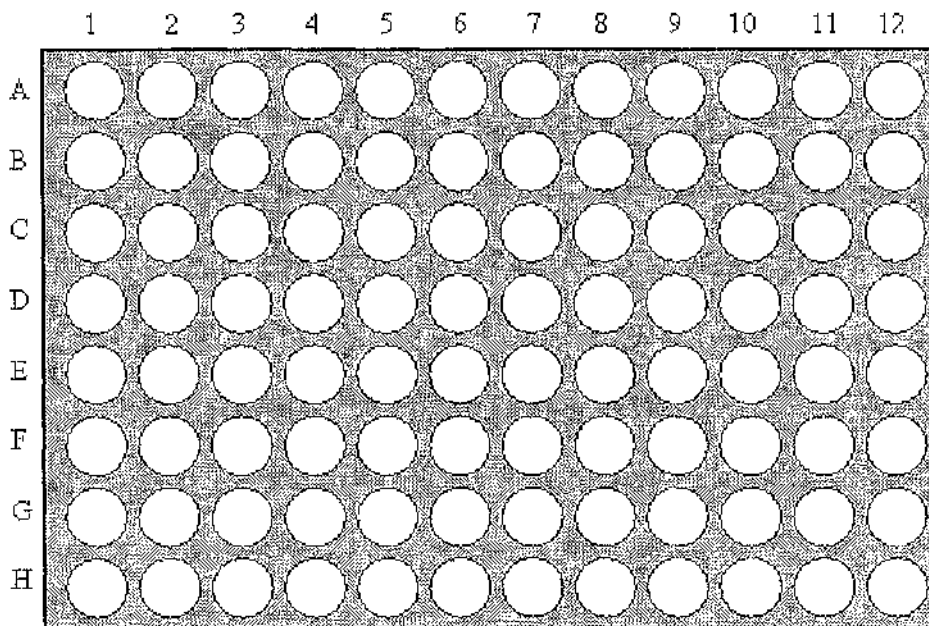
Table 4.1 Primer/ Probe sets used in detection of *Map* by Real-time PCR

Map Primer and Probe dilutions (nM)	
Primer Concentration	Probe Concentration
200	200
200	100
200	50
200	25
100	200
100	100
100	50
100	25
50	200
50	100
50	50
50	25
25	200
25	100
25	50
25	25

Table 4.2 Different primer/probe dilutions of *Map*

18S Primer and Probe dilutions (nM)	
Primer Concentration	Probe Concentration
400	200
400	100
400	50
200	200
200	100
200	50
100	200
100	100
100	50
50	200
50	100
50	50

Table 4.3 Different primer/probe dilutions of 18S



White circles represent the wells of the reaction plate.

Fig. 4.4 Template similar to 96-Well Reaction Plate

sealed reaction plate was then placed in the Applied Biosystems 7500 Real-Time PCR System (Applied Biosystems, Cheshire, UK), which was operated using the Applied Biosystems 7500 system software provided by the manufacturer installed onto a connecting computer. Thermal cycling parameters were 50°C for 2 minutes, followed by 95°C for 10 minutes and 45 cycles of: 95°C for 15 sec and 60°C for 1 minute.

4.2.2 Detection of *Map* and 18S template DNA in clinical samples by real-time PCR analysis

Premix solutions for *Map* and 18S were prepared as per the protocol which is based on optimised primer/probe concentrations (Table 4.4 and Table 4.5). A concentration of 50nM probe and 50nM primers were used for 18S premix and a concentration of 50nM probe and 100nM primers were used for *Map* premix in all assays to quantify the template DNA from samples. The procedure described above, was used, with 5µL sample volume per 25µL reaction.

4.2.3 Validating the real-time PCR results in the detection of *Map* and 18S.

(a) Cloning PCR products from *Map* and 18S reactions.

Two sets of gene cloning experiments were carried out; one with *Map* positive control and other with the 18S positive control. The selection of the controls for cloning was based on the reactions with the lowest C_{TP} values. The real-time PCR products were subjected to cloning without purification of the product as per the manufacturer's protocol. Real-time PCR products from *Map* and 18S were cloned using a commercially available kit, TOPO TA Cloning[®] Kit for Sequencing (with pCR[®]4-TOPO[®]) with One Shot[®] TOP10 chemically competent *Escherichia coli* (Invitrogen Ltd, Paisley, UK). The method used was as per the manufacturer's instructions. One micro litre of the real-time PCR product (*Map* or 18S) was added into a microcentrifuge tube, to which 1µL salt solution (included in the kit), 1µL TOPO[®] vector and sterile water were added to make up a volume of 6µL. The reaction was mixed gently and incubated for 5-30 minutes at room temperature, then placed on ice. *E. coli* were thawed on ice, 2µL TOPO[®] cloning reaction was added, mixed very gently without pipetting, and then incubated on ice for 5 minutes. The cells were heat-shocked for 30sec at 42°C

Constituents of Premix	Volume per reaction per well
PCR grade water	6.9375
Master Mix	12.5
Forward Primer (100nM)	0.25
Reverse Primer (100nM)	0.25
Probe (50nM)	0.0625
Total volume of Premix	20 μ L

Primers working stock solutions were at a concentration of 10 μ M/ μ L

Probe working stock solutions were at a concentration of 20 μ M/ μ L

Table 4.4 Map premix per well in Real-time PCR assay for test samples

Constituents of Premix	Volume per reaction per well
PCR grade water	7.1875
Master Mix	12.5
Forward Primer (50nM)	0.125
Reverse Primer (50nM)	0.125
Probe (50nM)	0.0625
Total volume of Premix	20 μ L

Primers working stock solutions were at a concentration of 10 μ M/ μ L

Probe working stock solutions were at a concentration of 20 μ M/ μ L

Table 4.5 18S premix per well in Real-time PCR assay for test samples

without shaking and immediately transferred to ice. Two hundred and fifty microlitres of S.O.C. medium was added to the cells and the tubes were incubated at 37°C in a shaking incubator (200rpm) for 1hr, placed horizontally. Volumes of 50µL and 200µL of transformed mix were spread on a prewarmed Luria Bertani (LB) plate (Appendix) containing 100µg/mL of ampicillin, and then incubated overnight at 37°C. Colonies were picked from the plates and subcultured overnight in LB broth containing 100µg/mL of ampicillin.

(b) DNA extraction from the cloned product

Plasmid DNA was isolated using the PureLink™ Quick Plasmid Miniprep Kit (Invitrogen Ltd, UK). 1mL of an overnight culture was centrifuged at 1000rpm for 5 minutes using a microcentrifuge and the supernatant discarded. The cell pellet was re-suspended thoroughly in 250µL re-suspension buffer (R3) with RNase A. Two hundred and fifty micro litre lysis buffer (L7) was added to the cell suspension and gently mixed by inverting the capped tube five times. The suspension was allowed to incubate for 5 minutes at room temperature. Three hundred and fifty micro litre of precipitation buffer (N4) was added and mixed immediately by inverting the tube until the solution was homogeneous. The mixture was centrifuged at approximately 12,000 x g for 10 minutes at room temperature to clarify the lysate from lysis debris. The spin column was placed in a 2mL wash tube into which supernatant from clarified cell lysate was added and centrifuged at approximately 12,000 x g for 1 minute. The flow-through was discarded and the column was placed back into the wash tube. Five hundred micro litre wash buffer (W10) was added to the column incubated for 1 minute at room temperature and it was centrifuged at approximately 12,000 x g for 1 minute. The flow through was discarded and the column was placed back into the wash tube. Seven hundred microlitres of wash buffer (W9) was added to the column, which was centrifuged at 12,000 x g for 1 minute. The flow-through was discarded and the column was placed back into the wash tube, and then centrifuged at approximately 12,000 x g for 1 minute to remove any residual buffer. The wash tube with the flow-through was discarded and the spin column was placed in a clean 1.5mL recovery tube. A volume of 75µL preheated TE was added in the centre of the column and the column was incubated for 1 minute at room temperature, to elute the DNA. After incubation, the column was

centrifuged at 12,000 x g for 2 minutes and purified plasmid DNA was eluted into a recovery tube.

(c) Restriction analysis of plasmid DNA obtained from cloned product

Before proceeding to sequencing, the plasmid DNA was analysed for inserts by restriction analysis. A volume of 10µL plasmid, 2µL React III buffer (Invitrogen Ltd, UK), 1µL *EcoR* I enzyme (Invitrogen Ltd, UK) were added in to a microcentrifuge tube and 7µL millipore water was added to make up a final volume of 20µL. The plasmid was digested by incubating at 37°C for 1hr and plasmid DNA was visualised by agarose gel/ polyacrylamide gel electrophoresis followed by ethidium bromide staining and gels were visualised under UV illumination using Gene flash (Syngene, Cambridge, UK) and photographed with monochrome video graphic printer (Sony, Hampshire, UK).

(d) Sequencing of plasmid DNA from cloned product

Plasmid DNA was sequenced using BigDye[®] Terminator v3.1 cycle sequencing kit (Applied Biosystems, Cheshire, UK). The sequence reaction was prepared by adding 4µL ready reaction premix, 2µL BigDye sequencing buffer, 2µL M13 forward primer (GTAAAACGACGGCCAGT), 5µL plasmid template to MicroAmp[™] Optical Reaction tube (Applied Biosystems, Cheshire, UK). The reaction tubes were placed on the GeneAmp[®] PCR system 9700 and the PCR system run as per BigDye[®] Terminator v3.1 cycle sequencing kit instructions. The PCR product was then purified by ethanol/sodium acetate precipitation in which 20µL PCR product, 80µL nuclease free water, 200µL 100% ethanol, 1µL sodium acetate were added in to a microcentrifuge tube. After incubation at -80°C for 30 minutes, the mixture was centrifuged at 12,000 x g for 15 minutes, and the supernatant discarded. The sediment was washed with 150µL 70% ethanol and centrifuged for 12,000 x g for 15 minutes. The supernatant was discarded; the tube was allowed to air dry and the sediment was resuspended with Hi-Di-formamide. A volume of 10µL Hi-Di formamide suspension was placed in MicroAmp[™] Reaction Plate (Applied Biosystems, Cheshire, UK). The samples were placed from well A1-H2 and considered as a single run, with unused wells filled with 10µL of Hi-Di formamide. The plate was sealed with the plate septa, then placed into a plate base and clamped with the plate retainer. The total plate

assembly was then placed in a Applied Biosystems ABI PRISM[®] 3100 Genetic Analyzer (Applied Biosystems, Cheshire, UK). The initial sample data was entered using ABI PRISM[®] 3100 data collection software and subsequently viewed and analysed by using ABI PRISM[®] DNA Sequencing Analysis Software. The plasmid DNA sequence was stored as an .ABI file. These files were later viewed and analysed using chromas (freeware) and Vector NTI advance 10 software (licensed to Invitrogen Ltd, UK).

(e) Agarose gel electrophoresis

A 1.5% agarose gel was prepared using research grade agarose (Invitrogen Ltd, Paisley, UK) in TBE buffer. Samples were prepared by the addition of 1 μ L 5X gel loading buffer (Invitrogen Ltd, UK) to 5 μ L PCR product and then loaded into each well. Φ X174 RF DNA/Hae III fragments (Invitrogen Ltd, UK) were used as a molecular size standard. The gel was run at 100V for 45 minutes (Bio-Rad Laboratories, UK) in TBE buffer before being removed and stained in buffer solution containing 0.5 μ g/mL ethidium bromide for 20 minutes. Gels were visualised under UV illumination using Gene flash (Syngene, UK) and photographed with monochrome video graphic printer (Sony, UK).

(f) Polyacrylamide gel electrophoresis

5–6% gels were prepared with 3mL of 30%: 0.8% acrylamide/bisacrylamide solution (Severn Biotech Ltd, UK) and 1.5mL of TBE buffer; distilled water was added to make up a volume of 15mL prior to the addition of 12.5 μ L of TEMED and 125 μ L of 10% ammonium persulfate (Sigma-Aldrich Ltd, UK). A gel cassette (Bio-Rad Laboratories, UK) on a casting stand (Bio-Rad Laboratories, UK) was prepared with two glass plates and spacers before preparing the solution. The solution was poured between the glass plates a comb was inserted. After polymerisation, gel cassettes were placed in the buffer tank (Bio-Rad Laboratories, UK), containing TBE buffer. The gel combs were removed and the wells were flushed with buffer. Samples were prepared by diluting the PCR products 5:1 with gel loading buffer; 12 μ L of each sample was then loaded well. Φ X174 RF DNA/Hae III fragments were used as a molecular size standard. The gel was run at 100V for 45 minutes in TBE buffer before being removed and stained in buffer solution containing 0.5 μ g/mL ethidium bromide for 20 minutes. These

gels were visualised under UV illumination using Gene flash (Syngene, Cambridge, UK) and photographed with monochrome video graphic printer (Sony, Hampshire, UK).

4.2.4 Quantification of DNA in samples

DNA quantification was performed by using the Qubit™ DNA Quantitation kit (Invitrogen Ltd, Paisley, UK). Quant-iT™ dsDNA BR assay kit was used as recommended by manufacturer with a sample concentration of 100pg/μL – 1μg/μL and an assay range of 2-1000ng. First, a 1:200 working solution of the Quant-iT™ dsDNA BR reagent was prepared in Quant-iT™ dsDNA BR buffer. Next 1:20 solution of Quant-iT™ standard-1 and standard-2, and a 1:20 solution of the test DNA were prepared. All tubes were incubated at room temperature for two minutes and then assayed in the Qubit™ fluorometer as per manufacturer's instruction. The readings were displayed either in ng/mL or μg/mL (QF value). The concentration of DNA in the sample is calculated using the formula.

$$\text{Concentration of sample DNA} = \text{QF value} \times \left(\frac{200}{X} \right) \mu\text{g/mL}$$

where X is amount of sample added to the assay tube.

4.2.5. Preparation of *Map* and 18S templates for standard curve analysis

Plasmid DNA containing cloned *Map* PCR product was used to construct a standard curve and estimate real-time PCR efficiency. DNA extracted from healthy bovine liver tissue (reported as disease free, especially Johne's disease based on post-mortem examination and clinical reports) was used for standard curve analysis of 18S gene. The DNA concentrations of DNA extracted from cloned *Map* and healthy bovine liver tissue were estimated using Qubit DNA quantitation kit.

Based on the amount of DNA present serial dilutions were made using a working stock solution prepared from 1000μL of TE buffer and 3μL of tRNA. This working stock solution helps obtaining the complete *Map* DNA without sticking to the walls of tubes. Using this working stock solution, a tenfold serial dilution of cloned *Map* DNA and a fivefold serial dilution for healthy bovine tissue DNA was performed. These dilutions were assayed using real-time PCR, as described above. The real-time

PCR efficiency (E) can be calculated from the slope of the dilution curve (S) using the equation

$$E = 10^{1/s} - 1$$

4.3. Results

4.3.1 Optimisation of primer and probe concentrations for detection of *Map* and 18S

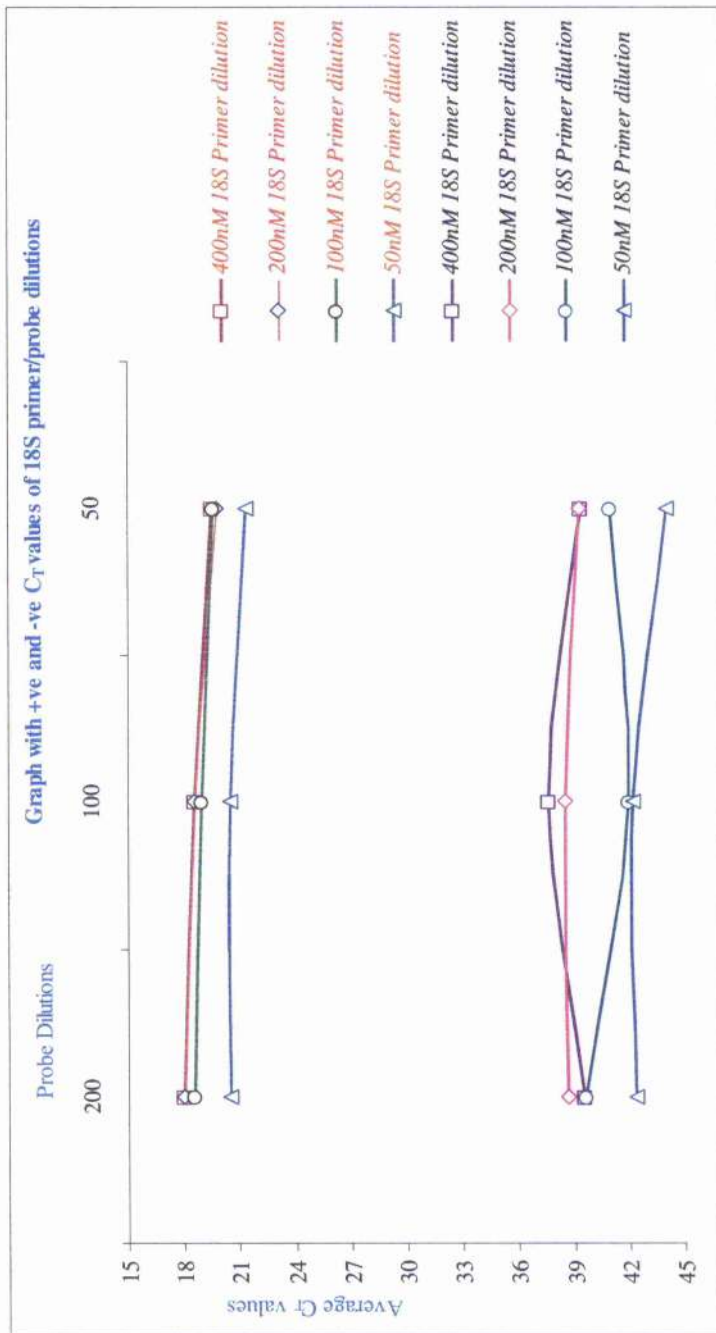
Optimal concentrations of primer and probes for *Map* and 18S real-time PCRs were determined by performing a series of assays with a range of primer and probe concentrations.

For detecting *Map* a range of 25–200nM was used. The margin of difference between the C_{TP} and NTC results at a 100nM primer concentration was greater than at 50nM and 25nM concentrations (Fig. 4.5). Maximal C_T values were observed when 50nM probe concentration was used with 200nM and 100nM primer concentrations; lesser concentrations of primer resulted in a decrease in C_T values. A concentration of 100nM of each primer and 50nM of probe was therefore chosen for all subsequent assays.

For optimisation of the 18S for real-time PCR assay (Fig. 4.6), primer dilutions ranged from 400–50nM and probe dilutions ranged from 200–50nM. All of the assays produced maximal C_T values regardless of primer/probe concentration within this range. A primer concentration of 50nM with 50nM of probe was therefore chosen for subsequent assays.

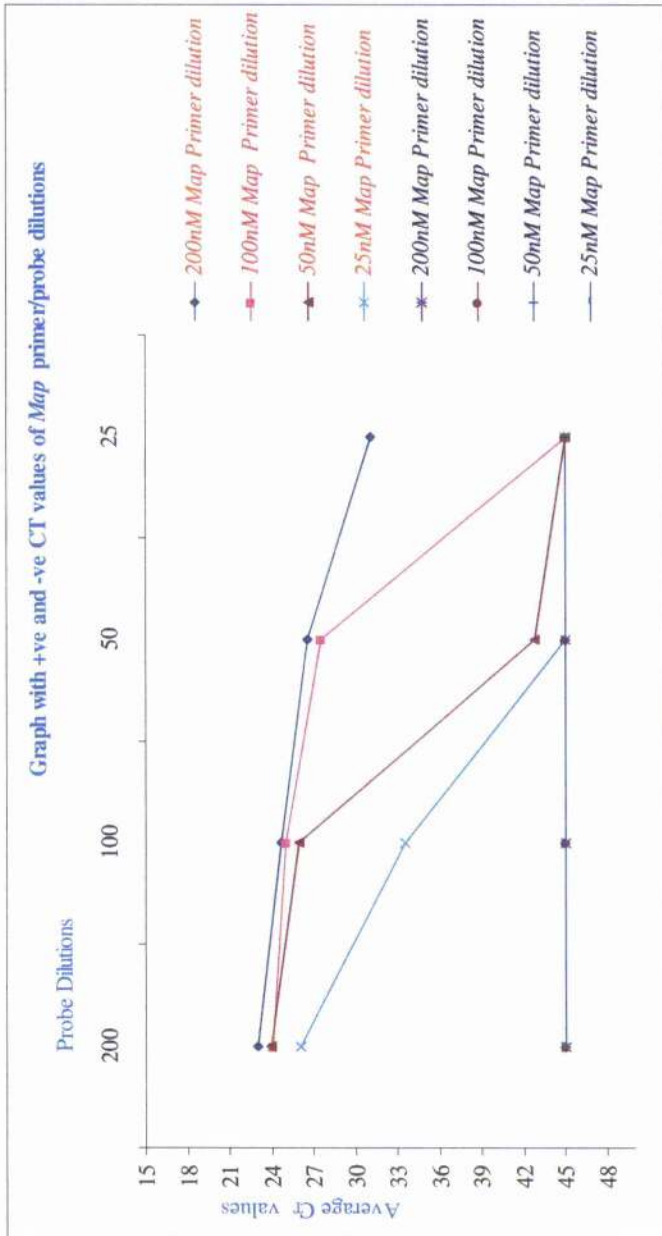
4.3.2 Validation of real-time PCR products for detection of *Map* and 18S

The total of 10 colonies were picked, these were grown overnight in bijoux tubes containing LB broth, following overnight growth of plated transformation reactions. Five most turbid tubes were selected for DNA extraction. Extracted plasmid DNA from the cloned product was analysed by restriction digest and visualised by agarose gel/polyacrylamide electrophoresis (Fig. 4.7). The total size of pCR[®]4-TOPO vector is 3956bp and size of plasmids of interest i.e. *Map* and 18S was 76bp and 66bp respectively. After observing the bands of plasmid DNA of interest on gel, sequencing of the respective plasmids was performed. This step was used as a checkpoint, if no bands were observed then the DNA extraction/ cloning experiment was repeated, if they



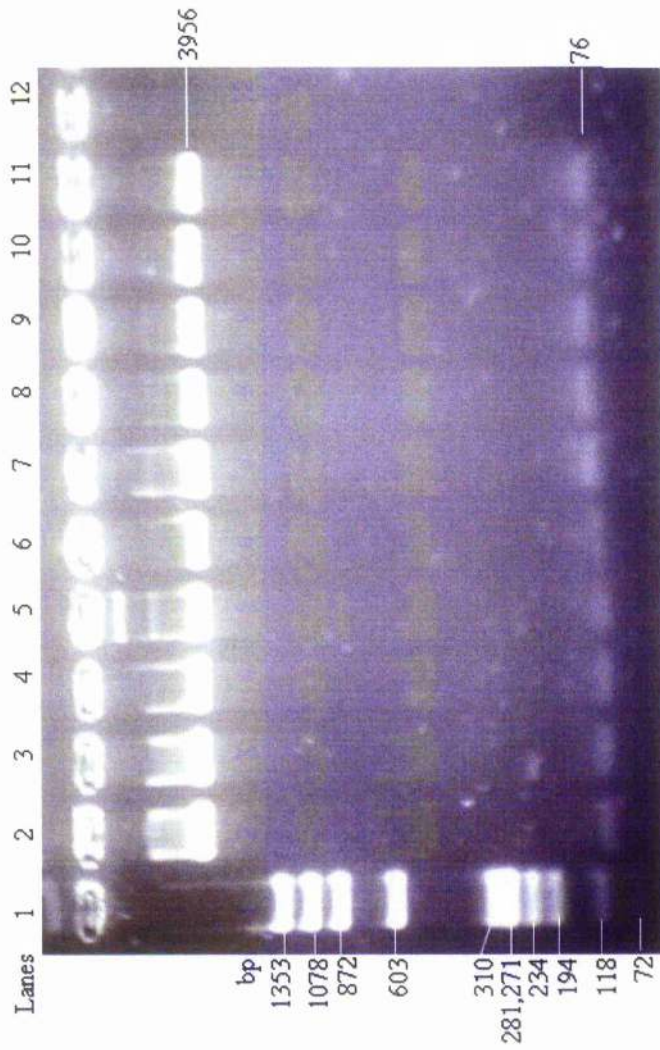
■ Coloured fonts to side are Positive 18S dilutions; ■ Coloured fonts to side are Negative 18S dilutions;
 Average of C_T values plotted against probe dilutions

Fig. 4.5 Line chart representing the C_T values of 18S primer and probe combinations for optimisation.



Coloured fonts to side are Positive 18S dilutions; Coloured fonts to side are Negative 18S dilutions; Average of C_T values plotted against probe dilutions

Fig. 4.6 Line chart representing the C_T values of Map primer and probe combinations for optimisation.



The plasmid DNA after TOPO cloning was analysed for *Map* inserts by restriction analysis. The bands towards the extreme left (Lane 1) were of the marker (Φ X174 RF DNA/Hae III fragments). *Map* insert of 76 bp length was visualised very faintly in between 118 bp to 72 bp. Highly visible bands which were more than 1353 bp were of pCR 4-TOPO plasmid vector.

Fig. 4.7 Cloned product of *Map* visualised on a 1.5% agarose gel

were present, sequencing was carried out. The sequence of primers and probes of interest for *Map* (i.e. IS 900) are given in the Appendix. The results of the cloned product exactly matches with the primer and probe set specific for IS900 (Fig. 4.8). Although there were a few nucleotide ambiguities in the forward primer and probe which was due to sequencing errors, the software predicts them to be similar to the primers and probes. Despite performing a series of transformation reactions followed by screening by of transformants by restriction digest for 18S recombinants, no clones containing 18S PCR product could be isolated.

4.3.3 Results of DNA quantification

The concentration of DNA was calculated from cloned *Map* sample and a liver sample from a healthy cow (free from any disease, especially Johne's disease, on post-mortem examination and clinical reports).

The DNA concentration of cloned *Map* after extraction was 45.8 μ g/mL. Given the plasmid size was 4.0Kb; 1 μ g of plasmid contains 2.275×10^{11} molecules (1 μ g of 1Kb = 9.1×10^{11} molecules). Hence, the concentration of plasmid was 1.04×10^{10} molecules/ μ L.

The DNA concentration of the healthy liver sample was 212 μ g/mL (212000pg/ μ L). This was used to estimate the total number of cells present in extracted DNA samples by detecting 18S fluorescence in real-time PCR assays. It was assumed that there was 6pg of DNA/ cell, thus 212000pg/ μ L is equivalent to 35333cells/ μ L. These samples were used to obtain a standard curve for *Map* and 18S real-time PCR assay.

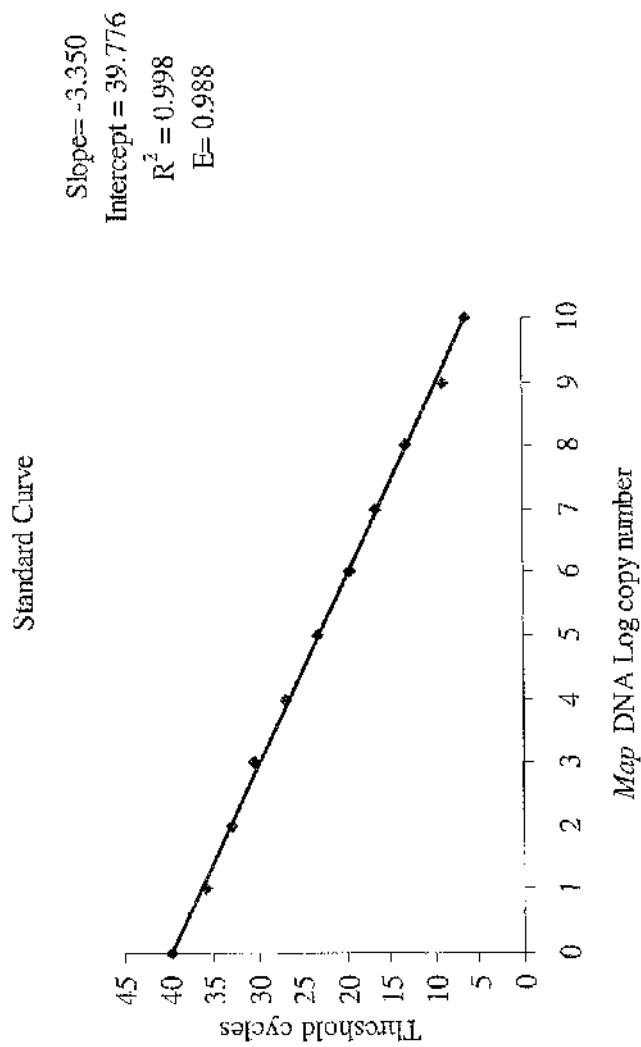
The real-time PCR results of serial dilutions were plotted on a graph to obtain a standard curve showing the linear range of quantification. The average C_T values were plotted against log copy number.

Cloned *Map* DNA was used to calculate the PCR efficiency and also estimate the amount of DNA at each C_T values. C_T values represent the input template amount; a linear relationship over 10 log decades with a correlation coefficient (R^2) of 0.9985 was revealed (Fig 4.9). A consistent detection of between 1.05×10^0 and 1.05×10^{10} copies was observed using cloned *Map* DNA, with low standard deviations ranging from 0.048% to 0.792% observed in triplicate assays indicating a high reproducibility of measurement. The real-time PCR efficiency is calculated using the slope value of standard serial dilutions. Thus, the calculated PCR efficiency is 0.986706.

1	TTTTG	GGGTT	ACCCC	NGNTA	CGGAG	GTGGT	TGTNT	TACAA	CCTGT	NTGGN
	AAAAC	CCCAA	TGGGG	NCNAT	GCCTC	CACCA	ACANA	ATGTT	GGACA	NACCN
51	CGGGC	GTGGA	CGCCG	GTAAG	GCCGA	CCATT	ACTGC	AAAGG	GCGAA	TTCGC
	GCCCG	CACCT	GCGGC	CATTC	CGGCT	GGTAA	TGACG	TTTCC	CGCTT	AAGCG
101	GGCCG	CTAAA	TTCAA	TTCGC	CCTAT	AGTGA	GTCGT	ATTAC	AATTC	ACTGG
	CCGGC	GATTT	AAGTT	AAGCG	GGATA	TCACT	CAGCA	TAATG	TTAAG	TGACC
151	CCGTC	GTTTT	ACAAC	GTCGT	GACTG	GGAAA	ACCCT	GGCGT	TACCC	AACTT
	GGCAG	CAAAA	TGTTG	CAGCA	CTGAC	CCTTT	TGGGA	CCGCA	ATGGG	TTGAA
201	AATCG	CCTTG	CAGCA	CATCC	CCCTT	TCGCC	AGCTG	GCGTA	ATAGC	GAAGA
	TTAGC	GGAAC	GTCGT	GTAGG	GGGAA	AGCGG	TCGAC	CGCAT	TATCG	CTTCT
251	GGCCC	GCACC	GATCG	CCCTT	CCCAA	CAGTT	GCGCA	GCCTA	TACGT	ACGGC
	CCGGG	CGTGG	CTAGC	GGGAA	GGGTT	GTCAA	CGCGT	CGGAT	ATGCA	TGCCG
301	AGTTT	AAGGT	TTACA	CCTAT	AAAAG	AGAGA	GCCGT	TATCG	TCTGT	TTGTG
	TCAAA	TTCCA	AATGT	GGATA	TTTTC	TCTCT	CGGCA	ATAGC	AGACA	AACAC
351	GATGT	ACAGA	GTGAT	ATTAT	TGACA	CGCCG	GGGCG	ACGGA	TGGTG	ATCCC
	CTACA	TGTCT	CACTA	TAATA	ACTGT	GCGGC	CCC GC	TGCCT	ACCAC	TAGGG
401	CCTGG	CCAGT	GCACG	TCTGC	TGTCA	GATAA	AGTCT	CCCGT	GAACT	TTACC
	GGACC	GGTCA	CGTGC	AGACG	ACAGT	CTATT	TCAGA	GGGCA	CTTGA	AATGG
451	CGGTG	GTGCA	TATCG	GGGAT	GAAAG	CTGGC	GCATG	ATGAC	CACCG	ATATG
	GCCAC	CACGT	ATAGC	CCCTA	CTTTC	GACCG	CGTAC	TACTG	GTGGC	TATAC
501	GCCAG	TGTGC	CGGTC	TCCGT	TATCG	GGGAA	GAAGT	GGCTG	ATCTC	AGCCN
	CGGTC	ACACG	GCCAG	AGGCA	ATAGC	CCCTT	CTTCA	CCGAC	TAGAG	TCGGN
551	CCGCG	AAAAA	TGACA	TCAAA	AACNC	CATTA	ACNTG	ATGTT	NTGGG	GNAAA
	GGCGC	TTTTT	ACTGT	AGTTT	TTGNG	GTAAT	TGNAC	TACAA	NACCC	CNTTT
601	TAAAA	TGTCA	GGCAT	GAGAT	NTNNA	AAAGG	NTTCT	NCCCT	ANATC	CTTTT
	ATTTT	ACAGT	CCGTA	CTCTA	NANNT	TTTCC	NAAGA	NGGGA	TNTAG	GAAAA
651	CCCTA	AAAGC	NGTCC	CNAAA	ACGGG	CTNAC	CCNGA	TNANN	TCNCT	ACTGG
	GGGAT	TTTCG	NCAGG	GNTTT	TGCCC	GANTG	GGNCT	ANTNN	AGNGA	TGACC
701	GCNTT	TGGAN								
	CGNAA	ACCTN								

Highlighted sequences are areas of interest; this is the site where the primers and probes bind to the target of *Map* DNA.

Fig 4.8 Gene fragment of cloned product of *Map*.



The average C_T values (Y) of *Map* clone were plotted against log copy number (X); correlation coefficient (R^2); calculated PCR efficiency (E) were given

Fig. 4.9 Standard curve generated from C_T values of the *Map* clone

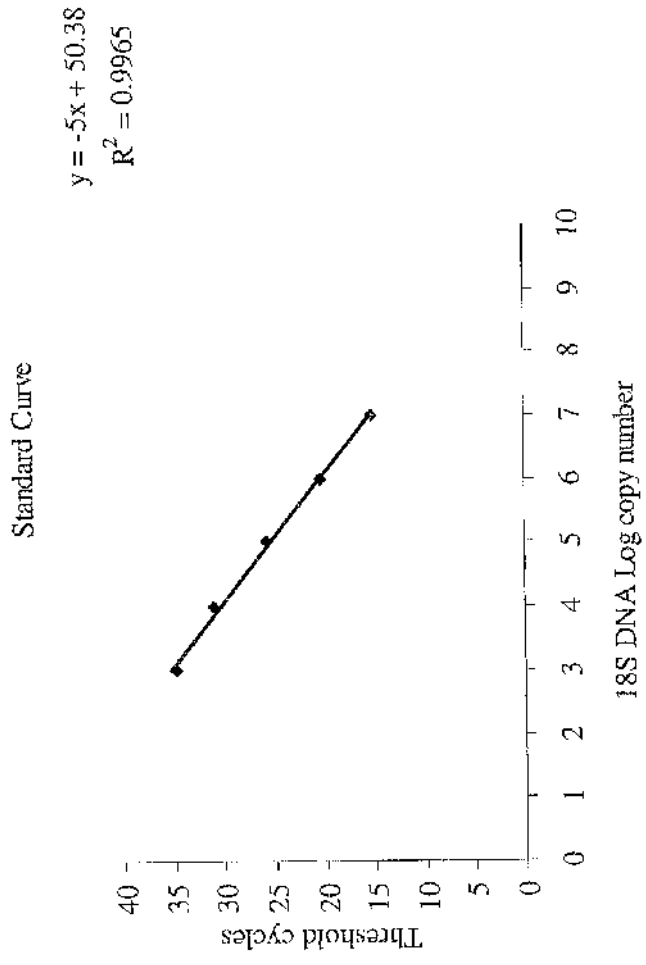
The standard curve for 18S was derived from serial dilutions of DNA from healthy bovine liver tissue. C_T values were plotted against 10 log decades; a correlation coefficient (R^2) of 0.9965 was revealed (Fig 4.10). Low standard deviations in a triplicate assays, ranging from 0.052% to 0.906%, indicate the high reproducibility of measurement; the slope value is -5 and the intercept is 50.38. PCR efficiency was 0.584893.

4.4. Discussion

In real-time PCR assay, selecting specific and sensitive primer and probe combinations, and also their effective concentrations in the premix plays a key role in yielding optimal results. In this study, *TaqMan*[®] probes were used as they are highly specific and sensitive, having advantages over the other probe chemistries. A potential and practical feature of the *TaqMan*[®] probe chemistries is their use of endpoint detection at room temperature, which is not possible with the Molecular Beacon probes that are fluorescent only at the elevated hybridization temperature (Täpp *et al.*, 2000). Also, SYBR-Green based detection strategies in real time analysis may lack specificity due to dye binding to non-specific DNA products (Hein *et al.*, 2001). So in order to detect *Map* from field samples highly specific and sensitive probe chemistry is necessary and also to reduce the optimisation steps, *TaqMan*[®] probes were used.

The primer and probe set using *TaqMan*[®] chemistry SF214/PR265/SR289 (Ravva and Stanker, 2005) was effective in detecting *Map* DNA from 100pg of template DNA. In this study the primer/probe/primer set was able to detect *Map* DNA from much less than 100pg cloned template DNA. The previous study used the cultured strains of *Map* (Ravva and Stanker, 2005); while in this study field samples were used.

To determine the optimal concentrations of primers and probes in the detection of both *Map* and 18S, a series of dilutions were made with different combinations and each combination was evaluated based on the C_T values. The *Map* primer/probe combination (100nM/50nM) used to detect the extracted DNA from field samples showed a strong fluorescence to wells positive for *Mycobacterium avium paratuberculosis*. No fluorescence was detected in NTC wells during 45 amplification cycles, thus confirming the specificity of the assay. The primer and probe combination used to detect 18S (50nM/50nM) were able to detect the 18S rRNA gene in all samples. Some fluorescence was observed in all wells with nuclease free PCR grade water



The average C_T values (Y) of healthy bovine tissue using 18S primers and probes were plotted against log copy number (X); correlation coefficient (R^2);

Fig. 4.10 Standard curve generated from C_T values of 18S

(NTC), all through this study. The difference between the C_T values of 18S positive control and NTC was always between 15-25cycles. Non-specific fluorescence in NTC wells was observed only after 35 cycles. This background fluorescence may be due to the amplification of 18S from contaminating DNA (Bustin and Nolan, 2004). Moreover, these primers are generally universal, so they will amplify the 18S gene from almost any eukaryote.

Gene cloning was carried out to confirm the *Map* and 18S positive results. This technique was used as it is difficult to grow *Map* and study its growth characters in one year, as the duration of this study was only one year. For this the TOPO TA Cloning® kit was used, in which *Taq* polymerase amplified PCR products directly inserted into a plasmid vector which can be sequenced and can be analysed for gene of interest. Gene cloning and sequencing were successful in case of *Map*, but was unsuccessful in the case of 18S. In the case of *Map*, the results were observed in the first attempt. In the case of 18S no colonies were observed until three attempts, once the colonies were observed they were subjected to restriction analysis. In restriction analysis results, bands were observed, at 66bp which agrees with the presence of 18S; at 3956bp which is the vector; and an unknown band occurred at the start of the well which is likely to be residual genomic template. In order to eliminate this band conventional PCR was used to amplify the sample DNA using the same primer concentrations but different sample volumes of 1 μ L and 5 μ L. In 1 μ L volume of sample the unknown band was not observed but it could be seen in the 5 μ L sample. This finding suggests that the unknown band was due to genomic DNA (template). When cloning was performed using a 1 μ L sample from the conventional PCR, colonies were observed and also clear bands, of an appropriate size, following restriction analysis. The negative results obtained after sequencing were a disappointment. Time constraints did not allow for further analysis and the reason why the 18S products could not be sequenced remains unclear.

In this study the primers and probes used in real-time PCR assay were able to detect the IS900 sequence of *Map* repeatably. The real-time PCR assay was readily able to detect a single copy of IS900 (*Map*) DNA repeatably. The results presented in this chapter confirm that it detects much less DNA than required to detect a single organism thus making real-time PCR far more sensitive than other methods of detection.

CHAPTER V

COMPARISON OF REAL-TIME PCR TO OTHER DIAGNOSTIC ASSAYS

5.1 Introduction

This Chapter describes the application of real-time PCR for *Map* to the samples collected from the cases described in Chapter 3. It further compares the results from Chapter 3 with results of the real-time PCR assay, finally interpreting all the results in detection of *Map* organisms.

5.2 Materials and methods

The materials and methods used were described in Chapter 2 and in section 4.2.2 of Chapter 4.

Different calculations were performed on the data obtained from the results of real-time PCR, to interpret the results. The C_T values were used to determine log copy number of *Map* and 18S and the formula used was as follows

$$\text{Copy number} = 10^{(C_T \text{ value} - \text{intercept of } Map \text{ standard curve or 18S standard curve} / \text{slope})}$$

The copy number of *Map* is the number of copies of DNA fragments detected on IS900 insertion sequence of *Map* genome using the primer/probe/primer set SF214/PR265/SR289. In the complete genome sequence of a *Map* organism, 17 copies of IS900 were detected (Li *et al.*, 2005), thus the total copy number divided by 17 gives the number of *Map* organisms present. The number of organisms present in 50 μ L of DNA extracted from samples can thus be calculated and expressed as organisms per gram of wet weight of a sample (faeces/tissues) or per millilitre of blood and milk samples.

18S is a housekeeping gene and is present in every eukaryotic cell. The copy number of 18S is the number of copies of DNA fragments detected on the 18S rRNA gene using the primer and probe set designed for this study. Using the methods outlined in 4.2.2, the copy number of 18S was used to calculate the equivalent number of cells present in a DNA sample. The number of *Map* organisms was divided by this calculated cell value and multiplied by 10^8 to derive the number of *Map* cells/ 10^8 tissue cells.

5.3 Results of the detection of *Map* DNA by real-time PCR in clinical samples

- (a) Efficiency of DNA extraction

The DNA extracted from clinical samples was assayed using real-time PCR and the results varied depending on the amount of DNA present in each sample (ranges 13.58 to 42.63). C_T values below the threshold level were regarded as negative and those above were considered positive. A minute variability in C_T values for both *Map* and 18S real-time PCR assays was observed from each individual well, which may be due to errors in adding the sample or may be due to variable DNA concentrations in the wells. The coefficient of variation for C_T values was less than 10% for almost 95% of the samples. Before examining the samples for detection of *Map*, fluorescence had to be observed in every well containing 18S primers and probes; to confirm the presence of DNA. If no fluorescence was detected in 18S wells, then the DNA extraction for those samples was repeated.

Initial experiments showed that the amount of DNA extracted from the samples was low, especially from faecal samples, which resulted in high C_T values for both *Map* and 18S. In order to lower the C_T value, more DNA should be present in each well. This was achieved by improving the DNA extraction technique, by altering some steps in the DNA extraction method provided by the manufacturer. The method described in Chapter 2 was altered, as follows: heating at 95°C for 20 minutes and sonication for 8-10 minutes were included, thus eliminating heating for 5 minutes at 70°C. An additional spin for 10 minutes was inserted after discarding the AW2 buffer and a final step of elution with 50µL of AE buffer was then added instead of the 200µL previously added. Even though the first few steps described above were not applicable to the tissues and other samples, the concluding steps were followed as per the protocol. Extracting DNA using this new method gave good results with decreased C_T values, which were described later.

(b) Results with *Map* and 18S primers and probes

18S specific primers and probes used throughout this study were effective in detecting fluorescence above the threshold level in all the samples, containing DNA. Background fluorescence was also frequently detected in NTC wells. However, given the degree of difference between positive samples (C_T values typically 16) and NTC wells (C_T values typically 35), this background had negligible effect on the assay and was disregarded.

In analysing the samples using *Map* specific primers and probes, there was a marked difference in C_T values between positive and negative controls (NTC), where negatives were below the threshold level. Triplicate wells showed slight variation in results for the same sample; hence, an average of three wells was taken all through this study. The *Map* primer and probe set used in this study were from a published source (Ravva and Stanker, 2005), where the fluorescence detection limits for *Map* was defined as 40 cycles. In this study, samples showing fluorescence after 40 cycles were considered as negative (-*), because at a C_T value of 39.77 one copy of an organism of *Map* was detected on a standard curve. Based on the above the cut off value was set to 40 cycles, above which it is regarded as negative.

(c) Results from clinical samples

All the results from bovine and ovine cases are shown in Table 5.1 and Table 5.2. The C_T values of *Map* in bovine ileal mucosa samples ranged from 20.54 to 27.03 whereas those from ovine ileal mucosa samples ranged from 13.58 to 32.75. In faeces there were no consistent results between animals, but it can be inferred that values <40 are definitely positive. In blood the C_T values were approximately 35, and other tissues had C_T values ranging from 21 to 42.33. This highest reading (mesenteric lymph node in Case 210716) was considered as negative, as it was >40 cycles, the cut off point.

(d) Results with C_T values greater than 40.

In bovine Cases 210716 (mesenteric lymph node), 211253 (ileocaccocolic lymph node) and in ovine Cases 210608 (prescapular lymph node; spleen; foetal liver) and 212384 (faeces) the detection of *Map* was observed at more than 40 cycles (Table 5.1 and 5.2), though 18S values were low (C_T). In bovine Cases 212260 (faeces) and 212261 (uterus) the 18S C_T values are greater than *Map* C_T values, making this a spurious result, for the purpose this study they were classified as negative. These results are not true negatives as the samples may give positive results if they are retested, but because of time constraints they were not repeated.

Samples	210444		210716		210717		211253		212260		212261	
	Map	18S										
Faeces	25.37	17.47	22.35	16.43	33.85	20.14	24.33	19.81	38.74	43.66	30.26	28.02
Heal mucosa	n	n	25.62	17.04	25.87	1724	20.54	16.68	27.03	10.33	21.28	15.78
Blood	37.37	14.47	34.1	17.91	36.32	21.38	37.18	19.88	37.75	20.49	35.38	18.17
Lymph Nodes												
Mesenteric	n	n	42.33	21.44	29.21	20.3	33.69	18.6	29.82	12.15	25.9	10.91
Ileocaecocolic	n	n	-	32.28	34.23	18.61	40.27	32.64	29.64	13.98	31.64	12.72
Iliac	n	n	-	24.52	n	n	36.57	30.92	28.22	10.08	31.71	13.87
Prescapular	n	n	n	n	n	n	n	n	28.98	12.36	37.09	14.42
Retropharyngeal	n	n	39.65	16.56	n	n	36.08	15.61	26.03	10.67	33.98	14.5
Popliteal	n	n	-	34.43	n	n	n	n	34.19	13.12	32.08	12.44
Supra mammary	n	n	39.35	24.86	n	n	37.22	18.8	31.93	10.81	32.96	12.41
Tonsil	n	n	31.39	10.97	n	n	35.57	18.4	28.7	9.79	32.35	11.83
Mammary Secretions	n	n	-	12.92	38.05	13.19	n	n	30.64	12.07	n	n
Mammary tissue	n	n	25.77	24.43	n	n	32.88	19.13	34.13	10.58	27.56	22.04
Uterus	n	n	28.08	18.31	38.47	19.86	30.52	15.68	31.82	11.98	34.9	-
Liver	n	n	n	n	n	n	28.88	13.66	29.56	9.94	n	n
Spleen	n	n	n	n	n	n	33.35	13.58	34.6	11.11	n	n
Kidney	n	n	n	n	n	n	36.34	11.61	32.28	10.04	n	n
Muscle	n	n	n	n	n	n	30.03	16.57	30.88	13.6	34.86	20.11
Ileocaecal valve	n	n	n	n	34.97	17.76	n	n	24.46	9.89	n	n

Values mentioned above are average C_T values of 3wells; n unable to collect the sample; - unable to detect fluorescence above threshold during 45 cycles; *Map* C_T values in wells with *Map* primers and probe; 18S C_T values in wells with 18S primers and probe.

Table 5.1 Real-time PCR results (C_T values) in various bovine tissue samples

Samples	209942		210552		210608		211056		212384	
	Map	18S								
Faeces	39.87	16.59	21.85	20.21	31.96	16.42	21.23	12.42	40.58	34.67
Ileal mucosa	28.32	16.89	15.19	10.62	32.75	12.3	13.58	12.34	17.3	13.19
Blood	34.46	15.99	n	n	35.29	18.22	n	n	n	n
Lymph Nodes										
Mesenteric	n	n	n	n	35.81	12.67	30.28	14.8	27.51	14.13
Ileocaecocolic	n	n	n	n	n	n	n	n	24.73	12.28
Iliac	n	n	n	n	39.07	14.27	n	n	31.04	17.03
Prescapular	n	n	n	n	41.46	17.49	n	n	34.79	18.32
Popliteal	n	n	n	n	n	n	n	n	27.32	13.79
Supra mammary	n	n	n	n	n	n	n	n	32.33	17.19
Mammary Secretions	n	n	n	n	n	n	n	n	34.24	15.48
Mammary tissue	n	n	n	n	34.77	14.98	n	n	31.05	16.51
Uterus	n	n	n	n	36.55	12.63	n	n	33.83	13.57
Liver	n	n	n	n	34.57	12.81	n	n	n	n
Spleen	n	n	n	n	41.33	17.5	n	n	n	n
Kidney	n	n	n	n	35.89	14.08	n	n	n	n
Muscle	n	n	n	n	-	15.82	n	n	21	19.13
Other samples	n	n	n	n	F	F	n	n	n	n

Values mentioned above are average C_T values of 3 wells; n unable to collect the sample; - unable to detect fluorescence above threshold during 45 cycles; F foetal samples; Map C_T values in wells with Map primers and probe; 18S C_T values in wells with 18S primers and probe.

Foetal samples of 210608		Map	18S
Membranes		37.02	13.31
Amniotic fluid		34.91	23.29
Other foetal fluids		32.96	18.83
Intestines		35.53	17.81
Spleen		38.78	12.68
Liver		42.63	15.35
Muscle		36.58	11.88

Table 5.2 Real-time PCR results (C_T values) in various ovine tissue samples; Right: foetal samples.

5.4. Calculation of the number of organisms present in each tissue

Using arithmetic calculations, an approximation of the number of organisms in each tissue was calculated based on the C_T values obtained from the real-time PCR (Table 5.3, Table 5.4). The calculations were presented in two ways, first the number of *Map* organisms present with respect to number of cells in each tissue (A), and second the number of *Map* organisms present with respect to the amount of sample taken, which is further equated to 1gram or 1millilitre of sample (B). The levels of *Map* organisms in varied widely from sample to sample, whether it was a sample from same case but different tissue or it was sample from same tissue in two different cases. So, a consistent level has not been found in any of the samples. In general low C_T values indicated that there were more organisms present, i.e. C_T values were inversely proportional to number of organisms present in each sample. The numbers of *Map* organisms were highest in the ileal mucosa samples followed mostly by faecal samples. In Case 211056 the C_T value of *Map* in ileal mucosa was 13.58 and the number of organisms in this sample by either method of calculation was highest, 9.5×10^6 organisms/ 10^8 cells and 1.5×10^9 organisms/gram. Faecal samples collected showed results ranging from 1 organism to a maximum of 1.2×10^6 organisms per gram of faeces: interestingly both were from ovine samples. The blood samples of 1mL also showed a moderate number of organisms in all the cases; the C_T value of *Map* in blood samples was highest in Case 212260 with 37.75 and their corresponding number of organisms detected were 25 organisms/ 10^8 cells (15 organisms/mL). In Case 210444, 34 organisms were found per 10^8 cells and 2.61×10^2 organisms were present per mL, the highest level in both bovine and ovine blood samples.

In mammary secretions the number of organisms varied from 1 to 1.56×10^3 /mL. The results for bovine mammary secretions, mammary tissue and supra mammary lymph node were quite surprising. In Case 210716 mammary secretions were negative for *Map* organisms, but supra mammary lymph nodes contained 62 organisms/ 10^8 cells (32 organisms/gram), also mammary tissue has 5.7×10^5 organisms/ 10^8 cells (3.5×10^5 organisms/gram). In Case 212260 mammary secretions has 68 organisms/ 10^8 cells (1.56×10^3 organisms/mL) but supra mammary lymph nodes has 16 organisms/cells (5.16×10^3 organisms/gram), while mammary tissue has 3 organisms/ 10^8 cells (1.14×10^3 organisms/gram). In ovine Case 212384 mammary secretions have 28 organisms/ 10^8 cells (1.32×10^2 organisms/mL) but supra mammary lymph nodes has

Samples	210444		210716		210717		211253		212260		212261	
	A	B	A	B	A	B	A	B	A	B	A	B
Faeces	3.07×10^4	5.86×10^3	1.51×10^5	4.67×10^2	3.09×10^2	1.73×10^2	1.84×10^3	1.19×10^2	—*	1.37×10^3	2.03×10^3	
Intestines	n	n	2.12×10^4	3.95×10^5	1.95×10^4	3.33×10^5	5.90×10^5	1.29×10^7	3.66×10^2	1.59×10^5	2.34×10^5	7.80×10^6
Blood†	3.4×10	2.61×10^2	9.3×10	1.45×10^2	1.00×10^2	3.2×10	2.8×10	1.8×10	2.5×10	1.5×10	4.4×10	6.0×10
Lymph nodes												
Mesenteric	n	n	—*	—*	8.07×10^3	3.35×10^4	1.70×10^2	1.54×10^3	1.24×10^2	2.34×10^4	1.04×10^3	3.25×10^5
Ileocaecocolic	n	n	—	—	1.18×10^2	1.06×10^3	—*	—*	3.27×10^2	2.65×10^4	4.6×10	6.30×10^3
Iliac	n	n	—	—	n	n	6.83×10^2	2.13×10^2	1.44×10^2	7.03×10^4	7.5×10	6.01×10^3
Prescapular	n	n	n	n	n	n	n	n	2.44×10^2	4.16×10^4	2	1.49×10^2
Retropharyngeal	n	n	†	2.6×10	n	n	8	2.98×10^2	8.52×10^2	2.98×10^5	2.1×10	1.26×10^5
Popliteal	n	n	—	—	n	n	n	n	1.0×10	1.09×10^3	3.0×10	4.66×10^3
Supra mammary	n	n	6.2×10	3.2×10	n	n	1.6×10	1.36×10^2	1.6×10	5.16×10^3	1.6×10	2.54×10^3
Tonsil	n	n	2.5×10	7.49×10^2	n	n	4.3×10	4.24×10^2	9.1×10	4.75×10^2	1.9×10	3.87×10^3
Mammary secretion†	n	n	—	—	†	1.0×10	n	n	6.8×10	1.56×10^3	n	n
Mammary tissue	n	n	5.75×10^5	3.56×10^5	n	n	3.78×10^2	2.69×10^2	3	1.14×10^5	5.59×10^4	1.04×10^5
Mammary tissue	n	n	7.02×10^3	7.28×10^4	n	n	3.91×10^2	1.36×10^4	2.9×10	5.57×10^3	n	n
Uterus	n	n	n	n	1.1×10	5.8×10	4.76×10^2	4.20×10^4	5.4×10	2.63×10^4	n	n
Liver	n	n	n	n	n	n	2.1×10	1.94×10^3	3	8.25×10^2	n	n
Spleen	n	n	n	n	n	n	n	2.50×10^2	9	4.06×10^2	n	n
Kidney	n	n	n	n	n	n	†	1.90×10^4	1.17×10^2	1.06×10^4	1.52×10^2	6.90×10^2
Muscle	n	n	n	n	n	n	8.25×10^2	n	1.75×10^3	8.77×10^3	n	n
Ileocaecal valve	n	n	n	n	4.8×10	6.40×10^2	n	n	n	n	n	n

A Number of *Map* organisms/ 10^6 cells based on their C_T values in 50 μ L extracted DNA; B Number of *Map* organisms per gram/mL based on their C_T values in 50 μ L extracted DNA. —* considered as negative, † all these samples are measured in millilitres hence the organisms are per millilitre

5.3 An approximate number of organisms present in various bovine samples based on their C_T values.

Samples	209942		210552		210608		211056		212384	
	A	B	A	B	A	B	A	B	A	B
Faeces	1	3	1.21×10 ⁶	6.59×10 ⁵	2.04×10 ²	6.33×10 ²	5.16×10 ⁴	1.00×10 ⁶	—*	—*
Ileal mucosa	3.09×10 ³	6.17×10 ⁴	1.43×10 ⁶	5.12×10 ⁸	1.8×10	2.94×10 ³	9.55×10 ⁶	1.55×10 ⁹	1.09×10 ⁶	1.20×10 ⁸
Blood†	3.0×10	1.14×10 ²	n	n	4.7×10	6.4×10	n	n	n	n
Lymph nodes										
Mesenteric	n	n	n	n	3	3.59×10 ²	3.07×10 ²	1.60×10 ⁴	1.51×10 ³	1.07×10 ⁵
Ileocaecocolic	n	n	n	n	n	n	n	n	4.36×10 ³	7.28×10 ⁵
Iliac	n	n	n	n	1	3.8×10	n	n	5.09×10 ²	9.52×10 ³
Prescapular	n	n	n	n	—*	—*	n	n	7.0×10	7.24×10 ²
Popliteal	n	n	n	n	n	n	n	n	1.47×10 ³	1.22×10 ⁵
Supra mammary	n	n	n	n	n	n	n	n	2.26×10 ²	3.927×10 ³
Mammary secretions†	n	n	n	n	n	n	n	n	2.8×10	1.32×10 ²
Mammary tissue	n	n	n	n	1.5×10	7.34×10 ²	n	n	3.98×10 ²	9.46×10 ³
Uterus	n	n	n	n	2	2.16×10 ²	n	n	1.5×10	1.40×10 ³
Liver	n	n	n	n	6	8.42×10 ²	n	n	n	n
Spleen	n	n	n	n	—*	—*	n	n	n	n
Kidney	n	n	n	n	5	3.40×10 ²	n	n	n	n
Muscle	n	n	n	n	—	—	n	n	1.32×10 ⁶	9.45×10 ⁶
Other samples	n	n	n	n	F	F	n	n	n	n

Foetal samples of 210608	Number of <i>Map</i> organisms per gram/mL based on their Ct values in 50µL extracted DNA	
	A	B
Membranes	2	1.56×10 ²
Amniotic fluid†	6.37×10 ²	8.3×10
Other foetal fluids†	3.12×10 ²	3.18×10 ²
Ileal mucosa	3.3×10	4.35×10 ²
Spleen	0.3	4.7×10
Liver	—*	—*
Muscle	1	2.12×10 ²

A Number of *Map* organisms/10⁶ cells based on their Ct values in 50µL extracted DNA, B Number of *Map* organisms per gram/mL based on their Ct values in 50µL extracted DNA.

—* considered as negative, † all these samples are measured in millilitres hence the organisms are per millilitre.

5.4 An approximate number of organisms present in various ovine samples based on their Ct values.

2.26×10^2 organisms/ 10^8 cells (3.92×10^3 organisms/gram) while mammary tissue has 3.98×10^2 organisms/ 10^8 cells (9.46×10^3 organisms/gram). The results indicate that *Map* organisms were present in high amounts in mammary lymph node and it remains uncertain why *Map* was not detected in the mammary secretions of Case 210716 even though it was detected in high amounts in mammary tissue.

All the lymph nodes showed reasonable numbers of organisms. Mesenteric lymph node contained high numbers of organisms ranging from 3 organisms/ 10^8 cells (3.59×10^2 organisms/gram) in ovine Case 210608, to 1.040×10^3 organisms/ 10^8 cells (3.25×10^5 organisms/gram) in bovine Case 212261. Second to mesenteric lymph nodes were the ileocaecocolic, iliac, retropharyngeal lymph nodes and tonsil. Liver contained more organisms when compared to the other visceral organs like spleen and kidney, which is as high as 4.76×10^2 organisms/ 10^8 cells (4.20×10^4 organisms/gram) in Case 211253. The most surprising results are from muscle tissue, where numbers of organisms present in a gram of tissue were as high as 9.4×10^6 in Case 212384 which is almost equal to a normal infected ileal mucosa. Even the ileal mucosa of Case 212384 contained numbers as high as 1.2×10^8 organisms/gram, which is to be noted. Negative results were observed in the muscle tissue of 210608, and foetal muscle tissue was also positive with *Map* numbers ranging from 1 organism/ 10^8 cells to 2.12×10^2 organisms/gram. The levels of organisms observed in the uterus were not very high. Interestingly, in Case 210608 the number of *Map* organisms present in uterus are as low as 2 organism/ 10^8 cells and 2.16 organism/gram, but numbers of *Map* organisms in the foetal samples are shown in Table 5.4, where foetal fluids and foetal ileal mucosa were shown to contain higher numbers than the uterus.

In this study a single cell of *Map* per gram was detected in Cases 209942 (faeces), 210608 (iliac lymph node), 210716 (retropharyngeal lymph node), 210717 (mammary secretions), 211253 (kidney), whose C_T values are 39.87, 39.07, 39.65,

5.5 Comparing the results of real-time PCR of *Map* with other diagnostic results in this study

The results of real-time PCR examination are compared with the earlier results in Table 5.5 and Table 5.6. Analysis of all the results from bovine and ovine samples showed variation in diagnostic results. Acid-fast staining was positive for *Map* in all Cases except Case 210444 and faecal smear of Case 212384. All the

Samples	210444			210716			210717			211253			212260			212261			
	ZN	HP	EA	RT															
Faeces	+		+	+		+	+		+		+	+		+		+		+	+
Ileal mucosa	+		+	+		+	+		+		+	+		+		+		+	+
Blood	+		+	+		+	+		+		+	+		+		+		+	+
Lymph Nodes	+		+	+		+	+		+		+	+		+		+		+	+
Mesenteric	+		+	+		+	+		+		+	+		+		+		+	+
Ileocaecocolic	+		+	+		+	+		+		+	+		+		+		+	+
Iliac	+		+	+		+	+		+		+	+		+		+		+	+
Prescapular	+		+	+		+	+		+		+	+		+		+		+	+
Retropharyngeal	+		+	+		+	+		+		+	+		+		+		+	+
Popliteal	+		+	+		+	+		+		+	+		+		+		+	+
Supra mammary	+		+	+		+	+		+		+	+		+		+		+	+
Tonsil	+		+	+		+	+		+		+	+		+		+		+	+
Mammary Secretions/ Milk	+		+	+		+	+		+		+	+		+		+		+	+
Mammary tissue	+		+	+		+	+		+		+	+		+		+		+	+
Uterus	+		+	+		+	+		+		+	+		+		+		+	+
Liver	+		+	+		+	+		+		+	+		+		+		+	+
Kidney	+		+	+		+	+		+		+	+		+		+		+	+
Spleen	+		+	+		+	+		+		+	+		+		+		+	+
Muscle	+		+	+		+	+		+		+	+		+		+		+	+
Ileocaecal valve	+		+	+		+	+		+		+	+		+		+		+	+

ZN Acid-alcohol fast staining; HP Histopathology; EA ELISA; RT Real-time PCR; - Negative result; + Positive result; -* unable to detect before 40 cycles; n unable to collect sample

Table 5.5 Summary of diagnostic results from suspected Johne's disease cattle used in this study

histopathology reports were positive for *Map*, apart from Case 210444 which was negative and Case 210608 which was only suspected to be *Map* positive. ELISA reports were given only in bovine cases and all reports were positive except for Case 210444. ELISA, post-mortem and histopathological examinations were completely based on the reports submitted to the clinicians whereas acid-fast staining and real-time PCR results were based on this work.

The most controversial case of all is Case 210444, where diagnosis by the commonly used tests failed to detect *Map* but real-time PCR assay detected it as *Map* positive in faeces and in blood. Acid-fast staining and histopathology reports were negative, even the widely accepted ELISA showed negative results. Even using real-time PCR the organisms could not be demonstrated initially, but after modified DNA extraction methods there was a remarkable decrease in C_T values. Other cases which showed some marked decrease in C_T values were, the faecal sample from Case 210444, where it has decreased from 41.79 to 25.37. Other samples which showed this difference are; a faecal sample from Case 210716 decreased from 35.1 to 22.35; ileal mucosa of Case 211056 decreased from 17.99 to 13.58; foetal membranes from the foetus of Case 210608 decreased from 39.01 to 37.02; foetal ileal mucosa from foetus of Case 210608 decreased from 38.42 to 35.53. The positive control was also decreased from 29.27 to 17.64. Case 210552, 211056 and 212384, had pigmented intestines and their C_T values were also low; and at the same time even though 209942 has pigmented intestines their C_T value was greater.

In this study *Map* organisms were detected in gastrocnemius muscle of cows by real-time PCR assay for the first time; 3/3 cases were positive for *Map*. Other bovine samples like faeces (5/6), blood (5/5), ileal mucosa (6/6), tonsil (4/4), retropharyngeal lymph nodes (4/4), mesenteric lymph nodes (5/5), supra mammary lymph nodes (4/4), mammary tissue (4/4), uterus (4/4), liver (2/2), spleen (2/2) and ileocaecal valve were also positive with real-time PCR assay. Tissue samples were negative in some cases: ileocaecocolic lymph node (2/5), iliac lymph node (1/4), prescapular lymph nodes (1/3), popliteal lymph node (1/3) and mammary secretions (1/3) were *negative*.

In this study *Map* was detected in foetal membranes, amniotic fluid, other foetal fluids, foetal ileal mucosa, foetal spleen, foetal liver and foetal muscle (*hind limb*) using a real-time PCR assay. The results were from Case 210608, which is surprising as all samples collected were positive for *Map* when assayed with real-time PCR despite the inability to demonstrate *Map* in these tissues. All other ovine samples collected were

positive for *Map* including the muscle tissue of Case 212384. The prescapular lymph node, muscle tissue and spleen samples from Case 210608 and faecal sample from Case 212384 were negative (Table 5.6).

5.6 Discussion

The results in this chapter, which comprise the real-time PCR results for *Map*, quantitation of the *Map* results and their interpretation are discussed below. Only a small number of cases were examined but the results obtained enabled the method to be evaluated and compared with results of conventional testing obtained in Chapter 3.

High numbers of *Map* organisms were found in all the ileal mucosal samples collected from both bovine and ovine cases. This could be due to the severity of *Map* in the intestines. Pigmented ovine Cases 211056 and 212384 showed high numbers of *Map* organisms in their ileal mucosa, but Case 209942 did not. The faecal samples showed a considerable amount of *Map* in all cases but results were not always as consistently high as those observed in ileal mucosa. This may be due to faecal consistency and/or the formation of micro-colonies or because of the tendency of *Map* to clump, thus resulting in a scattered distribution of organisms. The maximum numbers of *Map* were found in ovine samples; this may be due to their pellet form of faeces. The lowest numbers found were also in ovine samples and this can be due to clumping nature of the organisms, which can escape during collection of small volumes of faeces. In this kind of situations, a constant dry weight of faecal samples would prove to give more accurate results, which was not done in this study. All the lymph nodes and visceral organs showed reasonable numbers of organisms, which indicates they are disseminated throughout the body. When compared with histopathology all the bovine and ovine cases showed enlarged and necrosed lymph nodes, except Case 210444. Even though the pathology of lymph nodes is good they failed to show high numbers of organisms. The results may be quite interesting if a consistent sample collection was performed, especially in Case 210444. The mesenteric lymph node is a common site for high numbers of organisms. This can be explained by the fact that these organs drain the lymph from distal ileum, jejunum and colon which are predilection sites of *Map*. Ileocaecocolic and iliac lymph nodes are subordinate to mesenteric lymph nodes explaining why these have fewer numbers of *Map* compared to mesenteric lymph nodes. Tonsil and retropharyngeal lymph nodes have the highest numbers of organisms after the mesenteric lymph node which may be due to oral route of infection where the

primary site of infection is the tonsil which further passes in to the retropharyngeal lymph node. In mammary secretions the numbers of organisms varied in each sample, though these values may be due to various stages of infection or lactation. It remains uncertain why *Map* was not detected in the mammary secretions of Case 210716 even though it was detected in high amounts in mammary tissue. This may be due to the stage of infection, whether animals were entering the dry period or an animal entering lactation or perhaps *Map* milk was associated with inflammation. The levels of organisms observed in the uterus were not very high but in Case 210608 it is interesting to find organisms in various foetal samples. The results of other internal organs like liver, spleen and kidney are unusual since they contain high number of organisms, without any signs of gross pathology in these organs. This indicates that, although the *Map* predilection site is ileal mucosa it is disseminated throughout the body without even showing any signs of pathology in the respective organs. One finding which was detected grossly in this study was if the number of *Map* organisms was high in lymph nodes, it was lower in other visceral organs and vice versa. This can be observed in Cases 211253 and 212260. Perhaps this finding should be studied in detail with a greater number of samples; this may help in understanding the stages of infection and its shedding pattern.

The above results demonstrate *Map*'s dissemination inside the host body, and can support the view that spread of infection inside the body is via lymphatics (Payne and Rankin, 1961). Further it supports that it supports previous findings that *Map* can be detected in muscle (Bosshard *et al.*, 2006), and other foetal tissues (Lawrence *et al.*, 1956; Seitz *et al.*, 1989; Sweeney *et al.*, 1992). These results confirm that real-time PCR is more sensitive than ELISA and the microscopic staining techniques.

CHAPTER VI

GENERAL DISCUSSION

6.1 Introduction: Johne's disease

Johne's disease is one of the major diseases of cattle and sheep and also wildlife. Infection cannot be detected by the farmer until the initial clinical signs like diarrhoea, wasting and sub-mandibular oedema develop. These typically take 6 months to 5 years to develop in to a clinical infection thus, by the time an infection is diagnosed; the animal will be at a late clinical or advanced stage of infection. In the meantime, the animal sheds *Map* widely through faeces and milk, further contaminating the rest of the herd and the environment. Ultimately, the animal has to be slaughtered since there is no effective treatment, and also to limit the spread of infection. Although affected animals show signs of wasting and diarrhoea, there are no pathognomonic pre-clinical signs, making early diagnosis difficult. The affected animals gradually deteriorate in condition and succeed to secondary infections due to immunosuppression. Initially *Map* triggers the animals' immune system but later escapes by misdirecting the host inflammatory response, leading to chronic inflammatory lesions, mainly in the submucosa (Clarke, 1997). The mucosa and sub-mucosa lose their integrity and structure, which ultimately leads to chronic diarrhoea and wasting. It is not necessary for the animal to become a clinical case (Lawrence, 1956). The major problem in a *Map* affected cow is its silent stage of infection, as considerable economic losses are associated with sub-clinical infection, which must be controlled.

6.2 The importance of Johne's disease in animal trade and public health

The increasing prevalence of Johne's disease in cattle and sheep around the world makes it significant. It is a major hindrance to the trade of animals and their products and is of major economic importance. Even though it is not a major problem of interest in developing countries, there are reports of its prevalence in both domestic animals and wildlife (Siva Kumar *et al.*, 2005). The increased focus on *Map* playing a major role in Crohn's disease patients and concerns of public health importance like detection of *Map* in milk, river water etc, makes it as direct significance to human health (Grant, 2005).

6.3 Current methods of detection and their relationship to control measures

Even after extensive research for decades, there are no effective control measures to eradicate this disease; which is hampered by the lack of accurate and sensitive diagnostic methods and of a widely available and effective vaccine. The resistance of *Map* to disinfectants and in the environment allows it to survive for prolonged periods. The major requirement to control this disease effectively is a rapid method for early detection of infected animals. As there is no effective treatment for Johne's disease, the best control method is to prevent spreading and transmission to other animals. The transmission of *Map* is possible, even through animals shedding low amounts of *Map*. Small doses of organisms can establish infection (Sweeney, 1996) in any stage of animal's life, though there will be some age-related resistance. Transplacental transmission and direct transmission through milk/colostrum can take place. *Map* can be transmitted in absence of clinical signs of Johne's disease.

Presently, the fastest and easiest way to measure the prevalence of Johne's disease is by serum ELISA and later confirmation by isolation of organisms. In order to confirm a herd as Johne's affected, it takes at least 3 – 4 months or the finding of pathognomonic lesions at post-mortem. Real-time PCR is more sensitive and specific for detection of *Map* than all other techniques and gives results in 24 hrs.

In this study, the real-time PCR was shown to have advantages when compared to the other diagnostic tests used. Even though there are studies on using real-time PCR for detecting *Map*, still there are some problems in identifying specific primers and probes for detecting *Map*; routine methodology for extraction of DNA from clinical samples; its distribution in the host.

6.4 The value of real-time PCR results in diagnosis of Johne's disease

In this study real-time PCR detected as little as a single copy number of the insertion sequence IS900 of *Map* in field samples using the primer/probe combination of Ravva and Stanker (2005). This low amount of DNA was observed in the silent stage of infection and cannot be detected by using ELISA or other diagnostic tests presently used, therefore allowing early detection of infection in animals affected with Johne's disease. As the major predilection site for infection is the intestine, high numbers of organisms are present in ileal samples. As it is not feasible to take an intestinal sample

for diagnosis, other ante-mortem samples must be used for diagnosis including faecal, blood and milk samples. The next best sample after ileal mucosa with more number of organisms is the faecal sample though some lymph nodes showed more number of organisms. Collecting biopsy samples from lymph nodes or collection of lymph may help in getting early and good results but it is a cumbersome procedure. Blood and milk samples can also give good results much quicker than faecal samples, because DNA extraction is easier in these samples than from faeces. An alternate method of diagnosis which should be focused on is by examining rectal biopsies, which is already being used for diagnosing scrapie. The various foetal samples like placenta and other foetal fluids can be collected at the time of parturition and can be sent for routine diagnosis of Johne's disease on a farm. If *Map* organisms are present in these fluids there is more chance of transmitting them to the foetus, even though they may not be detected in the new born, initially. Diagnosis at this early stage is a real benefit, as it allows control of the silent spread of infection in the farm due to associated production losses.

6.5 The use of real-time PCR in carcass inspection

Most of the samples collected for this study may not be useful for carcass examination except muscle tissue, prescapular and popliteal lymph nodes and occasionally retropharyngeal lymph nodes. When muscles like gastrocnemius from a sheep were examined using real-time PCR assay results revealed a surprisingly high number of 9.4×10^6 of organisms in 1 gram. Though the results were not as high as sheep carcass, cattle carcasses showed 1.9×10^4 of organisms/gram. The prescapular lymph node showed the lowest organisms of all lymph nodes examined, but still numbers of *Map* were as high as 4.1×10^4 organisms/g. Popliteal lymph node showed smaller numbers of *Map* organisms in cattle carcasses but high number of 1.2×10^5 organisms per 1 gram were only found in only one sheep carcass. Real-time PCR therefore also allows the detection of carcass contamination by *Map* organisms. Further studies should be performed to evaluate the number of organisms in carcass tissues.

6.6 Relative costs of major diagnostic methods

The current prices in the UK for diagnosing Johne's disease animal as per DEFRA (Department for Environment, Food and Rural Affairs) and VLA (Veterinary

Laboratory Agencies) are; for detecting *Map* antibodies (serum) by ELISA – £6.90; for detecting *Map* antibodies (serum) by AGID – £8.00; for detecting *Map* by (faeces) ZN staining – £12.00; for detecting *Map* antibodies (serum) by CFT – £23.00; for detecting *Map* by (faeces) culturing – £30.70; for detecting *Map* DNA by using conventional PCR – £26.00; (SAC, 2007) for detecting *Map* DNA using real-time PCR – £22.50 (recently introduced). Among all tests the most specific and sensitive tests are culturing, PCR and real-time PCR, but the cheapest and quickest among these real-time PCR. This indicates that real-time PCR is the best diagnostic method in diagnosing Johne's disease, with quick and reliable results. At the start of this project VLA was not using real-time PCR for diagnosis of Johne's disease. According to VLA online literature, even though it is not yet accredited by United Kingdom accreditation service (UKAS), they achieved some good results from field samples. The real-time PCR technique used by VLA is a LightCycler® system which uses hybridisation probes, while in this study Applied Biosystems 7500 Real-Time PCR System (Applied Biosystems, UK) was used which in this study detects *Map* DNA of 1log copy/ μ L.

6.7 The findings of this study in relation to transmission and public health

In this study, the approximation of numbers of organisms, based on the real-time PCR results, gives an idea to a clinician as to how to react to a particular animal in a farm rather than just a positive or negative result. It can give an approximation and can predict how extensively the organisms are shed and spread to its immediate environment during the entire period of infection, resulting in better control of disease. The maximum numbers of organisms of *Map* contained in 1 gram of ovine faeces were observed to be 1.2×10^6 , which falls in between the estimated oral infectious dose of 10^6 – 10^8 bacilli in sheep (Whittington and Sergeant, 2001). So shedding of this nature in a farm may not only transmit the disease in that farm but also to wildlife like rabbits (Daniel *et al.*, 2003). This results in the transmission of organisms into a different ecosystem and food chain may occur where they in turn can transmit them to a whole new set of animals or can re-infect the same animals. An interesting result is finding an approximate numbers of *Map* organisms (9.4×10^6) in 1gram of an ovine muscle tissue, which is more than the estimated oral infectious dose of 10^3 bacilli in a sheep (Whittington and Sergeant, 2001). In this short study, it may be difficult to say how well it can establish infection, but certainly transmission can occur through this infected

meat. The possible routes of infection here can either be, through raw meat and also through other offal. The wild animals which can be infected through meat include foxes, stoats and weasels. Once these get infected they can shed the organisms throughout the environment. This study further supports Daniel and others (2003), where rabbit carcass included with a potentially infected lymph node can transmit the disease to foxes, stoats and weasels and further studies are needed to conclude the role of meat. Therefore, more attention has to be focussed on the infection of wildlife with *Map* on consumption of this meat, as they are the unknown silent shedders.

Detection of *Map* in the gastrocnemius muscle of bovine and ovine samples also raises an issue for public health, as consuming the meat from an infected animal could be a source of infection for humans. Humans may consume under cooked meat, and also meat consumed along with lymph nodes like popliteal. *Mycobacterium avium paratuberculosis* is able to survive in processed milk subjected to pasteurisation (Grant *et al.*, 2002). *Map* has a tendency to clump, and these clumped organisms demonstrate higher thermal resistance than the single organisms (Rowe *et al.*, 2000). Bearing the above two points in mind, more studies should be focussed on what are the possibilities of *Map* entering the food chain through raw meat/under cooked meat/completely cooked meat.

Low levels of *Map* organisms were observed in uterus samples including Case 210608, such that detection of *Map* in various foetal tissues of Case 210608 was surprising. Taking this case into consideration, if a Johne's diseased animal with such low numbers of *Map* organisms can transmit the disease to its offspring, what can be the level of transmission in animals with high numbers of *Map*?

Also a further study may provide information about their entry into the foetal tissues and their fate in those tissues i.e. what happens after the birth. If they are present in the neonatal animal, what are the chances of the neonate developing resistance/silent shedding/clinical disease? The factors which influence the dormancy of *Map* until the animal gives birth itself are unknown. If so what is the role of this dormancy in developing resistance to *Map*? What are the primary sites of *Map* in a foetus and why do they stay dormant instead of aborting the foetus? Do they only need macrophages to replicate and disseminate in the animal? In order to get the answers for questions further detailed research studies should be done. This study has opened a new discussion on transmission of *Map* through meat, but more detailed studies are required in order come to better conclusions.

In summary, a rapid and quantitative real-time PCR assay for *Map* using TaqMan[®] probes has been evaluated in field cases. This assay is effective in detecting at least a single *Map* cell even after extraction losses of DNA. It is also sensitive and specific and can be used for routine detection in clinical samples. As real-time PCR is expensive when compared to other diagnostic techniques, the concentration of primer/probe/primer dilutions has been reduced to an effective combination, so that it can reduce some cost. Also, real-time PCR assay in conjunction with automated culture techniques can reduce both time and cost in herd testing. Although problems with 18S standardisation were found, this problem will not be a hindrance in detecting *Map*. Further, it appears that it is better to use other housekeeping genes than 18S in the detection of *Map*.

As long as strict and well planned control programmes are not prepared, *Map* is likely to spread within infected herd and also among the other species of animals mainly through rodents as they are difficult to control. Considering the present status of the disease, "prevention is better than cure".

Appendix I

Reagents used in this study

Preparation of 1% Carbol fuchsin

Basic fuchsin	1gram
Absolute alcohol	10mL
5% phenol in distilled water	up to 100mL

Dissolve the basic fuchsin in absolute alcohol, then mix with the phenol solution, filter and use.

Preparation of 3% acid alcohol

3mL Hydrochloric acid is dissolved in 97mL of 95% alcohol; use.

Preparation of Loeffler's methylene blue

1% Methylene blue in 95% ethanol	30mL
1% potassium hydroxide	1mL
Distilled water	up to 100mL

Preparation of phosphate buffered saline (PBS)

Sodium chloride (NaCl)	8grams
Potassium chloride (KCl)	0.2grams
Sodium phosphate, dibasic (Na_2HPO_4)	1.15grams
Potassium phosphate, monobasic (KH_2PO_4)	0.208grams

Dissolve the ingredients in 800mL of distilled water, adjust the pH to 7.4 and make the volume up to 1000mL; use.

Ammonium Chloride lysis buffer

Ammonium chloride (NH_4Cl)	8.29grams
Potassium bicarbonate (KHCO_3)	1gram
EDTA disodium salt	37mg

Dissolve the ingredients in 900ml. of distilled water, adjust the pH to 7.2 and make the volume up to 1000mL; use.

Preparation of 10x TBE

Tris Base Fisher Scientific UK Ltd, UK)	216g
Boric Acid (Fisher Scientific UK Ltd, UK)	110g
EDTA (Sigma-Aldrich Company Ltd, UK)	16.9g

Dissolve the ingredients in 1.5 litre Millipore Distilled Water (Millipore Corporation, UK). Adjust pH to 8.2-8.3 using NaOH/HCL and make the volume up to 2 litres; use.

QIA amp[®] DNA stool mini kit (50), (QIAGEN Ltd, UK)

The kit includes Buffer ASL, Buffer AL, Buffer AW1, Buffer AW2, Buffer AE, Proteinase K, Inhibitex tablet, QIA amp spin columns with 2mL collection tube and 2 mL collection tubes.

QIA amp[®] DNA mini kit (50), (QIAGEN Ltd, UK).

The kit includes Buffer ATL, Buffer AL, Buffer AW1, Buffer AW2, Buffer AE, Proteinase K, QIA amp spin columns with 2mL collection tube and 2 mL collection tubes.

PureLink[™] Quick Plasmid Miniprep Kit

The kit includes resuspension buffer (R3), lysis buffer (L7), precipitation buffer (N4), TE Buffer (TF), wash buffer (W10), wash buffer (W9), spin columns, 2mL wash tubes, 1.5-mL recovery tubes.

Luria Bertani- medium:

Tryptone	10g
Yeast extract	5g
Sodium chloride (NaCl)	10g
Agar	15g

SOC medium:

Tryptone	2%
Yeast Extract	0.5%
NaCl	10 mM
KCl	2.5 mM

MgCl	210 mM
MgSO ₄	10 mM
Glucose	20 mM

Formulas

$$\text{Centrifugal force (g)} = 1.118 \times \text{Radius of rotor} \times \text{rpm}^2 / 10^5$$

2401 GCACGACGTG TTCGCCATGC CGTTCAGAC GATGCCCGAA TTCTTGAACC GGTCCCGGA CGCCGCAAG AGCTGSCCA GCGGGCCCG GCGCCGCTG
CGTCTGCAC AAGCGTACG GCAGCTCTG CTAGCGCTT ACAACTTGG CAAGCECTT GCGGCGTTC TTGCACTGGT CCGCCCGGGC GCGGCGCGAC
2501 GCGAGCTTCG CCGCGCCCG CCGACCCCG CCGGACGCGC ACCGGATCG
CGTCTGAAC GGGCCCGCC GGTGGCGG GCGTGCDCG TGGCTTAGC

REFERENCE LIST

Aho, A. D., McNulty A. M., and Coussens P. M. (2003). Enhanced Expression of Interleukin-1 {alpha} and Tumour Necrosis Factor receptor-associated protein 1 in ileal tissues of cattle infected with *Mycobacterium avium* subsp. *paratuberculosis*. *Infection and Immunity*; **71**, 6479-6486.

Animal Health Australia, 2007; website

<http://www.animalhealthaustralia.com.au/ahhc/programs/jd/nidcp.cfm>

Annau, E. (1958). Purified complement-fixing antigen from *Mycobacterium johnei*. *Nature*; **181**, 1206-1207.

Artus[®] M. paratuberculosis PCR kit by QIAGEN, Hamburg (March, 2006);

<http://www.qiagen.com/literature/protocols/artusMparatuberculosisPCRKitRUO.aspx>

Barrow, W. W., Wright E. L., Goh K. S., and Rastogi N. (1993). Activities of fluoroquinolone, macrolide, and aminoglycoside drugs combined with inhibitors of glycosylation and fatty acid and peptide biosynthesis against *Mycobacterium avium*. *Antimicrobial Agents Chemotherapy*; **37**, 652-661.

Bauerfeind, R., Benazzi S., Weiss R., Schliesser T., Willems H., and Baljer G. (1996). Molecular characterization of *Mycobacterium paratuberculosis* isolates from sheep, goats, and cattle by hybridization with a DNA probe to insertion element IS900. *Journal of Clinical Microbiology*; **34**, 1617-1621.

Beard, P. M., Daniels M. J., Henderson D., Pirie A., Rudge K., Buxton D., Rhind S., Greig A., Hutchings M. R., McKendrick I., Stevenson K., and Sharp J. M. (2001). Paratuberculosis infection of non-ruminant wildlife in Scotland. *Journal of Clinical Microbiology*; **39**, 1517-1521.

Begara-McGorum, I., Wildblood L. A., Clarke C. J., Connor K. M., Stevenson K., McInnes C. J., Sharp J. M., and Jones D. G. (1998). Early immunopathological events in experimental ovine paratuberculosis. *Veterinary Immunology and Immunopathology*; **63**, 265-287.

Bergey's Manual of Systematic Bacteriology (2001); 2nd edition by Bergey's Manual Trust.

Bendixen, P. H. (1977). Application of direct Leukocyte-Migration Agarose Test in cattle from a *Mycobacterium paratuberculosis* infected herd. *American Journal of Veterinary Research*; **38**, 2027-2028.

Beutler, B. and Cerami A. (1989). The biology of cachectin/TNF - A primary mediator of the host response. *Annual Review of Immunology*; **7**, 625-655.

Billman-Jacobe, H., Carrigan M., Cockram F., Corner L. A., Gill L. J., Hill J. F., Jessep T., Milner A. R., and Wood P. R. (1992). A comparison of the interferon gamma assay with the absorbed ELISA for the diagnosis of Johne's disease in cattle. *Australian Veterinary Journal*; **69**, 25-28.

Bogli-Stuber, K., Kohler C., Seitert G., Glanemann B., Antognoli M. C., Salman M. D., Wittenbrink M. M., Wittwer M., Wassenaar T., Jemmi T., and Bissig-Choisat B. (2005). Detection of *Mycobacterium avium subspecies paratuberculosis* in Swiss dairy cattle by real-time PCR and culture: a comparison of the two assays. *Journal of Applied Microbiology*; **99**, 587-597.

Bosshard, C., Stephan R., and Tasara T. (2006). Application of an F57 sequence-based real-time PCR assay for *Mycobacterium paratuberculosis* detection in bulk tank raw milk and slaughtered healthy dairy cows. *Journal of Food Protection*; **69**, 1662-1667.

Bustin, S. A. and Nolan T. (2004). Pitfalls of quantitative real-time reverse-transcription polymerase chain reaction. *Journal of Biomolecular Techniques*; **15**, 155-166.

Chen, Q. and Lentz B. R. (1997). Fluorescence resonance energy transfer study of shape changes in membrane-bound bovine prothrombin and meizothrombin. *Biochemistry*; **36**, 4701-4711.

Chiodini, R. J., Van Kruiningen H. J., and Merkal R. S. (1984). Ruminant paratuberculosis (Johne's disease): the current status and future prospects. *The Cornell veterinarian*; **74**, 218-262.

Chiodini, R. J. (1986). Biochemical characteristics of various strains of *Mycobacterium paratuberculosis*. *American Journal of Veterinary Research*; **47**, 1442-1445.

Christopher-Hennings, J., Dammen M. A., Weeks S., Epperson W. B., Singh S. N., Steinlicht G. L., Fang Y., Skaare J. L., Larsen J. L., Payeur J. B., and Nelson E. A. (2003). Comparison of two DNA extractions and nested PCR, real-time PCR, a new commercial PCR assay, and bacterial culture for detection of *Mycobacterium avium* subsp. *paratuberculosis* in bovine faeces. *Journal of Veterinary Diagnostic Investigation*; **15**, 87-93.

Clarke, C. J. and Little D. (1996). The pathology of ovine paratuberculosis: Gross and Histological changes in the intestine and other tissues. *Journal of Comparative Pathology*; **114**, 419-437.

Clarke, C. J. (1997). The pathology and pathogenesis of paratuberculosis in ruminants and other species. *Journal of Comparative Pathology*; **116**, 217-261.

Cocito, C., Gilot P., Cocne M., De Kesel M., Poupart P., and Vannuffel P. (1994). Paratuberculosis. *Clinical Microbiology Reviews*; **7**, 328-345.

Colgrove, G. S., Thoen C. O., Blackburn B. O., and Murphy C. D. (1989). Paratuberculosis in Cattle - A comparison of 3 serologic tests with results of faecal culture. *Veterinary Microbiology*; **19**, 183-187.

Collins, M. T., Kenefick K. B., Sockett D. C., Lambrecht R. S., McDonald J., and Jorgensen J. B. (1990). Enhanced Radiometric detection of *Mycobacterium paratuberculosis* by using filter-concentrated bovine faecal specimens. *Journal of Clinical Microbiology*; **28**, 2514-2519.

Collins, M. T. (1996). Diagnosis of paratuberculosis. *Veterinary Clinical North America Food Animal Practice*; **12**, 357-371.

Collins, M. T. (2004). Update on paratuberculosis: 3. Control and zoonotic potential. *Irish Veterinary Journal*; **57**, 49-52.

- Collins, M. T., Wells S. J., Petrini K. R., Collins J. E., Schultz R. D., and Whitlock R. H. (2005). Evaluation of five antibody detection tests for diagnosis of bovine paratuberculosis. *Clinical and Vaccine Immunology*; **12**, 685-692.
- Cousins, D. V., Whittington R., Marsh I., Masters A., Evans R. J., and Kluver P. (1999). *Mycobacteria* distinct from *Mycobacterium avium* subsp. *paratuberculosis* isolated from the faeces of ruminants possess IS 900 -like sequences detectable by IS 900 polymerase chain reaction: implications for diagnosis. *Molecular and Cellular Probes*; **13**, 431-442.
- Cox, J. C., Drane D. P., Jones S. L., Ridge S., and Milner A. R. (1991). Development and evaluation of a rapid absorbed enzyme immunoassay test for the diagnosis of Johne's disease in cattle. *Australia Veterinary Journal*; **68**, 157-160.
- Daniels, M. J., Hutchings, M. R., Beard, P. M., Henderson, D., Greig, A., Stevenson, K., and Sharp, J. M. (2003). Do non-ruminant wildlife pose a risk of paratuberculosis to domestic livestock and vice versa in Scotland? *Journal of Wildlife Diseases*; **39**, 10-15.
- DEFRA, 2007; website <http://www.defra.gov.uk/animalh/diseases/other/johnes.htm>
- de Lisle, G. W., Samagh B. S., and Duncan J. R. (1980). Bovine paratuberculosis II. A comparison of faecal culture and the antibody response. *Canadian Journal Comparative Medicine*; **44**, 183-191.
- de Lisle, G. W., Seguin P., Samish B. S., Corner A. H., and Duncan J. R. (1980). Bovine paratuberculosis I. A herd study using complement fixation and intradermal tests. *Canadian Journal Comparative Medicine*; **44**, 177-182.
- Fang, Y., Wu W. H., Pepper J. L., Larsen J. L., Maras S. A. E., Nelson E., Epperson W. B., and Christopher-Hennings J. (2002). Comparison of real-time quantitative PCR with Molecular Beacons to nested PCR and culture methods for detection of *Mycobacterium avium* subsp. *paratuberculosis* in bovine faecal samples. *Journal of Clinical Microbiology*; **40**, 287-291.

Goudswaard, J., Terportenpastoors W.W.M. (1972). Johne's disease in goats-comparison of serological tests. *Netherland Journal Veterinary Science*; **4**, 93-114.

Grant, I. R. (2005). Zoonotic potential of *Mycobacterium avium* subsp. *paratuberculosis*: the current position. *Journal of Applied Microbiology*; **98**, 1282-1293.

Grant, I. R., Ball H. J., and Rowe M. T. (2002). Incidence of *Mycobacterium paratuberculosis* in bulk raw and commercially pasteurized cows' milk from approved dairy processing establishments in the United Kingdom. *Applied and Environmental Microbiology*; **68**, 2428-2435.

Green, E. P., Tizard M. L., Moss M. T., Thompson J., Winterbourne D. J., McFadden J. J., and Hermon-Taylor J. (1989). Sequence and characteristics of IS900, an insertion element identified in a human Crohn's disease isolate of *Mycobacterium paratuberculosis*. *Nucleic Acids Research*; **17**, 9063-9073.

Greig, A., Stevenson K., Henderson D., Perez V., Hughes V., Pavlik I., Hines M. E., II, McKendrick I., and Sharp J. M. (1999). Epidemiological study of paratuberculosis in wild rabbits in Scotland. *Journal of Clinical Microbiology*; **37**, 1746-1751.

Hassall Associates report (2003); Financial and non-financial assistance measures for owners of beef cattle herds infected with BJD prepared for Animal Health Australia and Cattle Council of Australia.

Hein, I., Lehner A., Rieck P., Klein K., Brandl E., and Wagner M. (2001). Comparison of different approaches to quantify *Staphylococcus aureus* cells by real-time quantitative PCR and application of this technique for examination of cheese. *Applied and Environmental Microbiology*; **67**, 3122-3126.

Hines, S. A., Buergelt C. D., Wilson J. II., and Bliss E. L. (1987). Disseminated *Mycobacterium paratuberculosis* infection in a cow. *Journal of the American Veterinary Medical Association*; **190**, 681-683.

- Hiyoshi, M. and Hosoi S. (1994). Assay of DNA denaturation by polymerase chain reaction-driven fluorescent label incorporation and fluorescence resonance energy transfer. *Analytical Biochemistry*; **221**, 306-311.
- Holland, P. M., Abramson R. D., Watson R., and Gelfand D. H. (1991). Detection of specific polymerase chain reaction product by utilizing the 5'----3' exonuclease activity of *Thermus aquaticus* DNA polymerase. *Proceedings of National Academy of Sciences of the United States of America*; **88**, 7276-7280.
- Hope, A. F., Kluver P. F., Jones S. L., and Condron R. J. (2000). Sensitivity and specificity of two serological tests for the detection of ovine paratuberculosis. *Australian Veterinary Journal*; **78**, 850-856.
- Jark, U., Ringena I., Franz B., Gerlach G. F., Beyerbach M., and Franz B. (1997). Development of an ELISA technique for serodiagnosis of bovine paratuberculosis. *Veterinary Microbiology*; **57**, 189-198.
- Johnson, D. W., Muscoplat C. C., Larsen A. B., and Thoen C. O. (1977). Skin testing, faecal culture, and lymphocyte immunostimulation in cattle inoculated with *Mycobacterium paratuberculosis*. *American Journal of Veterinary Research*; **38**, 2023-2025.
- Jones, D. G. and Kay J. M. (1996). Serum biochemistry and the diagnosis of Johne's disease (paratuberculosis) in sheep. *The Veterinary Record*; **139**, 498-499.
- Jorgensen J.B. (1982). An improved medium for culture of *Mycobacterium paratuberculosis* from bovine faeces. *Acta Veterinaria Scandinavica*; **23**, 325-335.
- Kalis, C. H. J., Collins M. T., Hessclink J. W., and Barkema H. W. (2003). Specificity of two tests for the early diagnosis of bovine paratuberculosis based on cell-mediated immunity: the Johnin skin test and the gamma interferon assay. *Veterinary Microbiology*; **97**, 73-86.
- Khare, S., Ficht T. A., Santos R. L., Romano J., Ficht A. R., Zhang S., Grant I. R., Libal M., Hunter D., and Adams L. G. (2004). Rapid and sensitive detection of

Mycobacterium avium subsp. *paratuberculosis* in bovine milk and faeces by a combination of immunomagnetic bead separation-conventional PCR and real-time PCR. *Journal of Clinical Microbiology*; **42**, 1075-1081.

Kim, S. G., Shin S. J., Jacobson R. H., Miller L. J., Harpending P. R., Stehman S. M., Rossiter C. A., and Lein D. A. (2002). Development and application of quantitative polymerase chain reaction assay based on the ABI 7700 system (*TaqMan*) for detection and quantification of *Mycobacterium avium* subsp. *paratuberculosis*. *Journal of Veterinary Diagnostic Investigation*; **14**, 126-131.

Larsen, A. B., Merkal R. S., and Vardaman T. H. (1956). Survival time of *Mycobacterium paratuberculosis*. *American Journal of Veterinary Research*; **17**, 549-551.

Larsen, A. B., Merkal R. S., and Cutlip R. C. (1975). Age of cattle as related to resistance to infection with *Mycobacterium paratuberculosis*. *American Journal of Veterinary Research*; **36**, 255-257.

Larsen, A. B., Stalheim O. H. V., Hughes D. E., Appell L. H., Richards W. D., and Himes E. M. (1981). *Mycobacterium paratuberculosis* in the semen and genital organs of a semen-donor bull. *Journal of the American Veterinary Medical Association*; **179**, 169-171.

Lawrence W.E. (1956). Congenital infection with *Mycobacterium johnei* in cattle. *Veterinary Record*; **68**, 312-314.

Lec, L. G., Connell C. R., and Bloch W. (1993). Allelic discrimination by nick-translation PCR with fluorogenic probes. *Nucleic Acids Research.*; **21**, 3761-3766.

Lepper, A. W., Wilks C. R., Kotiw M., Whitehead J. T., and Swart K. S. (1989). Sequential bacteriological observations in relation to cell-mediated and humoral antibody responses of cattle infected with *Mycobacterium paratuberculosis* and maintained on normal or high iron intake. *Australian Veterinary Journal*; **66**, 50-55.

- Li, L., Bannantine J. P., Zhang Q., Amonsin A., May B. J., Alt D., Banerji N., Kanjilal S., and Kapur V. (2005). The complete genome sequence of *Mycobacterium avium* subspecies *paratuberculosis*. *Proceedings of the National Academy of Sciences*; **102**, 12344-12349.
- Livak, K. J., Flood S. J., Marmaro J., Giusti W., and Deetz K. (1995). Oligonucleotides with fluorescent dyes at opposite ends provide a quenched probe system useful for detecting PCR product and nucleic acid hybridization. *PCR Methods Applications*; **4**, 357-362.
- Manning, E. J. B. and Collins M. T. (2001). *Mycobacterium avium* subsp *paratuberculosis*: pathogen, pathogenesis and diagnosis. *Revue Scientifique et Technique de l'Office International des Epizooties*; **20**, 133-150.
- Masaki, S., Sugimori G., Okamoto A., Imose J., and Hayashi Y. (1990). Effect of Tween-80 on the growth of *Mycobacterium-avium* Complex. *Microbiology and Immunology*; **34**, 653-663.
- McCullough, W. G. and Merkal R. S. (1976). Iron-chelating compound from *Mycobacterium avium*. *Journal of Bacteriology*; **128**, 15-20.
- Merkal, R. S., Monlux W. S., Kluge J. P., Larsen A. B., Kopecky K. E., Quinn L. Y., and Lehmann R. P. (1968a). Experimental paratuberculosis in sheep after oral intratracheal or intravenous inoculation - histochemical localization of dehydrogenase activities. *American Journal of Veterinary Research*; **29**, 971-982.
- Merkal, R. S., Kluge J. P., Monlux W. S., Larsen A. B., Kopecky K. E., Quinn L. Y., and Lehmann R. P. (1968b). Experimental paratuberculosis in sheep after oral intratracheal or intravenous inoculation - histochemical localization of hydrolase activities. *American Journal of Veterinary Research*; **29**, 985-994.
- Merkal, R. S., Larsen A. B., Kopecky K. E., and Ness R. D. (1968c). Comparison of examination and test methods for early detection of paratuberculous cattle. *American Journal of Veterinary Research*; **29**, 1533-1538.

- Merkal, R. S., Kopecky K. E., and Larsen A. B. (1970). Immunologic mechanisms in bovine paratuberculosis. *American Journal of Veterinary Research*; **31**, 475-485.
- Merkal, R. S. and Richards W. D. (1972). Inhibition of fungal growth in cultural isolation of *Mycobacteria*. *Applied Microbiology*; **24**, 205-&.
- Merkal, R. S. and Curran B. J. (1974). Growth and metabolic characteristics of *Mycobacterium paratuberculosis*. *Applied Microbiology*; **28**, 276-279.
- Milner, A. R., Mack W. N., Coates K. J., Hill J., Gill L., and Sheldrick P. (1990). The sensitivity and specificity of a modified ELISA for the diagnosis of Johne's disease from a field trial in cattle. *Veterinary Microbiology*; **25**, 193-198.
- Muscoplat, C. C., Thoen C. O., Chen A. W., and Johnson D. W. (1975). Development of specific invitro lymphocyte-responses in cattle infected with *Mycobacterium bovis* and with *Mycobacterium-avium*. *American Journal of Veterinary Research*; **36**, 395-398.
- Mutharia, L. M., Moreno W., and Raymond M. (1997). Analysis of culture filtrate and cell wall-associated antigens of *Mycobacterium paratuberculosis* with monoclonal antibodies. *Infection and Immunity*; **65**, 387-394.
- NCBI taxonomy browser, (2007);
http://www.ncbi.nlm.nih.gov/Taxonomy/Browser/wwwtax.cgi?mode=Info&id=1770&lvl=3&p=mapview&p=has_linkout&p=blast_url&p=genome_blast&lin=f&keep=1&src_hmode=1&unlock.
- OIE (2004).): Manual of diagnostic tests and vaccines for terrestrial animals (Mammals, Birds and Bees); contributor Thorel, M.F.; Office International des Epizooties, Paris, France; 347-359, 464-473.
- OIE: Old classification of diseases notifiable to the OIE (2005) Animal diseases data;
http://www.oie.int/eng/maladies/en_OldClassification.htm#ListeB.
- O'Mahony, J. and Hill C. (2002). A real time PCR assay for the detection and quantitation of *Mycobacterium avium* subsp. *paratuberculosis* using SYBR Green and the Light Cycler. *Journal of Microbiological Methods*; **51**, 283-293.

- O'Mahony, J. and Hill C. (2004). Rapid real-time PCR assay for detection and quantitation of *Mycobacterium avium* subsp. *paratuberculosis* DNA in artificially contaminated milk. *Applied and Environmental Microbiology*; **70**, 4561-4568.
- Ott, S. L., Wells S. J., and Wagner B. A. (1999). Herd-level economic losses associated with Johne's disease on US dairy operations. *Preventive Veterinary Medicine*; **40**, 179-192.
- Payne J.M. and Rankin J.D. (1961). A comparison of the pathogenesis of experimental Johne's disease in calves and cows. *Research in Veterinary Science*; **2**, 175-179.
- Queen, D.S., Russell, E.G. (1979). Culture of *Mycobacterium paratuberculosis* from bovine foetuses. *Australian Veterinary Journal*; **55**, 203-204.
- Quinn, P. J., Carter, M. E., Markey, B. & Carter, G. R. (1994). Bacterial pathogens: Microscopy, culture and identification. In *Clinical Veterinary Microbiology*, 25-26. Edited by P. J. Quinn, M. E. Carter, B. Markey & G. R. Carter. Wolfe, London.
- Radostits OM, Gay CC, Blood DC, Hinchcliff KW. (2000) Veterinary Medicine: a textbook of the diseases of cattle, sheep, pigs, goats and horses, 9th ed: WB Saunders: 844-845.
- Rajeev, S., Zhang Y., Sreevatsan S., Motiwala A. S., and Byrum B. (2005). Evaluation of multiple genomic targets for identification and confirmation of *Mycobacterium avium* subsp. *paratuberculosis* isolates using real-time PCR. *Veterinary Microbiology*; **105**, 215-221.
- Ravva, S. V. and Stanker L. H. (2005). Real-time quantitative PCR detection of *Mycobacterium avium* subsp. *paratuberculosis* and differentiation from other *Mycobacteria* using SYBR Green and TaqMan assays. *Journal of Microbiological Methods*; **63**, 305-317.
- Ridge, S. E., Morgan I. R., Sockett D. C., Collins M. T., Condron R. J., Skilbeck N. W., and Webber J. J. (1991). Comparison of the Johne's absorbed EIA and the complement-

- fixation test for the diagnosis of Johne's disease in cattle. *Australian Veterinary Journal*; **68**, 253-257.
- Rothel, J. S., Jones S. L., Corner I. A., Cox J. C., and Wood P. R. (1990). A sandwich Enzyme-Immunoassay for bovine Interferon-Gamma and its use for the detection of tuberculosis in Cattle. *Australian Veterinary Journal*; **67**, 134-137.
- Rowe, M. T., Grant I. R., Dundee L., and Ball H. J. (2000). Heat resistance of *Mycobacterium avium* subsp *paratuberculosis* in milk. *Irish Journal of Agricultural and Food Research*; **39**, 203-208.
- Rubery, E. (2001). Review of the evidence for a link between exposure to *Mycobacterium paratuberculosis* (MAP) and Crohn's disease (CD) in humans: a report for the Food Standards Agency. [London]: Food Standards Agency.
- SAC report (May 2000): Workshop on assessment of surveillance and control of Johne's disease in farm animals in Great Britain; SAC Veterinary Science Division, UK.
- Seitz, S. E., Heider, L. E., Hueston, W. D., Bechnielsen, S., Rings, D. M., and Spangler, L. (1989). Bovine foetal infection with *Mycobacterium paratuberculosis*. *Journal of the American Veterinary Medical Association*; **194**, 1423-1426.
- Siva Kumar, P., Tripathi B. N., and Singh N. (2005). Detection of *Mycobacterium avium* subsp. *paratuberculosis* in intestinal and lymph node tissues of water buffaloes (*Bubalus bubalis*) by PCR and bacterial culture. *Veterinary Microbiology*; **108**, 263-270.
- Sockett, D. C., Conrad T. A., Thomas C. B., and Collins M. T. (1992). Evaluation of four serological tests for bovine paratuberculosis. *Journal of Clinical Microbiology*; **30**, 1134-1139.
- Somoskovi, A., Hotaling, J. E., Fitzgerald, M., O'Donnell, D., Parsons, L. M., and Salfinger, M. (2001) Lessons from a proficiency testing event for Acid-Fast Microscopy. *Chest*, **120**: 250-257.

- Stabel, J. R. (1998). Johne's disease: A Hidden Threat. *Journal of Dairy Science*; **81**, 283-288.
- Streeter, R. N., Hoffsis G. F., Bechnielsen S., Shulaw W. P., and Rings M. (1995). Isolation of *Mycobacterium paratuberculosis* from colostrum and milk of subclinically infected cows. *American Journal of Veterinary Research*; **56**, 1322-1324.
- Sweeney, R. W., Whitlock R. H., and Rosenberger A. E. (1992). *Mycobacterium paratuberculosis* isolated from foetuses of infected cows not manifesting signs of the disease. *American Journal of Veterinary Research*; **53**, 477-480.
- Sweeney, R. W. (1996). Transmission of paratuberculosis. *Veterinary Clinics of North America-Food Animal Practice*; **12**, 305-312.
- Täpp, L., Malmberg E., Rennel M., Wik M., and Syvänen A.C. (2000). Homogeneous scoring of single-nucleotide polymorphisms: comparison of the 5'-nuclease TaqMan assay and molecular beacon probes. *BioTechniques*; **28**, 732-737.
- Thelwell, N., Millington S., Solinas A., Booth J., and Brown T. (2000). Mode of action and application of Scorpion primers to mutation detection. *Nucleic Acids Res.*; **28**, 3752-3761.
- Thorcl, M. F., Krichevsky M., and Levy-Frebault V. V. (1990). Numerical taxonomy of mycobactin-dependent *Mycobacteria*, emended description of *Mycobacterium avium*, and description of *Mycobacterium avium* subsp. *avium* subsp. nov, *Mycobacterium avium* subsp. *paratuberculosis* subsp. nov, and *Mycobacterium avium* subsp. *silvaticum* subsp. nov. *International Journal of Systematic and Evolutionary Microbiology*; **40**, 254-260.
- Thoresen, O. and Saxegaard F. (1991). Gen-Probe rapid diagnostic system for distinguishing between *Mycobacterium-avium* and *Mycobacterium paratuberculosis* - reply. *Journal of Clinical Microbiology*; **29**, 2360-2361.
- Twort, F. W. and Ingram G. L. Y. (1912). A method for isolating and cultivating the *Mycobacterium enteritidis chronicae pseudotuberculosis bovis*, Johne, and some

experiments on the preparation of a diagnostic vaccine for pseudo-tuberculous enteritis of bovines. *Proceedings of the Royal Society of London Series B-Containing Papers of A Biological Character*; **84**, 517-542.

Vary, P. H., Andersen P. R., Green E., Hermon-Taylor J., and McFadden J. J. (1990). Use of highly specific DNA probes and the polymerase chain reaction to detect *Mycobacterium paratuberculosis* in Johne's disease. *Journal of Clinical Microbiology*; **28**, 933-937.

Whan, L. B., Grant I. R., Ball, H.G., Scott, R. and Rowe, M.T. (2001). Bactericidal effect of chlorine on *Mycobacterium paratuberculosis* in drinking water. *Letters in Applied Microbiology*; **33**, 227-231.

Whitlock, R. H. and Buerget C. (1996). Preclinical and clinical manifestations of paratuberculosis (including pathology). *The Veterinary Clinics of North America Food Animal Practice*; **12**, 345-356.

Whittington, R. J., Marsh L., Turner M. J., McAllister S., Choy E., Eamens G. J., Marshall D. J., and Ottaway S. (1998). Rapid Detection of *Mycobacterium paratuberculosis* in clinical samples from ruminants and in spiked environmental samples by modified BACTEC 12B radiometric culture and direct confirmation by IS900 PCR. *Journal of Clinical Microbiology*; **36**, 701-707.

Whittington, R. J. and Sergeant E. (2001). Progress towards understanding the spread, detection and control of *Mycobacterium avium* subsp *paratuberculosis* in animal populations. *Australian Veterinary Journal*; **79**, 267-278.

Whittington, R. J., Marsh I. B., Taylor P. J., Marshall D. J., Taragel C., and Reddacliff L. A. (2003a). Isolation of *Mycobacterium avium* subsp *paratuberculosis* from environmental samples collected from farms before and after destocking sheep with paratuberculosis. *Australian Veterinary Journal*; **81**, 559-563.

Whittington, R. J., Eamens G. J., and Cousins D. V. (2003b). Specificity of absorbed ELISA and agar gel immunodiffusion tests for paratuberculosis in goats with

observations about use of these tests in infected goats. *Australian Veterinary Journal*; **81**, 71-75.

Wittwer, C.T., Herrmann M.G., Moss A.A., and Rasmussen R.P. (1997) Continuous fluorescence monitoring of rapid cycle DNA amplifications. *BioTechniques*; **22**, 130-138.